BULK AMORPHOUS STEEL AS A COATING MATERIAL: HARDFACING APPLICATION

A THESIS SUBMITTED TO
THE GRADUATE SCHOOL OF NATURAL AND APPLIED SCIENCES
OF
MIDDLE EAST TECHNICAL UNIVERSITY

BY

HAFİZE ÇAKMAK

IN PARTIAL FULFILLMENT OF THE REQUIREMENTS
FOR
THE DEGREE OF MASTER OF SCIENCE
IN
METALLURGICAL AND MATERIALS ENGINEERING

JUNE 2018

Approval of the thesis:

BULK AMORPHOUS STEEL AS A COATING MATERIAL: HARDFACING APPLICATION

submitted by **HAFİZE ÇAKMAK** in partial fulfillment of the requirements for the degree of **Master of Science in Metallurgical and Materials Engineering Department, Middle East Technical University** by,

Prof. Dr. Halil Kalıpçılar _____
Dean, Graduate School of **Natural and Applied Sciences**

Prof. Dr. C. Hakan Gür _____
Head of Department, **Metallurgical and Materials Eng.**

Prof. Dr. M. Vedat Akdeniz _____
Supervisor, **Metallurgical and Materials Eng. Dept., METU**

Prof. Dr. Amdulla O. Mekhrabov _____
Co-Supervisor, **Metallurgical and Materials Eng. Dept., METU**

Examining Committee Members:

Prof. Dr. A. Macit Özenbaş _____
Metallurgical and Materials Eng. Dept., METU

Prof. Dr. M. Vedat Akdeniz _____
Metallurgical and Materials Eng. Dept., METU

Prof. Dr. Amdulla O. Mekhrabov _____
Metallurgical and Materials Eng. Dept., METU

Prof. Dr. Rıza Gürbüz _____
Metallurgical and Materials Eng. Dept., METU

Assist. Prof.Dr. Mehmet Yıldırım _____
Metallurgical and Materials Eng. Dept., Selçuk University

Date: 26.06.2018

I hereby declare that all information in this document has been obtained and presented with academic rules and ethical conduct. I also declare that, as required by those rules and conduct, I have fully cited and referenced all material and results that are not original to this work.

Name, Last Name: Hafize, Çakmak

Signature :

ABSTRACT

BULK AMORPHOUS STEEL AS A COATING MATERIAL: HARDFACING APPLICATION

Çakmak, Hafize

M.S., Department of Metallurgical and Materials Engineering
Supervisor: Prof. Dr. M. Vedat Akdeniz
Co-Supervisor: Prof Dr. Amdulla O. Mekhrabov

June 2018, 103 pages

In the industrial applications, surface modification/treatment techniques give preference to reach the better service life for components which encounter the problem of wear. In practice, worn components either have to be rejected or rebuilt by employing various surface treatment applications which actually do not only improve the wear resistant of the surface, but also it helps preserve against corrosion and oxidation problems at higher temperature. Among these industrial coating & surface treatment applications, hardfacing is a more conventional surface treatment technique, which is implemented by welding, to grade up the surface specialty of the base/substrate metals. In this coating application, the production of a new surface layer will be accomplished by homogeneous deposition of an alloy onto the surface of a relatively cheap conventional base/substrate metal by welding so as to obtain an enduring surface layer which has impact and wear resistance ability, erosion and corrosion resistance or any integration of these factors. Hence, the coating alloys should have some desired properties correspondingly**,** such as high hardness, demanded abrasion resistance/tribological properties, specific corrosion and heat resistance. On the other hand, bulk amorphous steels (BASs) have promising future due to their superior mechanical and physical properties compared with their

crystalline states. BASs display very high hardness, Young's modulus, wear and corrosion resistance due to their amorphous nature. This nature of the BAS is lack of any crystallographic defects such as grain boundaries and dislocations which provides better corrosion resistance and mechanical properties. These unique characteristics make the BASs a potential candidate for coating applications.

In this respect, the purpose of the thesis is to develop and make use of a new alternative coating material based on BAS in place of traditional coating materials which will be utilized in industrial coating and surface treatment implementations by hardfacing. For this application, the BASs were re-synthesized from cast iron scraps, which was derived from NOVALAB's theoretical approach in order to improve the glass forming ability of iron-based metallic glasses, by arc melting under controlled atmosphere. Suction casting technique has been employed for the direct production of 3 mm in diameter BAS rod, subsequently utilized as a filler material in TIG welding process. Hardfacing application was applied on relatively cheap low/medium carbon steel (S275) and stainless (304) steel substrates. Coating quality, its coherency and conformity were examined in two different cooling environments. It was observed that owing to high bulk glass forming ability (BGFA), BAS coating material preserved their amorphous structure with extreme high hardness, 3-4 times higher than the substrate metal and displayed good wear/abrasion and corrosion resistance in various extreme environments.

Keywords: Hardfacing, Hardfacing with Bulk Amorphous Alloys, Surface Treatment, Coating Applications

ÖZ

İRİ HACİMLİ CAMSI ÇELİKLERİN KAPLAMA MALZEMESİ OLARAK KULLANILMASI: SERT KAPLAMA UYGULAMASI

Çakmak, Hafize

Yüksek Lisans, Metalurji ve Malzeme Mühendisliği Bölümü
Tez Yöneticisi: Prof. Dr. M. Vedat Akdeniz
Ortak Tez Yöneticisi: Prof Dr. Amdulla O. Mekhrabov

Haziran 2018, 103 sayfa

Endüstriyel uygulamalarda kullanılan yüzey modifikasyon teknikleri, aşınma problemi ile karşılaşan bileşenlerin daha iyi servis ömrüne erişmeleri için tercih edilmektedir. Pratikte, aşınmış bileşenlerin ya reddedilmesi ya da sadece yüzeyin aşınmaya karşı dayanıklılığını geliştirmekle kalmayıp, aynı zamanda daha yüksek sıcaklıkta korozyon ve oksidasyon problemlerine karşı korunmasına yardımcı olan çeşitli yüzey işleme uygulamaları kullanılarak yeniden yapılması gerekmektedir. Bu endüstriyel kaplama ve yüzey işleme uygulamaları arasında, sert kaplama, baz/esas metallerinin yüzey özelliklerini sınıflandırmak için kaynak ile uygulanan daha geleneksel bir yüzey işleme tekniğidir.

Bu kaplama uygulamasında, yeni bir yüzey tabakasının üretimi, bir alaşımın, nispeten ucuz bir konvansiyonel baz/esas metalin yüzeyi üzerine homojen olarak kaynak yöntemi ile biriktirilmesiyle, darbe ve aşınma direnci yeteneği, erozyon ve korozyon direnci veya bu faktörlerin herhangi bir entegrasyonu gibi özelliklere sahip kalıcı bir yüzey tabakasının elde edilmesi ile gerçekleştirilecektir. Bu nedenle, kaplama alaşımları, yüksek sertlik, talep edilen aşınma direnci/tribolojik özellikler, çok özel korozyon ve ısı direnci gibi uygun özelliklere sahip olmalıdır. Bunun yanı sıra, İri Hacimli Camsı Çelikler (İHCÇ'ler), kristal yapıları ile karşılaştırıldığında üstün

mekanik ve fiziksel özelliklerinden ötürü umut verici bir gelecek vaat etmektedirler. İHCÇ'ler, amorf doğaları nedeniyle çok yüksek sertlik, Young modülü, aşınma ve korozyon direnci gösterirler. İHCÇ'ler, tane sınırları ve dislokasyon gibi herhangi bir kristalografik kusurdan yoksun oldukları için daha iyi korozyon direnci ve mekanik özellikler sağlarlar. Bu benzersiz özellikler İHCÇ'leri kaplama uygulamaları için potansiyel bir aday haline getirmektedir.

Bu açıdan tezin amacı, endüstriyel kaplama ve yüzey işleme uygulamalarında kullanılacak olan geleneksel kaplama malzemelerinin yerine İHCÇ'e dayalı yeni bir alternatif kaplama malzemesinin geliştirilmesi ve kullanılmasıdır. Bu uygulama için İHCÇ'ler, NOVALAB'ın teorik yaklaşımından türetilen demir esaslı metalik camların cam şekillendirme kabiliyetini arttırmak için kontrollü atmosfer altında eritilmesiyle, dökme demir parçaları kullanılarak yeniden sentezlenmiştir. Emme döküm tekniği, 3 mm çapında İHCÇ çubuğunun doğrudan üretimi için kullanılmış, daha sonra bu çubuk TIG kaynak işleminde dolgu malzemesi olarak kullanılmıştır. Sert kaplama uygulaması, nispeten ucuz düşük / orta karbonlu çelik (S275) ve paslanmaz (304) çelik yüzeylere uygulanmıştır. Kaplama kalitesi, tutarlılığı ve uygunluğu iki farklı soğutma ortamında incelenmiştir. Yüksek cam şekillendirme kabiliyeti sayesinde, İHCÇ kaplama malzemesi amorf yapısını koruduğu için aşırı yüksek sertlik sonuçları (esas metalden 3-4 kat daha yüksek) ve çeşitli aşırı aşındırıcı ortamlarda iyi bir aşınma ve korozyon direnci gösterdiği gözlenmiştir.

Anahtar Kelimeler: Sert Kaplama, İri Hacimli Camsı Çeliklerle Sert Kaplama, Yüzey İşlem, Kaplama Uygulamaları

To my lovely family;

ACKNOWLEDGEMENTS

First and foremost, I would like to express my sincere gratitude to my supervisors Prof. Dr. M. Vedat Akdeniz and Prof. Dr. Amdulla O. Mekhrabov for their limitless and continuous guidance, giving me the opportunity to carry out my research project and their endless patience and understanding in preparation of this thesis.

I would like to express my gratitude to METU Welding Technology and Non-Destructive Testing Research / Application Center; especially to Dr. Koray Yurtışık and Dr. Süha Tirkeş for their support in this study.

I would like to thank my colleagues and friends Dr. Göksu Gürer, Burak Özcan, Baran Tunç, Ayşe Duman, Melis Kaplan, Mehmet Çağırıcı, OlgunYılmaz, who helped me along this way. The technical assistance and suggestions of Nilüfer Atak, Yusuf Yıldırım, and Kubilay Savcı Yeşildemir are also gratefully acknowledged.

My deepest gratitude goes to my beloved mother Emine Çakmak, father Fahri Çakmak and my lovely sister Şerike Çakmak Selvi for their unconditional love, support, and understanding.

TABLE OF CONTENTS

LIST OF TABLES

TABLES

LIST OF FIGURES

FIGURES

CHAPTER 1

INTRODUCTION

During the past several years, because of the future demands and rapid progress of technology, new and unrivaled materials have been the primary research topics for scientists. Advanced materials can be defined as the control microstructure of materials in order to get demanding properties. Developers have recently focused on basically the enhancement of the properties and performance of present materials and/or synthesizing completely novel materials which have better performance than available materials [1]. The first investigation of the unordered atomic arrangement was carried out with highly cooling rates in ($\sim 10^6$ K/s) and they were named as metallic glasses/amorphous alloys. Bulk metallic glasses (BMGs) with millimeter scales dimensions were enhanced in 1982 [2, 3]. Among all classes of BMGs, iron-based BMGs have a substantial effect due to their unique mechanical properties and ferromagnetic behaviors. The difference between Bulk Amorphous Steels (BASs) and BMGs is that BASs behave as non-ferromagnetic. Hence, thanks to these properties, they are widely used in several areas spreading from medical applications to built-in purposes according to their conventional types. [4, 5].

According to theoretical calculations and experimental results from previous studies in NOVALAB, in the first part of the study we intended to re-synthesize the BASs from scrap cast irons by conventional production techniques [6, 7]. The base of the BASs system contains 60 at. % cast iron scraps and pure elements such as B, Mo, Y, and Cr which were selected according to theoretical and experimental backgrounds extracted from published literature works. One of the important parameters in the production of BAS's is the Glass Forming Ability (GFA) of the samples which was tried to be increased by various elemental additions. As a result of all the studies performed in NOVALAB, Manganese (Mn) with 7at. % was found

to be the best among others having good thermal stability with amorphous steel systems and lower fabrication costs.

In the second part of the study, we aimed to use the synthesized sample in surface treatment applications since they have the proper characteristics. As mentioned before, the BAS's have extreme mechanical properties, corrosion and wear resistances which make them good candidates for surface treatment applications. In this part, the prepared samples were used as a hardfacing substance. The main purpose of the hardfacing application is to obtain an invulnerable surface on the substrate metal and to enhance the durability properties of the substrate in the light of amorphous structure preservation after the coating application as well as good wear resistance, abrasion, corrosion or any combination of these properties. In the industrial applications, metallic glass have not been yet fully commercialized in surface modified/coating applications but, their encouraging wear and corrosion characteristic make these materials an alternative for structural applications [8].

This thesis consists of six chapters. Introduction of the thesis is detailed in the first chapter. Theoretical background and related experimental information about processes are explained in the second chapter. The experimental procedure for production and surface treatment application of bulk amorphous steel is explained in the third chapter. The fourth chapter presents the experimental results and discussion about the production part of the BASs and the hardfacing application. In the fifth chapter, the final acquired results of the study are summarized. The final chapter is the sixth chapter that concludes the thesis.

CHAPTER 2

THEORETICAL REVIEW

2.1. A Brief History of Metallic Glasses

Although the metallic materials have been used since pre-historic ages, the development in material science and technology have had an upsurge by the industrial revolution. The traditional definition of metallic materials is considered as crystalline in nature and their atoms are arranged uniformly in three dimensions. However, in 1960, an Au-Si alloy was developed in the glassy state by applying sudden solidification at rates of 10^5–10^6 K/s [1]. After the crystallization examination, no crystalline peaks were realized in X-ray diffraction (XRD) of the Au–Si alloy. This situation was claimed by two graduate students and this was the indication of the presence of the noncrystalline structures [1]. According to our general knowledge, the term "Glass" refers to an amorphous oxide which is obtained by the rapid cooling process of molten mixture in order to protect crystallization [9]. While the material is in this state, in the liquid mixture, rearrangement into regular three-dimensional crystalline structure is not possible. Likewise, "Metallic Glass" also defined as amorphous alloy was synthesized by the rapid solidification of molten alloy [10]. The amorphous state basically can be described as the kinetic freezing of the liquid structure without passing through the crystallization [10].

In the 1970s and 1980s, because of the new perspective in the science and potential applications, interest in metallic glasses gained momentum [11-13]. Turnbull et. al. [12, 13] proved that there are some similarities between metallic and conventional glasses according to thermal analysis reports and it was understood that metallic glasses also got glass transition temperature similar to glasses and this is one of the essential part of metallic glasses.

Before 1970s, production methods allowed systemization of the micron size bulk metallic glasses only. However, in 1970s, Chen et. al. [14] changed this fact and they produced the first metallic glass in millimeter-sized successfully. These metallic millimeter-sized glasses were named as bulk metallic glasses (BMGs). In 1980s, nearly one centimeter-sized BMG was produced by Turnbull and coworkers with lowering cooling rates [2, 3]. After these encouraging developments, BMGs were engendered as the novel materials had to be developed.

The main topics of the BMGs studies in literature are summarized as following:

- The development of the new amorphous alloys while achieving supernal glass-forming ability during production
- The improvement of the fundamental properties of the newly developed amorphous alloys
- The synthesis of the new bulk amorphous alloys via different production techniques for future applications

After the production of the new amorphous alloy with new atomic configuration, lots of characteristics, like promising mechanical properties, desired physical properties and good chemical properties [11, 12, 15] came to light [16].

The experimentally produced amorphous specimens are usually either in rod or in powder form since the high cooling rates ($\approx 10^6$ K/s) limits the specimen geometry.

2.1.1. General View of BMG Systems and Their Features

BMGs can be described as the noncrystalline solids which were synthesized by rapidly cooling from the liquid state that are at least few millimeters in thickness. According to common knowledge, metallic glasses with at least 1mm diameter or thickness are defined as “bulk” noncrystalline [1].

Before 1960s, all metals were considered as crystalline materials, but then omitting the nucleation and crystallization steps were made possible within a very high cooling rate ~10^6K/s and non-crystalline (amorphous) alloys were introduced into the material science. However, BMGs cannot be produced from pure alloy systems. There are some requirements and limitations to produce BMGs. So, in the production part of the BAS, there are several kinds of points to take into consideration.

2.1.2. The Kinetic and Thermodynamic Approach of Metallic Glasses

The thermodynamic point of view is the most critical part during the determination of the phase stability. The characteristic of glass forming ability can be determined by this view. The Gibbs free energy (ΔG) is used to determine the stability of phases.

$$\Delta G = \Delta H_{tr} - T\Delta S_{tr} \text{ and } \Delta G = G_g - G_c \qquad (2.1)$$

In the formula ΔH_{tr} is represents the transformation enthalpy and ΔS_{tr} is represents the transformation entropy.

As can be easily understood from Eq.2.1, it is obvious that to obtain more negative ΔG, either the ΔH_{tr} term should be decreased or the ΔS_{tr} term should be increased.

Production with the high glass forming ability is quite useful for the production part. To obtain favorable glass forming ability, the Gibbs free energy should be kept as negative as possible. Stated in other words, to obtain the non-crystalline structure it must have lower free energy than crystalline phase. The low driving force for nucleation step provides a high glass forming ability.

The major property for metallic glasses is the high number of constituent elements. As known from the literature, entropy is proportional to the number of states. The

interaction between the atoms will also influence the enthalpy of formation. Increase in the entropy leads to lower the Gibbs free energy.

The viscosity is a kinetic parameter for glass formation since atomic mobility is connected to viscosity in the supercooled state. The change of viscosity as a function of undercooling is a parameter for liquids because it leads to the change of the atoms while supercooling [17]. Viscosity can be calculated following relation[17]:

$$\eta=\eta_0 \exp\left(\frac{D^*T_0}{T-T_0}\right) \qquad (2.2)$$

where T_0 is temperature, η_0 is limit of viscosity at high T and D^* is the brittleness parameter. The high values of D^*provide high stability of the glass phase.

Previous studies in literature which were related to metallic glasses [18] have proved that the liquid form in the production step of the BMGs has a similar kinetic approach to the silicate.

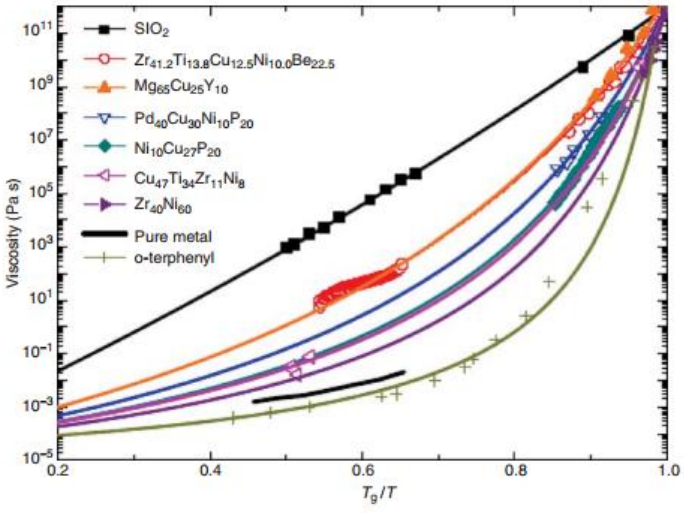

Figure 2.1. Related viscosities of different liquids[19]

From related studies, it can be summarized that a high viscosity and small free volume at the melting point of the liquid gives high GFA results. As represented in

Figure 2.1, SiO_2 shows the strongest glass formability with high melt viscosity [1]. According to general point of view, the change of viscosity, changes the movement capability of atom during supercooling state. Figure 2.1 shows the viscosities of some different liquids [20] and, it is obvious from the figure that the SiO_2 is the has strongest glass former ability.[18].

Because of the high viscosity and inhibition of the formation and growth of the thermodynamically stable phases with insufficient mobility of the constituents, system will reach the large GFA [18].

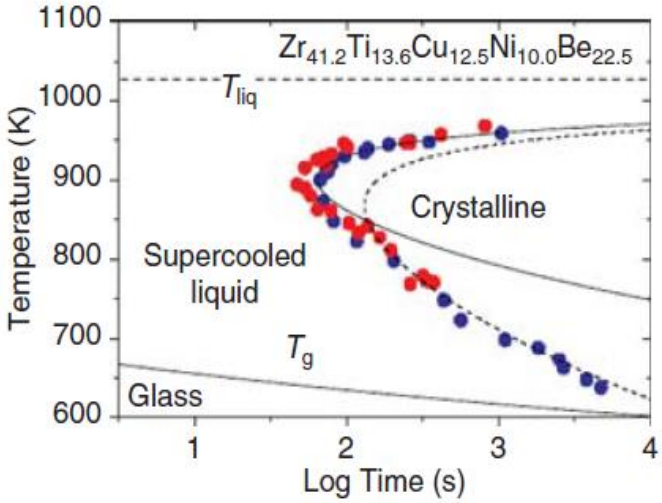

Figure 2.2. TTT diagram for the primary crystallization[19]

In Figure 2.2, the diagram shows the typical C shape that is the result of the conflict between the driving force for crystallization and the diffusivity of the atoms. Driving force for crystallization tends to increase whereas diffusivity of the atoms tends to decrease. With the achievement of slower cooling rates, the fabrication of big sized metallic glasses can be possible and these large pieces will stimulate the usage of the BASs in the industrial applications. According to general knowledge, if more components are added to the alloy, the glass forming ability will show tendency towards an increase and hence, the molten phase will become more stable compared to the crystalline phases [21].

2.1.3. Design Criteria for Production of BMG Alloys

As mentioned before, bulk term is defined as the sample which has minimum 1 mm thicknesses or diameters dimension. At the end of the experiment, to obtain larger sized specimen, cooling rate should be as low as possible. As illustrated in Figure 2.3, there is a comparison between the critical cooling rate of silicate glass, BMGs and conventional metallic glasses with respect to reduced glass transition temperature (T_{rg}). From this figure, to obtain BMGs, 10^4K/s or lower cooling rate is needed during production. As estimated, the critical cooling rate is a very essential parameter for BMGs design.

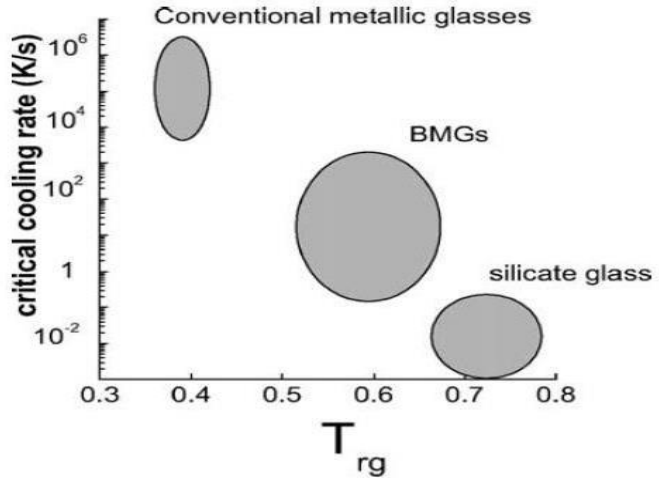

Figure 2.3. Critical cooling rate comparison with respect to T_{rg} [18]

In 1996, Inoue specified the criteria for the production of the BMG systems as:

1- The developed novel alloy system must include minimum three ingredient elements [22]

2- These ingredients must have variable (not identical) atomic radius [22]

3- Negative heats of mixing must be achieved between these ingredients [22].

As it was mentioned in Section 2.1.2, the first criterion is related to thermodynamics. It states that any increase in the number of the components will increase the system's entropy which will cause a decrease in the Gibbs free energy.

Hence, it makes the glassy phase formation possible rather than the crystalline phases. Furthermore, increasing the ingredient number also increases the viscosity of the molten state which leads to a better glass former melt. As a result of the increase in the viscosity of the system, atomic diffusivity will decrease. Hence, by applying the first criterion, both nucleation and growth rates can be reduced.

As mentioned in the second criterion, due to the addition of ingredient elements with varying atomic radius the alloy system cannot choose a viable crystal structure so, glass forming of the system increases [1, 23, 24]. Moreover, if the systems have deep eutectics, it will have better glass forming ability because liquid stability at lower temperatures is also an important parameter for glass forming ability. Hence, according to above discussions, BMGs alloys should include more than three components with different atomic size and a developed composition which is nearby the eutectic point. Moreover, there is a study to support this view point. Akdeniz et.al [25] show that, when the system achieves the peritectic and eutectic reactions points with high enthalpy ratio, it gains high glass forming ability. Their schematic representations are given on Figure 2.4**.**

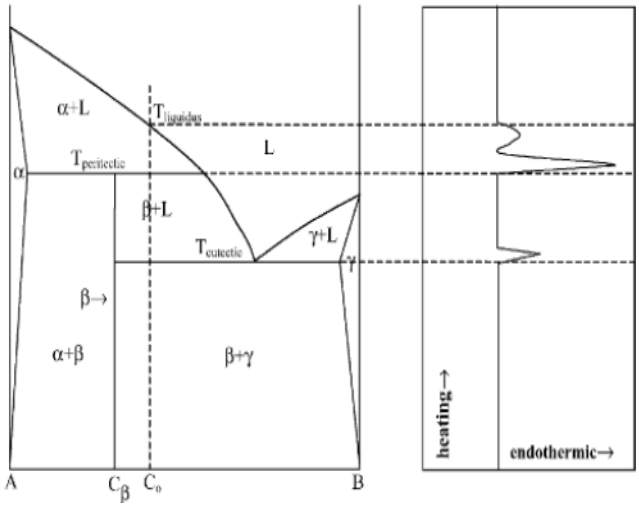

Figure 2.4. Phase diagram and thermal pattern of peritectic and eutectic reactions

2.2. Glass Forming Ability (GFA) and Parameters

"The glass-forming ability is predefined as the transformation ambition of the metals into the glassy state [1]." While synthesizing metallic glasses, the glass forming ability of BMGs has to be enhanced as needed. As it is well known, when the free transformation energy condition is low, desired GFA is achieved. According to the relationship of Gibbs free energy; $\Delta G = \Delta H_f - T\,\Delta S_f$, the low ΔG value can be derived in the presence of small ΔH_f and large ΔS_f values. Large ΔS_f can be measured in multi-component alloying structures because it is commeasurable to the number of micro-states.[16] While determining the GFA of the systems, there are a great number of parameters that have been identified in the consideration of the thermal characteristics of the systems.

2.2.1. Reduced Glass Transition Temperature (T_{rg})

While cooling a liquid from the molten phase, the division of the glass transition temperature, (T_g) to the liquidus temperature (T_l), is a good indicator of the GFA of the alloy. The alloy which has higher T_g and lower T_l will have easy glass formation.

$$T_{rg} = \frac{T_g}{T_l} \qquad (2.3)$$

Turnbull suggested that the ratio which is larger than 2/3 provides retention of the homogeneous nucleation. However, even if this ratio is not attained successfully, $T_{rg} \approx 0.50$ is a sufficient value for the glassy phase formation. The other critical process in the glass formation is to exceed the critical cooling rate. However, achieving separate successful results from both criteria is not sufficient because, if the solidification carried out at slower rate than the critical cooling rate, there will be no glass formation in the system, even if it has high T_{rg} [1].

2.2.2. Supercooled Liquid Region (ΔT_x)

Supercooled liquid region (ΔT_x) is roughly described as the interjacent region of the T_g and the T_x by Inoue. If this region can be designed to be broader, the glassy phase will be more stable and it will not have enough driving force to crystallization step, and it will be relatively easy to locate the T_g. Moreover, as stated by Inoue, the alloy with wide ΔT_x will have lower critical cooling rate. However, some other studies showed that this prediction is not completely correct for all materials, e.g. Pd-based metallic glasses. In reality, we cannot easily locate the T_g in every large ΔT_x condition.

$$\Delta T_x = T_x - T_g \qquad (2.4)$$

2.2.3. The γ and γ_m Parameters

Besides the general knowledge for glass formation, Lu and Liu [26] claim that the glass formation is not carried out in only one aspect. It involves the prevention of the liquid phase stability and the resistance to crystallization. To cover these two aspects, a new parameter, γ, was developed [1]. According to thermodynamic stability, by lowering T_l higher the stability can be obtained in the liquid phase. Moreover, by T_g calculation, some predictions related to crystallization resistance can be carried out. Combination of these two views give us:

$$\gamma = \frac{T_x}{T_g + T_l} \qquad (2.5)$$

Then, this criterion had been improved by adding the supercooled stability term because, hereinbefore, the wider the ΔT_x the more stable liquid is. So, the parameter was expanded as:

$$\gamma_m = \frac{2T_x - T_g}{T_l} \qquad (2.6)$$

2.2.4. The α and β Parameters

After the invention of γ and γ_m parameters, Mondal and Murty [27], suggested α parameter that defines the stability of the amorphous phase information. α parameter can be expressed as the stability of the liquid in the scope of the liquidus temperature.

$$\alpha = \frac{T_x}{T_l} \qquad (2.7)$$

If we take the T_{rg} parameter into consideration, β parameter can be driven from the equation:

$$\beta = \frac{T_x}{T_g} + \frac{T_g}{T_l} = 1 + \alpha \qquad (2.8)$$

2.2.5. The ω Parameter

Another GFA parameter is ω and it defines the average T_n temperature,

$$T_n = \frac{T_g + T_l}{2} \qquad (2.9)$$

which is the temperature at the nose of the C-curve. With lower T_n, higher GFA could be obtained. [28]

$$\omega = \frac{T_g}{T_x} - \frac{2T_g}{T_g + T_l} \qquad (2.10)$$

2.2.6. Structures Model of BMG Systems

In the literature, the commonly used BMGs structures are classified into three types, which are, metal and metal-type alloys, metal with metalloid type alloys and the Pd-metalloid type which was shown in Figure 2.5[18].

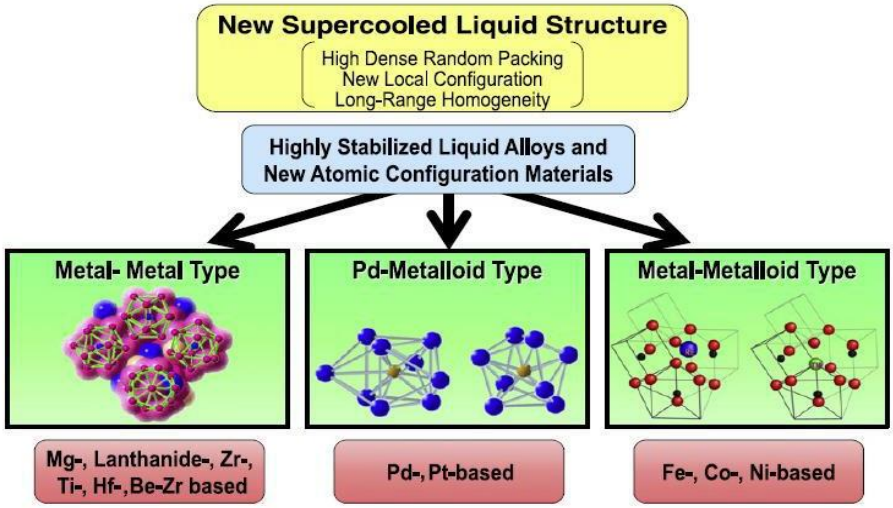

Figure 2.5. Supercooled liquid structurers [29]

The structure of liquids was uncertain for many years however, in 1959, "random dense packing model [30]" was defined for liquids. This model includes five Bernal polyhedrons which are shown in Figure 2.6.

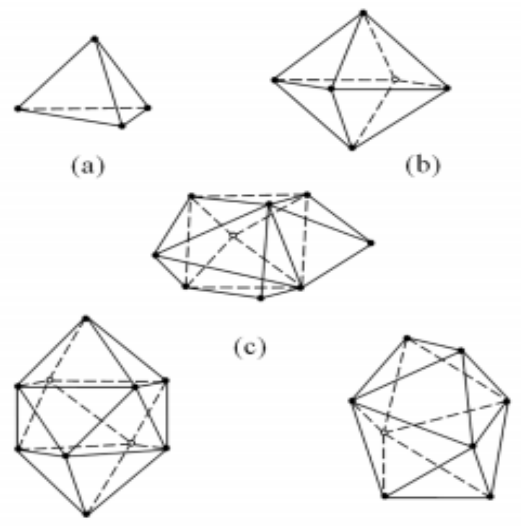

Figure 2.6. Five Bernal polyhedral: (a) tetrahedron, (b) octahedron; (c)trigonal prism capped with three half octahedral; (d) archimedean antiprism capped with two half octahedral; (e) tetragonal dodecahedron Bernal [30]

Due to maximum packing with 73%, tetrahedron might be considered as the most basic structure for liquid structures [30].

Table 2.1. The percentage of five Bernal polyhedrons[30]

Type	Number of Percentage	Volume Percentage
Tetrahedron	73%	48.4%
Octahedron	20.3%	26.9%
Trigonal prism capped with three half octahedral	3.2%	7.8%
Archimedean antiprism capped with two half octahedral	0.4%	2.1%
Tetragonal dodecahedron	3.1%	14.8%

These structural models bring together the features of randomness, short-range forces, and medium-range forces [31]. The disordered structure provides superior properties to the metallic glasses because atomic structure specifies the properties of the BMG systems.

2.3. Iron-Based Bulk Metallic Glasses

In the beginning stage of BMGs production, it was seen that the studies broadly focused on Zr and Pd based systems which have high material costs. However, among the BMG alloys, Fe-based BMGs have shown an attractive potential with their relatively low cost, good mechanical and physical properties including soft magnetic, relatively strong and satisfied corrosion resistance characteristics[32]. After having an understanding of significant engineering properties of iron-based glassy alloys, development of iron-based bulk metallic glasses (BMGs) with advanced glass forming ability attracted huge attention [33].

Iron-based BMGs usually include Boron, Carbon, and Phosphor as the principal metalloids. The Young's modules of binary and ternary Fe-metalloid glasses was reported nearly 3.3GPa [34]. Moreover, iron-based bulk glassy alloys show soft magnetic characteristic and high electrical resistivity.

The first iron-based BMG in the bulk form was synthesized with the Fe–Al–Ga–P–C–B alloy composition by Inoue and their team members in 1995 [35]. In Table 2.2 the previously investigated Fe-based BMGs were listed. These studies are a good example for the production requirements of the BMGs. As mentioned in the production requirements, all systems in Table 2.2 have at least 3 or more constituent elements to decrease in the high cooling rate requirement. As known from theoretical knowledge by adding more ingredient elements, the critical cooling rates of the systems could be reduced to ~10-10^2K/s [35].

Table 2.2. Previously investigated Fe-based BMG systems.

Fe- based BMG Systems	Year	References
Fe–(Ti,Zr,Hf,Nb,Ta)–B-Cu	1991	[36]
Fe-(Al, Ga)-(P, C, B, Si, Ge)	1995	[9]
Fe–(Nb,Mo)–(Al,Ga)–(P,B,Si)	1995	[9]
Fe–(Co,Cr,Mo)– (Ga,Sb) -(P,C,B)	1999	[37]
Fe–Ga–(P,C,B,Si)	2000	[37]
Fe–Nb-B-P	2001	[38]
Fe–Mn–Cr–Mo–C–B	2003	[37]
Fe–Cr–(Ln,Y)–Mo–C–B	2004	[37]
Fe-(Co,Cr,Mo)-(C,B)-Y	2005	[37]
Fe–(Cr,Mo)–(C,B)-Tm	2006	[39]
Fe-(Nb, Cr)-(P, B, Si)	2010	[40]

2.3.1. General Properties of Iron-Based Bulk Metallic Glasses

Metallic glasses are in amorphous form and they are not in the atomic order, they do not include any microstructural features. These unique characteristics provide them lots of extreme properties. Due to these unique characteristics, Fe-based systems are regarded as the most encouraging class of BMGs with thermal, physical and mechanical properties.

2.3.1.1. Magnetic Characterization of Fe-Based BMGs

After the production of ferromagnetic BMGs, their magnetic behavior also drew attention. In electrical and electronic industries, magnetic properties of materials have fundamental importance [35].

In the history, hard magnetic characteristics were first mentioned in the literature as annealing amorphous precursors [41-43]. After that, the soft magnetic behavior of Fe-based BMGs was developed by alloying them with Al, Ga, P, C, B, Si, Co-Ni, Zr, Nb, etc. Later, high saturation magnetization (mainly between 0.75 to 1.5T), low coercivity (generally between 100 to 1000 A/m), high magnetic permeability (usually between 900 to 1200) and soft magnetic characteristics emerged in related literature research [44-47]. According to the knowledge sources in material science, the soft magnetic characteristics of alloys are an outcome of the consolidation of the non-crystal structure with a small magneto crystalline anisotropy [32].

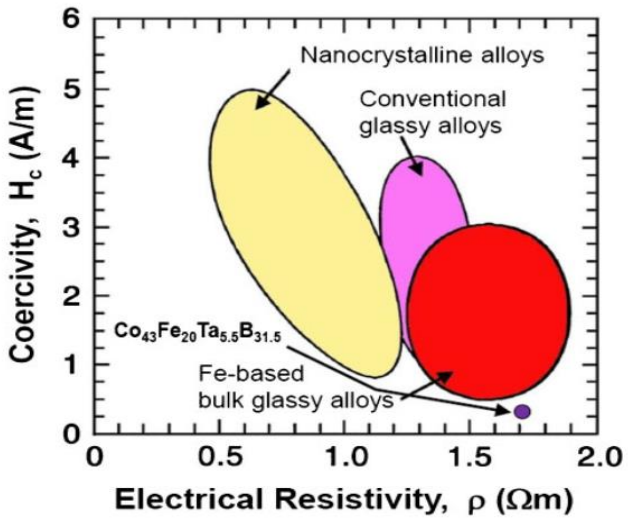

Figure 2.7. Representation of the coercivity and electrical resistivity relationship for iron-based glassy alloys [35]

And finally, non-ferromagnetic iron-based metallic glasses were introduced in the history of the BMGs. The fundamental factor for non-magnetic characteristic is correlated with Curie temperatures which is the magnetic transition temperatures. If their transition temperature is lower than the room temperature, they act as non-ferromagnetic [48]. The main reason of lower Curie temperature is the addition of alloying elements like Chromium and Manganese.

2.3.1.2. Mechanical Properties of Iron-Based BMGs

Another substantial feature of iron-based BMGs is their extreme mechanical properties. The BMGs are widely known for their very high strength and hardness compared to their crystalline counterparts. Because of these properties, Fe-based BMGs be an alternative for structural studies. According to fundamental knowledge in material science, materials should have some plasticity for structural applications. On the contrary, iron-based metallic glasses expose little or almost zero plasticity. To improve their plasticity there exists lots of studies since any potential improvement in plasticity would obviously increase the application and usage area of the Fe-based BMGs [35].

As illustrated in Figure 2.8, Fe-based BMGs exhibit highly satisfied fracture strengths between 2500 to 3000MPa that is 2.5-3 times higher than the conventional materials. Due to these encouraging results, there are lots of studies about the mechanical characterization of iron-based BMGs (Table 2.3).

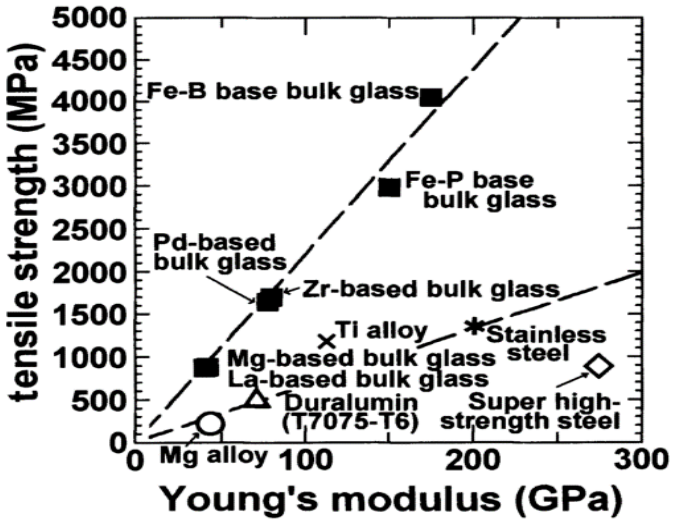

Figure 2.8. Representation of the variety fracture strength and Young's modulus for metallic glasses compare with other materials [16]

Table 2.3. Some critical mechanical properties of typical iron-based BMGs [49]

Alloy Compositions	σ_y (GPa)	σ_f (GPa)	ε_{pl}(%)	E(GPa)	υ
$Fe_{65}Mo_{14}C_{15}B_6$	3.40	3.80	0.60	195	0.334
$Fe_{59}Cr_6Mo_{14}C_{15}B_6$	3.80	4.40	0.80	204	0.317
$Fe_{49}Cr_{15}Mo_{14}C_{15}B_6Er_1$	3.75	4.14	0.25	220	0.320
$Fe_{66}Mo_{10}P_{12}C_{10}B_2$	2.55	3.25	1.17	176	0.330
$Fe_{65}Cr_2Mo_9P_{10}C_8B_6$	2.90	3.55	1.00	177	0.330
$Fe_{49}Cr_{15}Mo_{14}C_{13}B_8Er_1$	3.90	4.04	0.10	220	0.320

Compared with other mechanical characteristics, iron-based BMGs also have promising hardness values. As indicated in Figure 2.9, hardness values of Fe-based BMGs changes between 900 to 1300HV which are much higher than conventional steels and stainless steels.

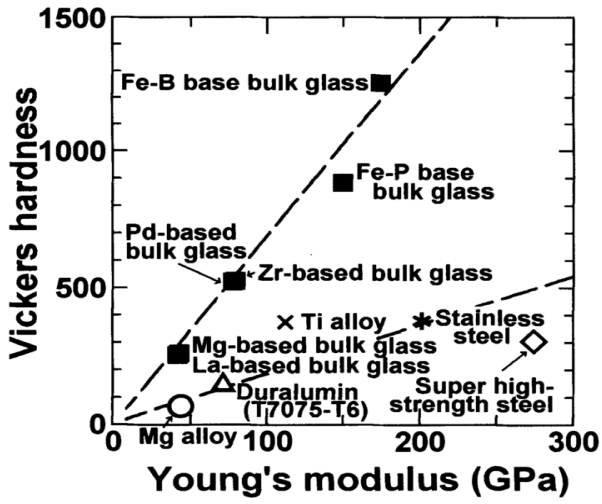

Figure 2.9. Representation of the Vickers hardness of metallic glasses and conventional materials with respect to Young's modulus [16]

2.3.1.3. Thermal Characteristics of Iron-Based BMGs

Metallic glasses reach meta-stable equilibrium at low temperatures and they are diversified from crystalline solids with heating process. They show deviant thermal properties such as structural relaxation and glass transition behaviors. In reality, the glass transition does not take place at a confidential temperature, it requires a temperature separation. However, in literature, an individual temperature is preferred for definition, that is the midpoint of the temperature range. For characterization of thermal properties differential scanning calorimetry (DSC) is commonly used [50]. Thermal parameters of BMGs include glass transition temperature (T_g), crystallization temperature (T_x), supercooled liquid region (ΔT_x) and liquidus temperature (T_l). To attain thermal stability in BMGs, T_g and ΔT_x values are taken into consideration. In the production stage of BMGs, high T_g and, wider ΔT_x cause losing the amorphous characteristic at exalted temperatures so, the supercooled liquid is balanced in the system. Table 2.4 shows thermal characteristics of the iron-based BMGs systems in the theoretical studies.

Table 2.4. Thermal characteristics of the iron-based BMGs in the theoretical studies [7]

Alloy Compositions	T_g (K)	T_x (K)	ΔT_x (K)	References
$Fe_{76}Sm_4B_{20}$	805	824	19	[51]
$Fe_{52}Co_{10}Nb_8B_{30}$	907	994	87	[52]
$Fe_{43}Cr_{16}Mo_{16}C_{10}P_{15}$	880	910	30	[53]
$Fe_{50}Cr_{15}Mo_{14}C_{15}B_6$	839	874	45	[34]
$Fe_{61}Cr_6Mo_{14}C_{15}B_6$	806	858	52	[34]
$Fe_{48}Cr_{15}Mo_{14}Y_2$	839	886	47	[54]

From literature point of view, the T_g of iron-based BMGs vary from 500 to 950K with a supercooled liquid region between 20 and 160 K. Wider supercooled liquid region allows to the production of different shapes of materials. Moreover, there is a relation between GFA and T_g so, higher T_g represents higher GFA (section 2.4) and this leads to smaller cooling rate. The reduction in critical cooling rates means easier, cheaper and more conventional production methods for metallic glasses so, the chance of adaption to the industry will be easier which is the main goal of this study.

2.3.1.4. Corrosion Characteristics of Iron-Based BMGs

According to literature reviews good corrosion resistance is based on:

- Premeditating a chemically uniform and flawless microstructure [55]
- Premeditating an alloy that have rare-earth element or transition metals in the substantial form [55]

Metallic glasses do not comprise metallurgical features. In the crystalline structures, corrosion activities are mostly preferred to these features; which leads to worse corrosion resistance. From literature, even though Zr-based bulk metallic alloys provide good corrosion resistance in H_2SO_4 and NaCl solutions, they do not have corrosion resistant in aggressive HCl solutions and in this study same solution was used as a corrosion environment in order to see the differences [56].

The potential of Fe-metalloid alloys was increased after addition of chromium which has high corrosion resistance. In 1974, studies showed that amorphous iron-metalloids with enough amount of chromium exhibit high corrosion resistance [55]. After that point, it turns out that chromium has a huge influence and this can be improved with Mo addition [35].

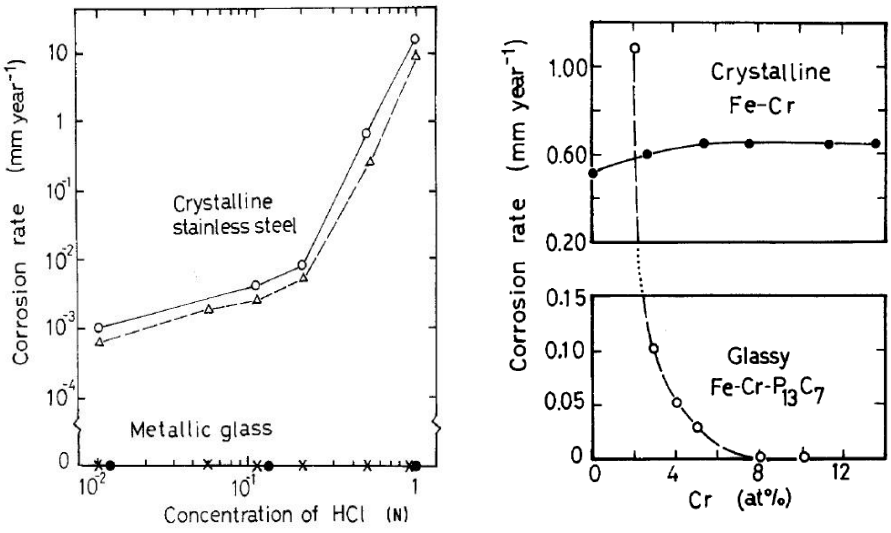

Figure 2.10. Comparison of corrosion conduct of amorphous and crystalline systems a) HCl solution b) NaCl solution [57]

Figure 2.10 represents the conduct of amorphous and crystalline systems in the diversified extreme environmental conditions. So, it is evident that amorphous system has very good performance than crystalline system in the in the aggressive environments [57].

2.4. Iron-based Bulk Amorphous Steels

Although metallic glasses provide unique characterizations, BASs also have the specific soft magnetic properties. Moreover, like BMGs, they provide desired corrosion resistance, good fracture strength, and high T_g. Thus, they could be a part of the industry and evaluated in various applications with these specific characteristics.

2.4.1. Properties of BASs

Fe-based bulk amorphous steels have lower glass forming ability than Pd and Cu-based BMGs. However, as we know, by adding constituent, GFAs could be increased. Because of various pure and rare constituent elements, the costs of BASs are high to use commercially. However, by applying cooling rate improvement to BASs that have high GFA, they might be used in conventional industrial implementations.

2.4.2. Effects of Alloying Elements

While making a new metallic material, addition of extra element and preparation of a new alloy have been always applied as a metallurgical technique.The influence of the additions on the glass formation can be examined according to thermodynamic and kinetic point of view. In the thermodynamic examination, the undertaking parameters are the supercooled liquid region (ΔT) and the liquidus temperature T_l that represent the thermal stability characteristic of the liquid phase. According to common knowledge, large ΔT indicates higher crystallization resistance and initiates to a high GFA for many of the BMGs [58]. While deciding on the design of the bulk amorphous steels, the effects of alloying elements should be taken into consideration. The results of the elemental additions can be summarized as below:

- While alloying of Zr, Fe, Ti and rare earth elements with metalloids like C, B, and Si large negative heats of mixing are achieved which improves the GFA of the alloys.

- The minor alloying elements destabilize the competing crystalline phase and some alloying elements, such as Y or Gd, may also act as oxygen holder which induce to the demolition of heterogeneous nucleation and improvement in the GFA [59]. However, there should be some limitations while adding the alloying

elements. For example, the amount of Y is commendable in between 1at. % and 5at. %, in which range, the liquid stabilization can be achieved [5, 60].

- The Yttrium has important role while justify the composition of the BMGs closer to a the eutectic point [58].

- According to common knowledge, high T_g leads to higher temperature resistance and better GFA. By interpolation of the refractory materials (Zr, Nb, Mo), higher T_g can be obtained as a result of viscosity increase.

- Hereinbefore, amorphous steels are soft magnetic so, the influence of the alloying elements on magnetic properties must be reviewed during preparation of BAS systems. Because of the soft magnetic properties of Ni, it could be used to build systems with perfectly soft magnetic characteristics. Moreover, Cr and Mn are classified as diamagnetic elements, and hence they have a nonplusing effect on ferromagnetic characteristic.

- For the Young's modulus (E) improvement of BASs, refractory metals should be taken into consideration [4]. Due to chemical bonding approach between Fe and B, when B atoms are added to the structure, fracture strength of the BAS alloys increase.

- Corrosion resistance is an important property of amorphous steels and corrosion resistance is being improved by the supplementation of Cr and Mo. However, excessive amount of Mo supplementation prevents the dissolution of Cr during passivation.

- According to research and experimental data in NOVALAB [6, 61], Fe-Mo system shows more negative heat of mixing, and relatively lower critical cooling rate values that provide desired and high glass forming ability.

2.4.3. Production Methods of Bulk Amorphous Steels

2.4.3.1. Arc Melting with Suction Casting

Most frequently used method of synthesizing BMGs is arc melting with suction casting method. The designed alloy composition is melted with arc melting from under argon atmosphere and during the experimental procedure, the melted alloy mixture was re-melted multiple times to obtain preferable homogeneity. When the homogeneous mixture is obtained, molten alloy suck into water-cooled copper mold by the help of the non-equal pressure between the melting and the casting chambers. While alloy designing, the possibility of the high melting points difference between the elements, the arc-melting technique is mostly preferred. The most accustomed and simple design of the casting mold is in the a cylindrical or rod-shaped form about 3 mm in diameter and 15 cm in length. [1].

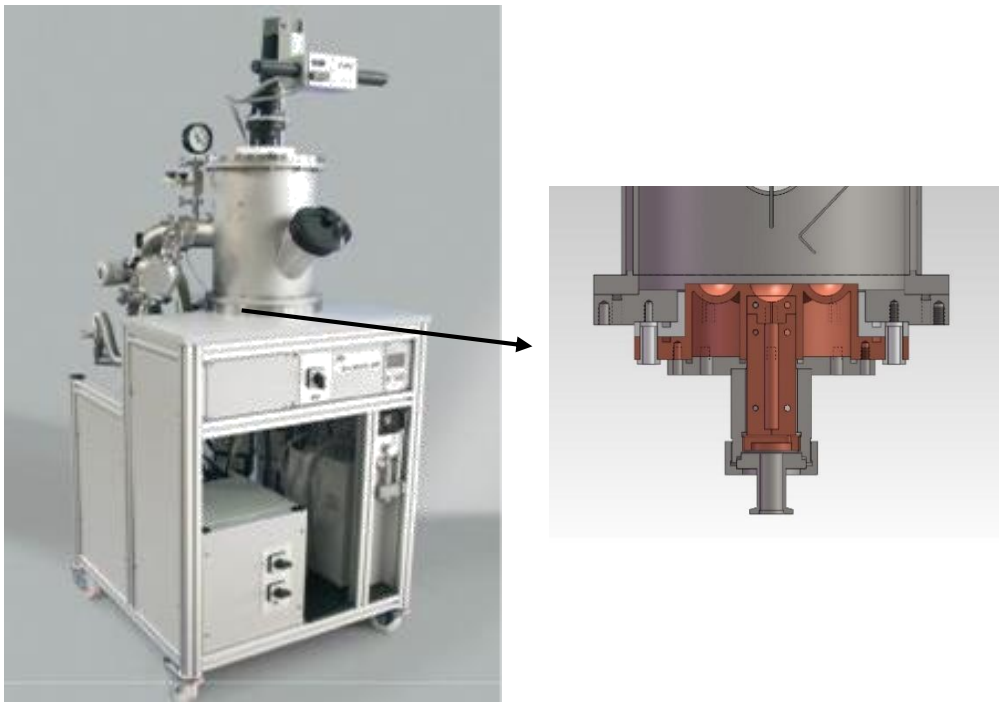

Figure 2.11. Edmund Bühler Arc melting with suction casting device

2.5. Potential Applications of BAS

After the successful production of the BAS, the next step is the adaption of the BASs to their potential applications. The application range is determined based on their unique characteristics. The advantages and disadvantages of the properties were listed as;

Table 2.5. Properties of Metallic Glasses related to applications [11]

Properties	Advantages	Disadvantages
General	• Featureless microstructural such as grain and phase boundaries	• Relatively high cost of components and processing
Mechanical	• High hardness, implicitly giving good wear and abrasion resistance • Good yield strength • High specific strength • Low mechanical damping	• Can be show brittle property by annealing • Low fracture toughness Kc • Small production size (d<1mm) leads to embrittlement of the larger components
Electrical and magnetic	• High magnetic permeability • Good Resistivity with almost independent of temperature	• Under the oscillation, there will be energy loss due to the magnetostriction
Chemical	• Good corrosion resistance, implicitly lack of grain structure • Biocompatible fortune	• (Zr, Ti) -based compositions are sensitive to oxygen, which causes to crystallization and embrittlement

2.5.1. Surface Treatment Applications

In the industry, carbon steels are the most preferred material in the design and the manufacturing of metallic parts is the result of easy machining ability, good weldability, relatively low cost and validity. However, because of their chemical characteristics, under highhanded environments they can easily form oxides, since they have low chemical resistance. Because of the low chemical durability, the surface protection is a feebleness implementation for carbon steels [62]. Due to these reasons, BASs were selected in order to use in surface treatment application with their supportive properties.

There are lots of industrial coating & surface treatment applications which are thermal spray, cold spray, high pressure and so on. Most frequently preferred methods for amorphous material coatings are laser and thermal spray techniques. The studied coating technique in this thesis was obtained with the favor of depositing the amorphous sample on the substrate which was melted by welding. After that, by applying re-cooling application the hardened layer was converted to amorphous structure. While processing, amorphous alloy was treating by energy input so, it might result in surfaces which consist of crystalline phases embedded in amorphous matrix or it might be fully amorphous depending on the procedure parameters. Beside the laser based and thermal spray based methods, more conventional methods can also be used during coating applications like hardfacing process [8]. During the historical development of the hardfacing studies, lots of different materials and welding processes has been studied and the importance of this surface treatment application has significantly increased after the year 1999. Parallel to the industrial demand, the number of the hardfacing studies has slightly increased and today these studies are still a hot topic among all the other surface treatment applications. Surface modification techniques are preferred to obtain better service life for components and hardfacing is one of such techniques, which is applied by welding, to enhance surface characteristics. Nearly all industrial components face the problem of wear and the worn components either have to be rebuilt or rejected. By applying hardfacing, the enhancement of the surface

hardness and wear resistant layers can be achieved. Moreover, “it does not only help in resisting to wear, but also helps to prohibit corrosion and high temperature oxidation [63] ”.

Advantages of Hardfacing

- **Reduces downtime:** Extended service life cycle means minimum number of replacement in the components. Hardfacing decreases the downtime and less shutdowns are needed while replacing of the components.
- **Any steel material:** For hardfacing processes, any steel material can be used according to welding processes.
- **Desired property:** According to desired properties like hardness, wear resistance, a special base material can be designed by using different alloying elements.
- **Longer service life:** Hardfacing provides longer service life with fewer replacements of parts.
- **Better productivity:** Better wear life means increase in the productivity and profits [64].

Table 2.6. Previously investigated Hardfacing Studies [65]

Author	Year	Material & Method
Jha A. K., & Parsad B. K.	1999	Iron Based Material
Kumar S., & Mondal D. P.	2000	Fe-Cr Material
Fernández J. E., Vijande R., Tucho	2001	Cast Iron Alloy
Chatterjee S., & Pal T. K.	2006	Preheating / Without preheating and Single/Double Layer
Choteborsky R., & Hrabe P.	2008	Fe-Cr-C and GMAW Process
Balasubramanian V., & Varahamoorthy R.	2009	Steel & SMAW, MIG, TIG, SAW and PTAW Processes
Coronado J. J, & Caicedo H. F.	2009	ASTM A36 carbon steel plates and FCAW & SMAW processes

2.5.1.1. Laser Processing for Amorphous Coatings Applications

In the application steps of the processing, a suitable beam that has supernal intensity is inflicted on the sample and the electrons affect the atoms in the lattice. The advantage of laser processing is the chance of the high cooling application rates (which is higher than10^{3}°C/s). However, there are still some difficulties which are listed below:

- Rarefaction from the system results with alteration in composition which reduces the glass forming ability [8]
- Irregular thermal data might be faced during laser processing [8]

2.5.1.2. Thermal Spray Processing of Amorphous Coatings

Application of thermal spray has a wide range of material possibility which might be metallic, ceramic, cermet, and polymers. In this process, material can be used in three-different forms which are powder, wire, and rod. The molten state material is expedited with high speed and interacted with the material substrate to form a coating. The commonly preferred thermal spay processes which are specific for metallic glass surface treatment applications are high velocity oxy fuel (HVOF) and plasma spray processes which provides high cooling rates and this is a substantial presupposition for preservation of the amorphous feature on the surface [8].

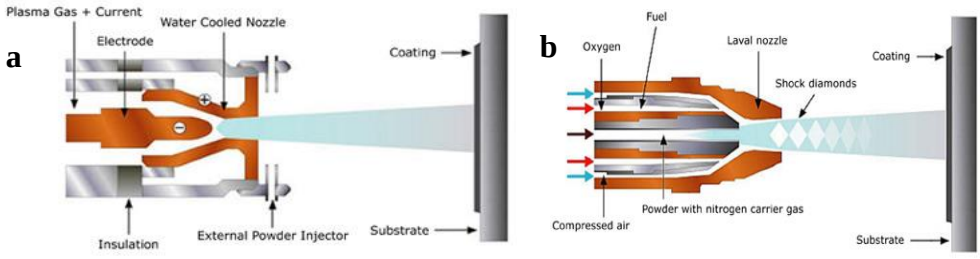

Figure 2.12. Schematic representation of a) plasma spray and b) high velocity oxy fuel (HVOF) processes [66]

2.5.1.3. Hardfacing by Welding

Hardfacing was first developed and patented by J. W. Spencer in 1896 using welding. Like lots of other processes, it was not developed for the industry for a long time. S. Z. Ferranti published a new patent in 1919 that includes cobalt nickel alloys for steam valves protection. Then, hardfacing alloys have started to be used in oil well drilling for the facing of the cutting edges of the rotary drills in 1922. The success of this application has brought big demand for the hardfacing rod. The development of this application has come into life in United States due to the lack of oil wells in Great Britain.[67].

"Hardfacing is an application which is applied by welding, spraying, or allied welding processes to decrease wear or destruction of a material under different sorts of service conditions [68]" and it can be defined as "the deposition of a special alloy material on a metallic part, by various welding processes, to obtain more desirable wear properties and/or dimensions [69]. "

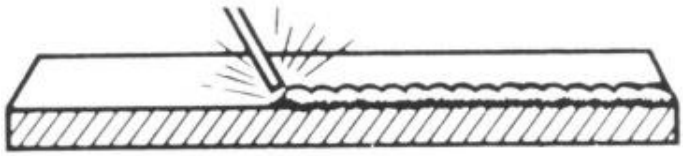

Figure 2.13. Schematic representation of the Hardfacing Process [68]

The main purpose of the hardfacing applications is to obtain an enduring surface layer to a substrate metal to improve the properties like impact & wear resistance ability, contact surface stress, erosion and corrosion resistance or any integration of these factors. It is reported that 50-60% of machine elements are worn due to erosive and abrasive wear. To improve the service life of the components, the alloys should have some desired properties**,** which are very good hardness, demanded abrasion resistance /tribological properties, specific corrosion resistance and heat resistance. If the materials face with the wear problem, their related properties can be improved by applying a hardfacing onto a cheaper base material. Hence, by

supplying inexpensive, easy machining metals with the desired specific properties, the usage of coatings will be extremely attractive [70].

The main scope of the this surface treatment application is for the materials, which requires surface protection to minimize the downtimes and to minimize the replacement cost of expensive parts [71].

Hardfacing with welding applications are favored for applications in which thickness of the coating is essential (due to deposition rates). Welding forms most usually utilize the covering material in the form of rod or wire [65].

Hardfacing coatings come with big advantages when they are compared with other coating systems. The metallurgical bond of the substrate weld is not easily influenced by spallation and is free of porosity. Welded deposits can be applied in high thickness on surfacing alloys. The thickness is greater than most of the other techniques (3 to 10 mm). Most importantly, iron-based hardfacing alloys provide a wide range of desirable properties including low cost [72].

The main reasons to perform hardfacing applications can be summarized as;

- Reduce costs – saving usually 20 - 70% of the cost by avoiding replacement
- Maintain equipment life - extending life 40 – 400 times,
- Drop the downtime – the longer life time, the fewer shutdowns are required
- Reduce the stock of the parts - no need to keep back-up part [69].

There are basically two main usage areas of hardfacing process which are:

- To ameliorate the abraded /worn parts: Actually, there is not any known resolution for metal wear. So, after reaching the upper limit the useful life stage must be replaced.
- The conservation of the metal parts in the wild against the metallic loss: Hard facing surface provides better wear resistance than the original substrate material thus, the life cycle of the component can be increased [69].

“Hardfacing is the deposition of a special alloy material on a metallic part, by various welding processes, to obtain more desirable wear properties and/or dimensions [69]. ”

In the industrial applications, metallic glass have not been yet fully commercialized in surface modified/coating applications but, their encouraging wear and corrosion characteristics make these materials an alternative for structural applications [8].

2.6. Processes Used in Hardfacing

The decision of the most compatible welding process depends on:

- Type of work which is to be hard-faced
- Majority operation of the components,
- Base metal chemical composition,
- Dimension limit of the component,
- Within easy reach of the weld equipment,
- Description of repairable components,
- Number of the items to be hard-faced etc.

There are lots of methods for hardfacing application. A small part of those can be grouped as:

Hardfacing by Arc Welding (SMAW, Flux Cored Arc, Welding, SAW) [73]
Hardfacing by Gas Welding (Deposition by Oxy-Acetylene Gas Welding) [73]
Hardfacing by integration of Arc and Gas (TIG, Gas Metal Arc Welding) [73]
Powder Spraying – (Flame Spraying, High Velocity Oxy-Fuel Process, Electric Arc Spraying, Plasma Transferred Arc) [73]
Laser Hardfacing (Laser Cladding) [73]

2.6.1.1. Tungsten Inert Gas (TIG) Welding Application

Within the bounds of possibility, surface treatment technique was selected as hardfacing with welding application. In Tungsten Inert Gas (TIG), the heat input is produced by an electric arc that is hit between an inexhaustible tungsten electrode and the work piece to dissolve the metal and generate a molten welding pool. The filler metal is fed manually.

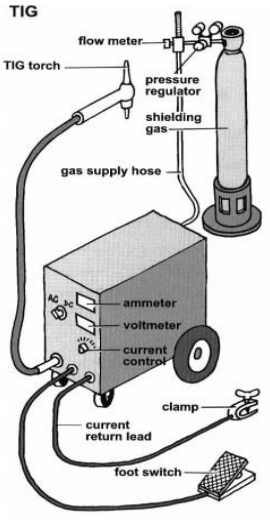

Figure 2.14. A typical TIG welding setup [69]

Predominantly, in arc welding processes, the arc is hit from an inexhaustible electrode to the work however, in TIG process due to using of the high melting point tungsten, there is no consumption in the electrode. During the welding process argon or helium is selected as the protective shielding gas. TIG welding can be carried out both AC & DC. For Al and Mg alloys AC is suggested and for stainless steel, Cu, Ti, Ni Alloys DC is suggested. [74].

TIG Welding has the advantages of concentrated heating of work piece, effective protection of the weld pool by an inert shielding gas, independency from filler material and no slag or spatter production after treatment which is good for welding thin with dissimilar and similar material. Gas Tungsten Arc Welding has some disadvantages. The disadvantages are more costly equipment, slower deposition rate and requirement for a skilled hand-eye coordinated operator [67].

CHAPTER 3

EXPERIMENTAL PROCEDURE FOR PRODUCTION AND SURFACE TREATMENT APPLICATION OF BULK AMORPHOUS STEEL

3.1. Production of Bulk Amorphous Steel

3.1.1. Crude Materials

For this study, BAS samples had been evolved by using scrap cast iron pieces. The weight percentages of the scrap cast iron are tabulated in the Table 3.1.

Table 3.1. The elements analysis of the scrap cast iron with weight percentages

Element	Wt.%	Element	Wt.%	Element	Wt.%
Fe	92.770	Co	0.016	Ti	0.016
C	4.330	As	0.005	V	0.016
Si	2.090	Zn	0.005	B	0.001
Mn	0.400	Zr	0.004	Ca	0.002
Cu	0.210	Mo	0.004	Sn	0.003
Ni	0.090	Pb	0.003	Al	0.003
Cr	0.060	S	0.059	P	0.050

The denoted scrap cast iron is named as “M” in the designed composition. To obtain BAS, scrap cast iron is alloyed by highly pure elements that are tabulated in in Table 3.2.

Table 3.2. The alloying elements with their purity grades

Element	Grade
Mo	99.95%
Y	99.90%
Mn	99.90%
Al	99.90%
Ti	99.80%
V	99.80%
B	99.50%
Cr	99.20%

In this thesis, studied alloy (**$M_{60}Cr_{13}Mo_{10}B_8Y_2Mn_7$)** was identified as the best composition in the previous studies for unique/superior and improved properties of bulk amorphous steels produced by scrap cast irons. The prepared compositions were selected according to the relevant GFA and the thermal stability requirement of the system beside the statistics.[75, 76]

3.1.2. Production of the Samples

The $M_{60}Cr_{13}Mo_{10}B_8Y_2Mn_7$ alloy was produced by arc melting machine under argon atmosphere. During the experimental procedure, elements were re-melted four-five times to enhance the homogeneous mixing. The Edmund Bühler Arc Melting device with water-cooled suction casting section was used during the production steps in this study. This cooling has arranged holes on it and it allowed to the synthetization of rod forms by suction casting. By applying rapid cooling, fully amorphous structure could be achieved by suction casting.

3.1.3. Arc Melting

To prepare designed compositions, Bühler arc melting which was using under argon atmosphere was utilized. Before each experimental study, by using special cleaning

solution, copper mold was cleaned to avoid any kind of contamination. Moreover, applying evacuation process with rotary and diffusion pump, oxygen in the arc melting chamber is minimized by applying argon flushing for at least 4-5 times. To obtain full homogeneity sample it was re-melted for four to five times.

3.1.3.1. Suction Casting

The suction casting is the rapid solidification part of the metallic glass production. The suction casting unit is adorned into Edmund Bühler device. To obtain fully homogenized alloy, arc melting process followed by suction casting operation. The archived final shapes of the specimens were 3 mm in diameter and fully 15 cm in length. For this study, by using arc welding and suction casting, rod form specimens were produced having 3-millimeter diameters size (Figure 3.1) which can be named as in bulk form.

Figure 3.1. The produced by suction casting

3.2. Hardfacing Application Procedure

Hardfacing, by definition, means a combination of different processes that weld the protective coating to the surface which is needed to be protected. This application is also known as weld overlay. Different from thermal spray processes, surface is needed to be melted from a physical, chemical and metallurgical interface in the hardfacing technique [77].

The melting temperature that is needed to weld materials in TIG welding might approach 2500°C in the presence of an inert gas [argon, helium, or a mixture of helium and argon] which protects from atmospheric contamination. The welding temperature occurs by an arc between a tungsten alloy electrode and the work piece. This arc burns between a gas-backed tungsten electrode and the work piece within a hardfacing process. Then the arc melts the base metal and the wire or rod-shaped weld filler material. There develops a fusion welded joint between base metal and surfacing bead. Hardfacing material is in rod form for manual welding process. The benefits of TIG process are good control of welding arc and simple manual operation [77].

Amorphous steels could be used in industrial coating/surface treatment application due to their high hardness values. There are lots of processes for surface treatments, but within the bounds of possibilities for this study, hardfacing applications were preferred.

3.3. Hardfacing Application of Iron Based Bulk Amorphous Steel

According to published reports and performed experiments, iron-based bulk metallic glasses display very high hardness, Young's modulus, wear and corrosion resistance due to absence of crystallographic defects in the microstructure such as grain boundaries and dislocations. During this study an amorphous coating application was carried out with $M_{60}Cr_{13}Mo_{10}B_8Y_2Mn_7$ bulk amorphous steel onto S275 carbon steel substrate (70x50x15 mm) via TIG welding processing. For hardfacing application Tungsten Inert Gas (TIG) welding also known as GTA (Gas Tungsten Arc) in the USA and WIG (Wolfram Inert Gas) in Germany, was favored because it can be used with different types of materials, like, steels, titanium and aluminum alloys etc. The produced bulk metallic glass ($M_{60}Cr_{13}Mo_{10}B_8Y_2Mn_7$) was used as a filler material in TIG welding process.

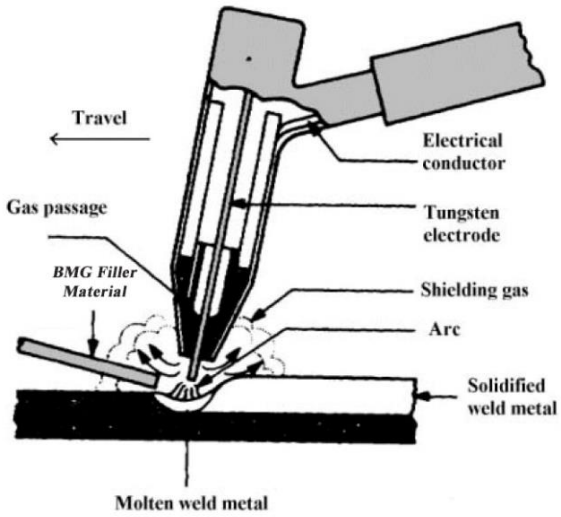

Figure 3.2. Schematic representation of TIG welding process [78]

3.4. Characterization Techniques

To determine the structure of the samples, various characterization techniques were operated, which are microstructural evolution, thermal characteristics and mechanical characteristic of the BAS samples.

3.4.1. X-Ray Diffractometer

To analyze the amorphous structure, samples were examined by X-Ray Diffraction (XRD) analysis by Bruker S8 Tiger Diffractometer. During the structure analysis by applying monochromatic Cu K_α, diffraction angle (2θ) in the range of 5-110° and the scanning rate of 1°/min were selected as diffraction analysis parameters. According to obtained XRD data, qualitative phase analyses of the samples were performed.

3.4.2. Microstructural Characterization

During microstructural characterizations, the designed samples were investigated with FESEM/FEI NOVA NANO430 scanning electron microscope (SEM) which

was supported with energy dispersive spectroscopy (EDS). The main purpose of EDS is to identify the composition the present phases in the microstructure.

The preparation of samples for microstructure investigation include bakelite mounting, grinding with grinding papers and polishing with diamond polisher. Moreover, for microstructural examination, polished samples were etched with Marble solution, containing 10gr $CuSO_4$, 50ml HCl and 50ml water in the solution. The main reason for choosing this strong etchant was the resistance behavior of the samples against to corrosive environments.

3.4.3. Thermal Characterization with Differential Scanning Calorimetry

Thermal behavior is a characteristic feature for the BASs. During the investigation of the thermal behavior, some critical thermal parameters had to be identified. These parameters can be summarized as; glass transition temperature (T_g), crystallization temperature (T_x) and melting temperature (T_m). During investigation of these parameters, studies were carried out with SETSYS-16/18 high temperature differential scanning calorimeter (DSC). Experiments were conducted with a heating and a cooling rate of 40K/min under constant argon gas flow in a temperature range between 296-1673K. In this analysis, 5-10 mg of sample was used. In the calibration process, the reason of using board range of temperatures and scanning rates is related to inclusion of high purity elements.

3.4.4. Magnetic Characterization with Vibrating Sample Magnetometry

The magnetic characterization of the samples can be measured via using Vibrating Sample Magnetometer (VSM) as a function of applied field. During these experiments samples are vibrated towards the up and down directions in the enclosed coli region[10]. For this thesis, determination of magnetic characteristic experiment was conducted with ADE Magnetics EV9 Vibrating Sample Magnetometer (VSM). In the implementation part, magnetic field was applied up to 1.8KOe at the room temperature and the related data was recorded for understanding the magnetic characterizations.

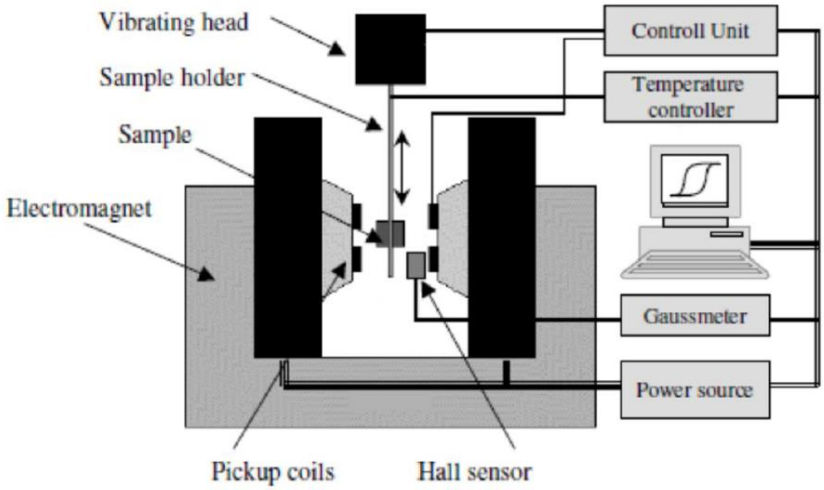

Figure 3.3. The vibrating sample magnetometer (VSM) [10]

3.4.5. Micro-Hardness Measurements

Vickers micro-hardness measurements of all produced samples were performed by an automated micro-hardness tester Shimadzu-2 Micro-hardness Tester by applying 1kgf load. The reported averages of micro-hardness values were the sum of minimum six measurements from the surface of the specimens.

3.4.6. Corrosion Resistant Implementations

By applying extreme corrosive environment, corrosion resistances of BASs samples were measured. Five different samples, which are bulk amorphous steel, pig iron, carbon steel (S275), titanium (pure) and stainless steel (304) and three different corrosive solutions were prepared. Five different samples were subordinated to these solutions throughout 80 and 120 days which were tested in the identical testing apparatus.

The chosen-up solutions were:

i. An acidic solution with 1.12 pH which is 0.5M H_2SO_4,
ii. A basic solution with 14 pH which is, 1M NaOH,
iii. A salt solution with 7 pH which is 0.6M NaCl.

The calculations were carried out according to measurement of the weight loss for per area. Before the experiment, the primary weight and primary surface areas of the samples were measured and in interval of five days, weight and surface area changes were persuaded.

3.4.7. Wear and Tribological Properties

In the case of harder particle participation onto the metallic surface, abrasive wear case becomes relevant for this surface. Rather than using more expensive material for achieving good wear resistance, improving surface characteristic of a cheaper material will be more sufficient. Hence, wear resistant coating will be extremely attractive. "While carrying out the hardfacing material designing steps, niobium, titanium, molybdenum, boron and carbon should be in consideration due to their encoring mechanical, thermal, magnetic and physical properties [70]." Moreover, due to their capability of carbide formation chromium are mostly used in the hardfacing implementations. To improve the service life of the materials, hardfacing alloy should have some specific properties which are listed below [68]:

- Hardness,
- Abrasion resistance,
- Tribological properties,
- Corrosion resistance,
- Heat resistance.

For understanding the tribological properties, CMS+ Instruments Pin-on-Disc testing machine was used. "The pin-on-disc test can be described as a model test that includes a stable ball slippery against a revolving disc during friction force is permanently measured, see Figure 3.4. [64] ."

During the experiment, to create the wear, a sample is fixed on a turning stage. The perpendicular force is applied on a zirconia ball, that is contacted with the sample

surface. The pin-on-disk test is usually used during determination of the tribological properties of the materials with the friction coefficient (COF) output. At the end of the experiment, volume loss of the sample enables wear rate calculation.

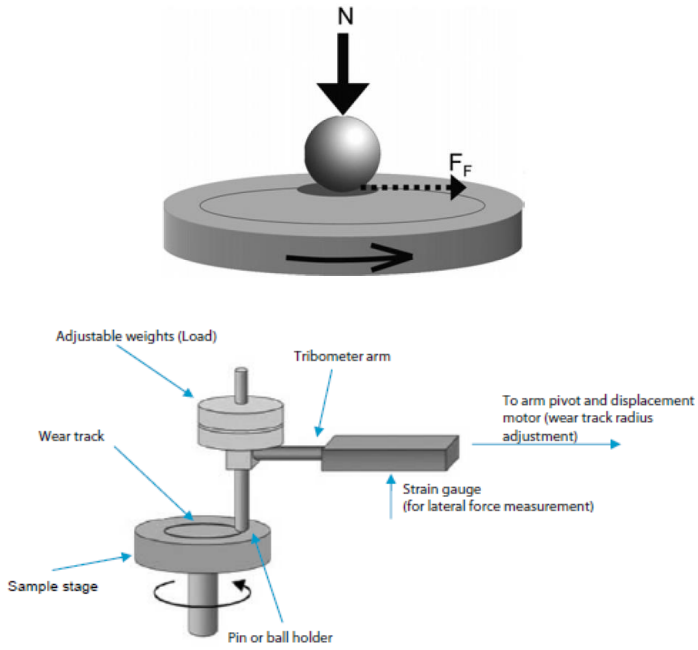

Figure 3.4. Schematic image of the ball-on-disc set up, N is the applied normal force and F_F is the measured friction force.[64] [79]

To gain insight about wear/abrasion properties of hard-faced layer which was prepared by using BAS, tribological test was carried out under computer controlled pin-on-disk tribometer (TRB, CSM+ Instruments, Switzerland) in the Photocatalytic Materials Laboratory (E103). A normal load of 7 N with 100 Hz rate was applied at room temperature using parameters stated in Table 3.3 and during the tribological tests ASTM G99-17 standard was followed as a reference document.

Table 3.3. Pin- on disk tribometer test parameters

Testing Parameter	Test Conditions
Ball Material	High purity zirconia
Ball Radius	3 mm
Tested Material	Fe-based Bulk Metallic Glass after Hardfacing application
Applied Load	7 N
Sliding Speed	5 cm/s
Application Rate	100 Hz
Sliding Distance	158 m
Testing Environment	Ambient atmosphere
Testing Temperature	Room temperature

CHAPTER 4

RESULTS AND DISCUSSIONS

4.1.Production of Bulk Amorphous Steel

Recent studies and investigations have related with synthesizing and developing new materials and/or the enhancement of the characteristics and performance of existing materials. The rapid development of technology and demands in the future have constituted attention on improved materials that have higher hardness and those materials that could be used in more aggressive environments.

In the initial part of this study, the impulsion point was the re-production of economical BASs from scrap cast iron which was synthesized and developed according to previous simulation and experimental studies in NOVALAB.

4.1.1. Near Equilibrium Solidification and Microstructural Investigation

The equilibrium structure is related with liquid and the crystal's stability. Due to the complex crystal structure of the amorphous phase, a heat treatment operation was applied to obtain equilibrium structure and evaluate the glass forming ability and microstructural characterization of the sample. The sample was heated up to 1700K to obtain liquefied structure and it was slowly cooled. The first examination will be related with the glass forming ability of the sample and GFA parameters was calculated according the DSC results.

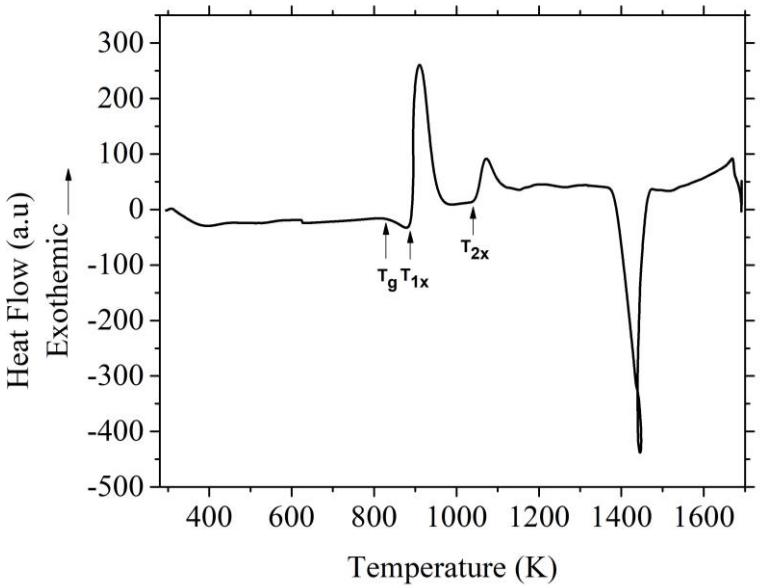

Figure 4.1. DSC analysis of the $M_{60}Cr_{13}Mo_{10}B_8Y_2Mn_7$ alloy

Table 4.1. Critical temperatures for $M_{60}Cr_{13}Mo_{10}B_8Y_2Mn_7$ alloy

T_g (K)	T_{1x} (K)	T_{2x} (K)	T_l (K)	ΔT_x (K)
861	898	1079	1487	37

Table 4.2. GFA parameters of $M_{60}Cr_{13}Mo_{10}B_8Y_2Mn_7$ alloy

T_{rg}	γ	γ_m	α	β	ω
0.579	0.382	0.629	0.604	1.604	0.225

According to previous studies on iron based amorphous steel, T_g values differ between ~780-830K with ΔT_x ~55-75K[80]. Moreover, $T_{rg} \approx 0.50$ is a sufficient value for the glassy phase formation. These results show that, re-produced sample has high glass forming ability and it could form amorphous structure during rapid solidification.

The second examination is related to the identification of the stable phases. The slowly cooled samples were exposed to XRD to detect the present phases in the system and Figure 4.2 shows the XRD data.

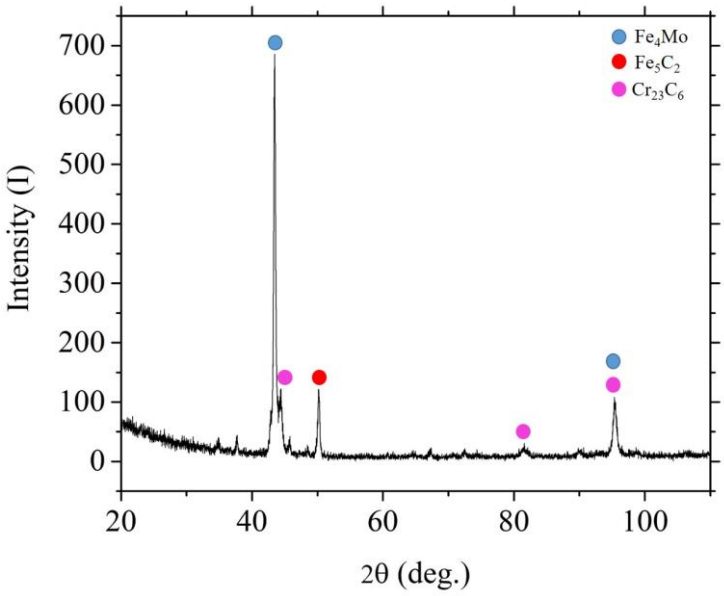

Figure 4.2. XRD diffractogram of near equilibrium $M_{60}Cr_{13}Mo_{10}B_8Y_2Mn_7$ alloy

Due to the lots of constituent element and the complex phases, present phases in the diffractogram could not be clearly identified and not be labeled. However, some candidate phases could be specified which were Fe_4Mo, Fe_5C_2 and $Cr_{23}C_6$. The XRD pattern was led to the investigation of the microstructure with SEM and for determination of the phases, EDS were applied.

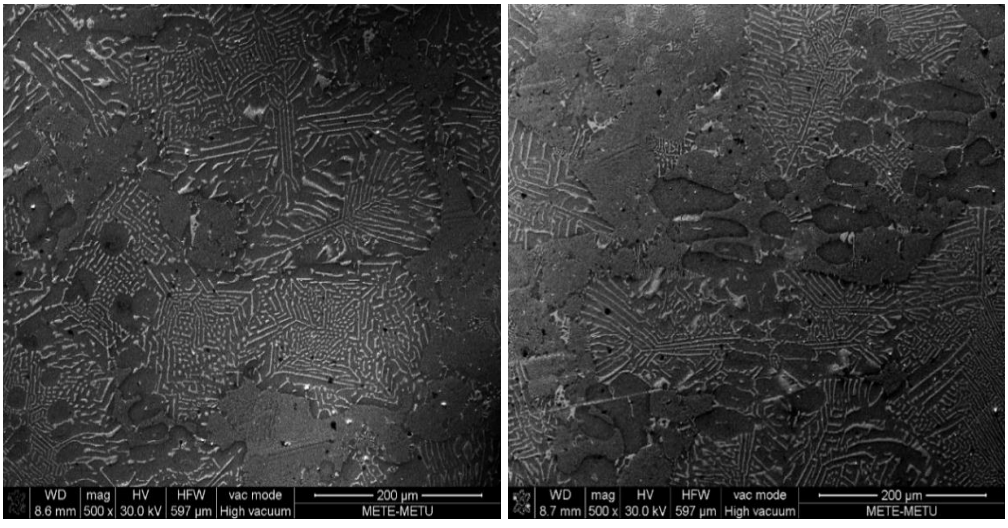

Figure 4.3. Microstructural investigation of near equilibrium ($M_{60}Cr_{13}Mo_{10}B_8Y_2Mn_7$) alloy with SEM

The microstructure of heat treated $M_{60}Cr_{13}Mo_{10}B_8Y_2Mn_7$ alloy shows a eutectic phase mixture which is clearly seen from Figure 4.3 with two phase mixtures. These phases could not be identified clearly; however, EDS scans showed that there are two dominant areas which are Fe-Cr rich and Mo rich areas. In Figure 4.3, the darker areas include higher Fe-Cr, while the lighter zones containes higher Mo content.

The difference in the microstructure also affects the hardness. The hardness of samples was illustrated in Figure 4.4, it was in the range of 500-600 HV.

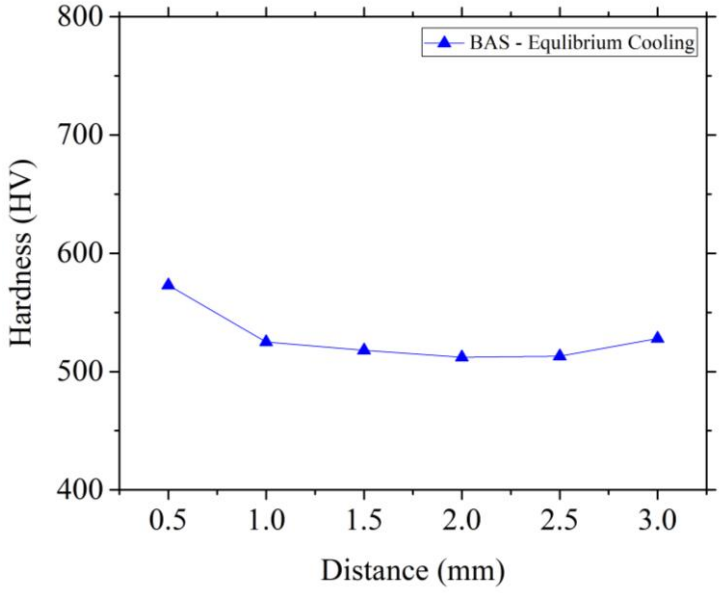

Figure 4.4. Hardness results of the near equilibrium ($M_{60}Cr_{13}Mo_{10}B_8Y_2Mn_7$) alloy

After obtaining the expected promising result, similar experimental results will be compared for rapid cooling case and the changes will be reported.

4.1.2. Re-Production and Characterization of Base Alloy

According to theoretical calculations and experimental results from previous studies in NOVALAB [6, 7], best alloy composition has been decided to be $M_{60}Cr_{13}Mo_{10}B_8Y_2Mn_7$. In this notation, cast iron scrap was denoted as M in alloy compositions. During preparation section, scrap pieces were initially polished to

get rid of the oxide layer on it to eliminate demolishing effect of the oxygen on glass forming ability. The design of the BAS systems requires some specifications during preparation such as:

- The developed novel alloy system must include minimum three ingredient elements
- During the designing of the BAS system, their soft magnetic behavior must be taken into consideration.
- To obtain high GFA, the designed alloy must show large T_g and low T_l values.
- For adaptation of the industrial applications, corrosion resistance must be inconsideration and during alloying step, corrosion resistant elements should be used like Cr and Mo.
- According to previously referenced master researches, Mn amount should be optimized for obtaining stable system.
- According to other rare earth elements, Y has also an important effect in the designing part due to high radius difference [7].

During the production of the sample, designed alloy composition was casted into pre-cooled copper mold which is in wedge shaped. Because of the high viscosity of molten alloy, melting point of the alloy could not be observed with naked eye, however it was clearly seen from DSC analysis with 1487 K. The examination of the amorphous phase was carried out with DSC, XRD analysis and with SEM investigations; these results were given in Figure 4.5 from (a) to (c) respectively. From the DSC curve of the design sample, it is seen that the glass transition (T_g) performs at nearly 861 K with 37 K supercooled liquid region ($\Delta T_x = T_x - T_g$). The XRD pattern of the sample is a typically amorphous structure shape which has board, wide and low intensity peaks. According to XRD result analysis, these peaks have iron carbide characteristic however, the exact composition is not clear because of the closer point data.

a)

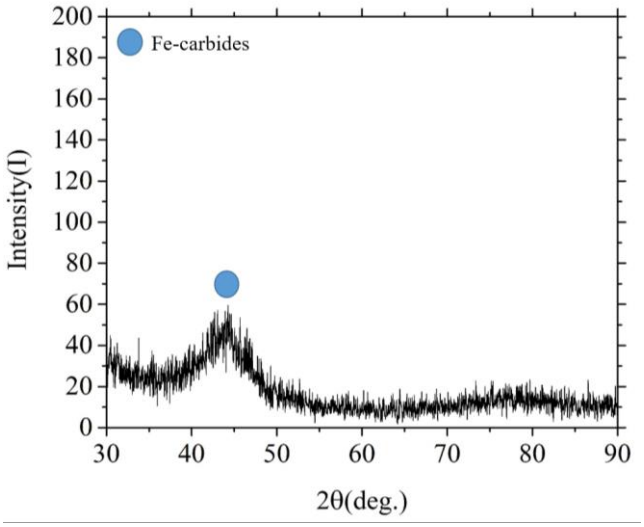

b)

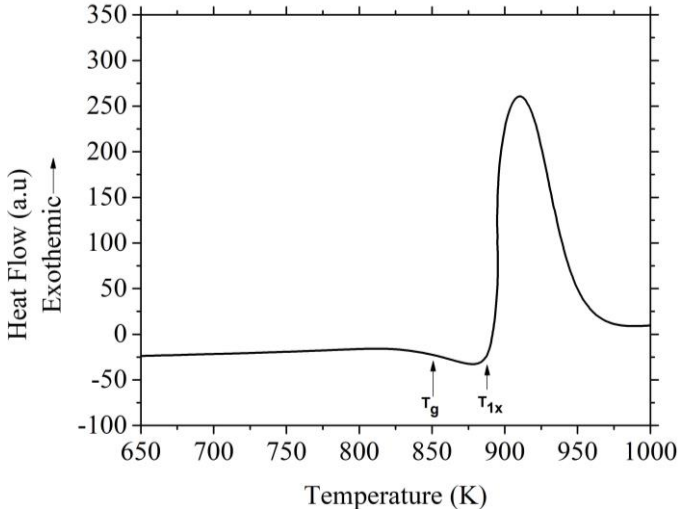

c)

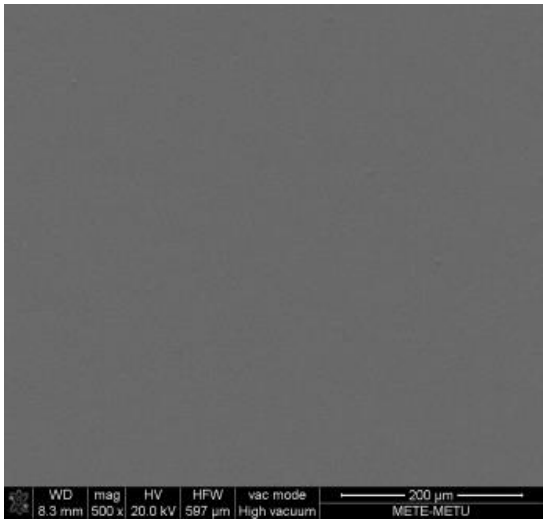

Figure 4.5. a) XRD b) DSC and c) SEM results of designed alloy

a) The XRD pattern of the prepared BAS sample shows the characteristic amorphous halo shaped patterns. While there exists the XRD pattern of the near equilibrium condition in Figure 4.2, there is not any candidate phase identification in in Figure 4.5a.

b) For thermal analysis, samples were heated to 1773 K in the DSC. The critical thermal parameters were determined. If the system shows glassy phase, there will be glass transition peak predate in the supercooled region and exothermic reaction peak in the thermal analysis diagram.

c) In contrast to the microstructural investigation of the near equilibrium condition Figure 4.3, the fully amorphous structure does not show any contrast in SEM images. In the rapid solidification part, liquid shows lower disposition to form crystal structure. Hence, before reaching the eutectic and peritectic points, the system have higher driving force to liquid formation than the solid [25, 81].

All critical temperatures of $M_{60}Cr_{13}Mo_{10}B_8Y_2Mn_7$ bulk amorphous steel are listed in Table 4.3.

Table 4.3. Critical thermal parameters of the $M_{60}Cr_{13}Mo_{10}B_8Y_2Mn_7$

	$M_{60}Cr_{13}Mo_{10}B_8Y_2Mn_7$
T_g	861 K
T_x	898 K
ΔT_x	37 K
T_{rg}	0.579
γ	0.382
γ_m	0.629
α	0.604
β	1.604
ω	0.225

The produced sample images having 3 mm in diameter and 15 cm in length were given in Figure 4.6.

Figure 4.6. $M_{60}Cr_{13}Mo_{10}B_8Y_2Mn_7$ samples fabricated by suction casting

4.1.3. General Properties of Synthesized BAS

Amorphous structures contain some specific properties and after the design and production part, related properties should be checked to be sure that the produced sample is amorphous.

4.1.3.1.Magnetic Properties of Synthesized BAS Sample

According to previous knowledge of BASs, they should be non-ferromagnetic alloy systems. Hence, after the the production of the BASs, their ferromagnetic behavior should be checked. By using Fe-Nd-B magnet, and by applying controlled magnetic field hysteresis, loops could be generated by acquiring magnetic response.

While making decision about the success of the BAS, magnetic characterization of the samples is substantial due to their soft magnetic behavior at room temperature. According to VSM results, the designed sample act as soft magnets with 145.39 Oe (11.57 kA/m) coercive field (H) and 73.23 emu/gr saturation magnetization (M_s).

As indicated in the Figure 4.7 it has almost near zero squareness which is also the evidence of the amorphous structure.

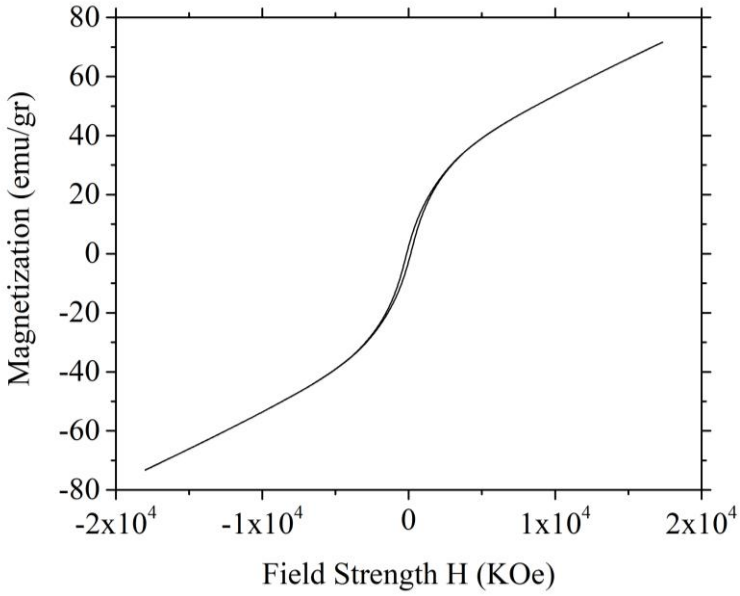

Figure 4.7. $M_{60}Cr_{13}Mo_{10}B_8Y_2Mn_7$ hysteresis loop

While defining the magnetic characteristic of the samples, the shape of the hysteresis loop is named as squareness. The squareness of the designed sample was 0.107 in base alloy which is near to zero.

4.1.3.2.Mechanical Properties of Synthesized BAS Sample

4.1.3.2.1. Hardness Studies

As it is known from the basic knowledge, rapidly solidified samples usually exhibit higher hardness values among their equilibrium cooling condition. The measured values vary between 1100 and 1180 HV. As indicated in Figure 4.8, these hardness values are very high compared to other conventional materials.

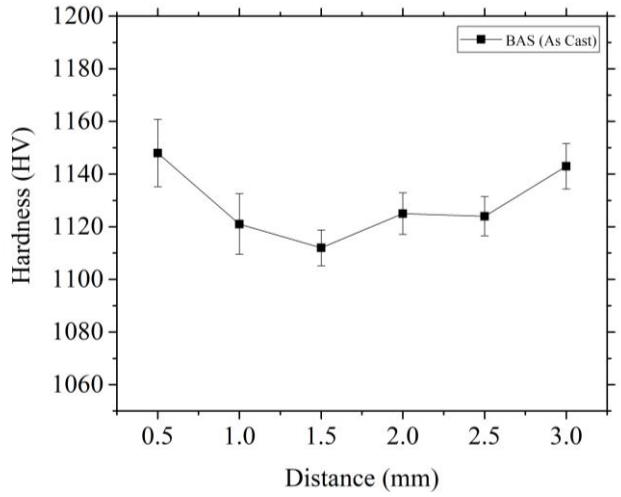

Figure 4.8. Hardness distributions of as cast $M_{60}Cr_{13}Mo_{10}B_8Y_2Mn_7$

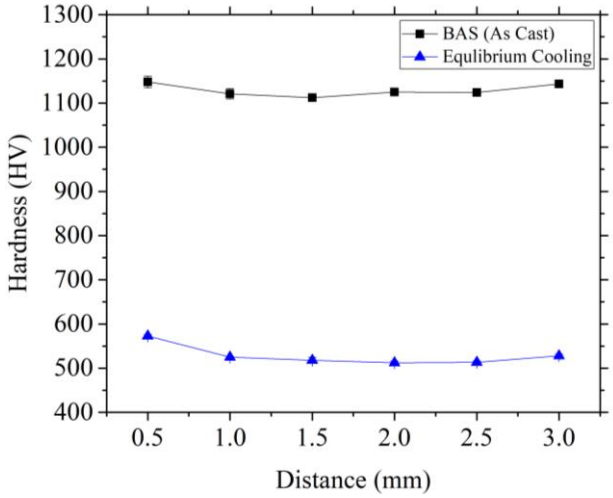

Figure 4.9. Hardness distributions of as cast and equilibrium condition of $M_{60}Cr_{13}Mo_{10}B_8Y_2Mn_7$

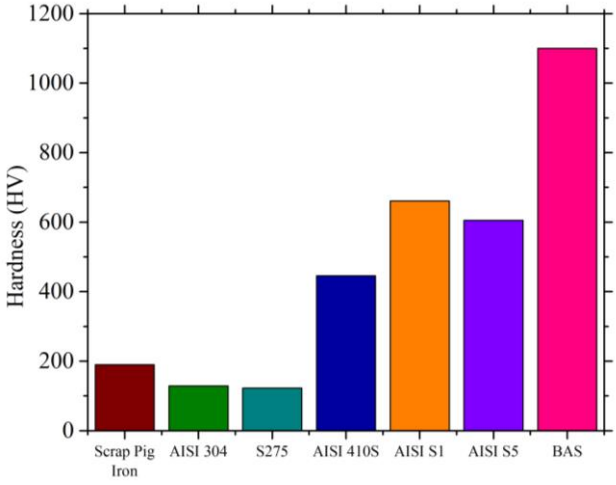

Figure 4.10. Hardness values of $M_{60}Cr_{13}Mo_{10}B_8Y_2Mn_7$ and some conventional materials [82]

As shown in the Figure 4.9, there is huge difference between rapid cooling (as-cast) and near equilibrium cooling condition. From the Figure 4.10, it is certainly clear that glassy structure had a significant effect on hardness when it is compared to conventional steels. Tsai et. al. [83] published in their studies that the micro hardness values are usually around 1150-1250 HV. The result which was obtained from $M_{60}Cr_{13}Mo_{10}B_8Y_2Mn_7$ sample is comparable and coherent with these previously published hardness values.

4.1.3.2.2. Corrosion Studies

While determining the corrosion characteristics of $M_{60}Cr_{13}Mo_{10}B_8Y_2Mn_7$ sample, sinking in an aggressive solution technique was used. Before every sinking test, the surfaces of the samples were polished carefully.

For corrosion testing, 0.5M H_2SO_4 acidic solution with 1.12 pH solution, 1M NaOH basic solution with 14 pH solution and 0.6M NaCl salt solution with 7 pH solution were preferred. The corrosion performance of BAS sample was compared with the scrap pig iron which is the base ingredient of BAS production, carbon steel (S275), titanium (pure) and stainless steel (304 SS).

For corrosion testing, all of the samples were kept in three extreme environments for 120 days and change of weight and surface area of the specimens were measured in each 5 days' period of time. Hence, the weight losses were calculated and tabulated according to the initial surface area and weight change in the system. The corrosion behavior of the samples in different solutions was shown in Figure 4.11, Figure 4.12 and Figure 4.13.

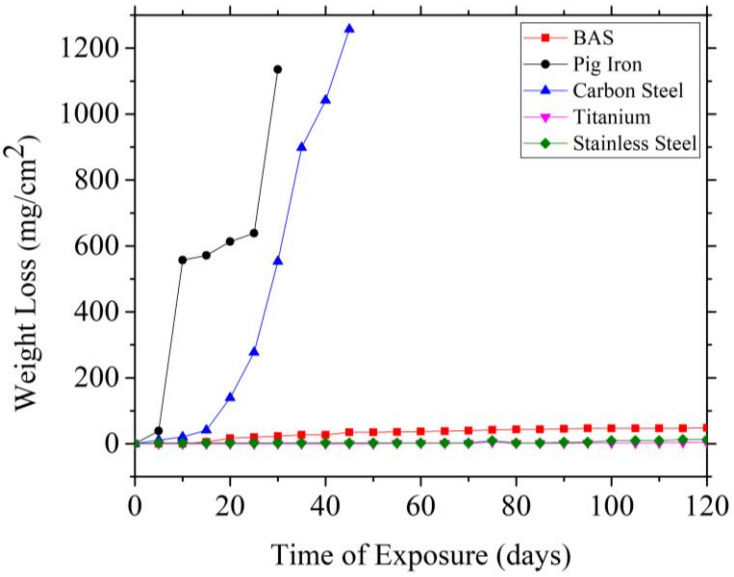

Figure 4.11. Weight loss vs time graph of the samples in 0.5M H_2SO_4 (1.12 pH) solution

As illustrated in Figure 4.11, at the end of 30 days, pig iron sample was decomposed in the acidic solution. Similarly, at the end of the 45 days, carbon steel (S275) sample was also decomposed. While the pig iron and carbon steel samples decomposed immediately in acidic solution, the weight loss of the titanium (pure) and stainless steel (304) was relatively low at the end of 120 days. Furthermore, $M_{60}Cr_{13}Mo_{10}B_8Y_2Mn_7$ sample did not show significant weight change in highly acidic solution.

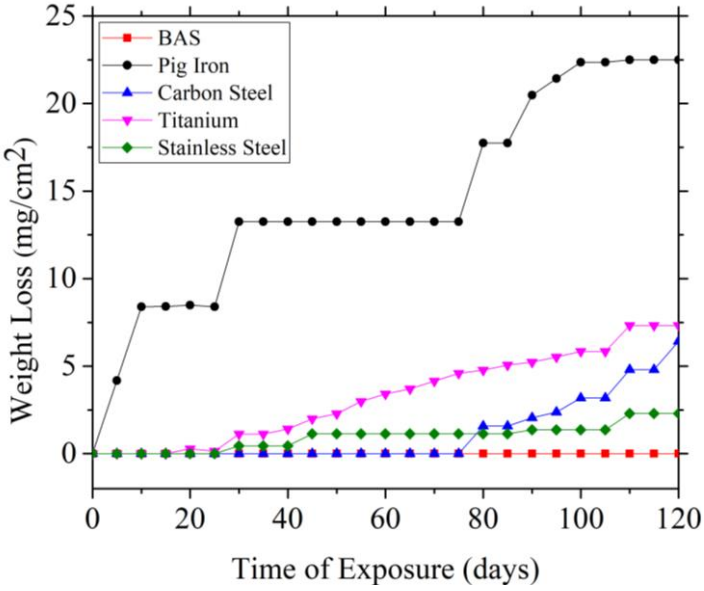

Figure 4.12. Weight loss vs time graph of the samples in 1M NaOH (14 pH) solution

The corrosion behaviors of the samples were illustrated inFigure 4.12. It is clear that there are low weight changes in 1M NaOH solution according to 0.5M H_2SO_4 solution and 0.6M NaOH solution. Moreover, there is not any weight loss in the $M_{60}Cr_{13}Mo_{10}B_8Y_2Mn_7$ BAS system. However, there are weight losses in all other materials, and the most weight loss was monitored from pig iron sample.

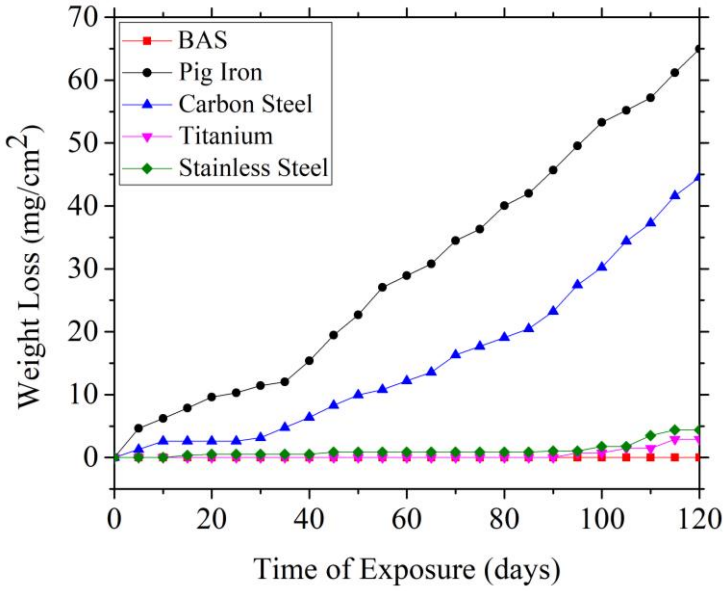

Figure 4.13. Weight loss vs time graph of the samples in 0.6M NaCl (7 pH) solution

There is also weight loss in 0.6M NaCl environment. Although the weight losses are lower than 0.5M H_2SO_4 acidic environment, salt solution has affected the surfaces of the all tested samples. Oxidized layers were observed on the surface of the pig iron and carbon steel specimens. Calculations were proceeded after removing the oxide layer. Most importantly, $M_{60}Cr_{13}Mo_{10}B_8Y_2Mn_7$ showed no weight change for 120 days.

The all corrosive environmental results are tabulated in Table 4.4 and detailed representation of the results are shown in the Figure 4.14, Figure 4.15 and Figure 4.16.

Table 4.4. Corrosion study results for 120 days

Material	Corrosive Environment	Total Weight Loss (mg/cm^2)	Weight Loss Percentage
BAS (As Cast)	0.5M H_2SO_4	48.105	10.38%
	1M NaOH	0	0%
	0.6M NaCl	0	0%
Pig Iron	0.5M H_2SO_4	1135.458	100%
	1M NaOH	22.502	3.09%
	0.6M NaCl	64.970	3.78%
Carbon Steel (S275)	0.5M H_2SO_4	1257.784	100%
	1M NaOH	6.421	0.51%
	0.6M NaCl	44.561	2.95%
Stainless Steel (304)	0.5M H_2SO_4	12.457	1.72%
	1M NaOH	2.294	0.23%
	0.6M NaCl	4.377	0.41%
Titanium (Pure)	0.5M H_2SO_4	3.820	0.55%
	1M NaOH	7.332	1.05%
	0.6M NaCl	2.887	0.43%

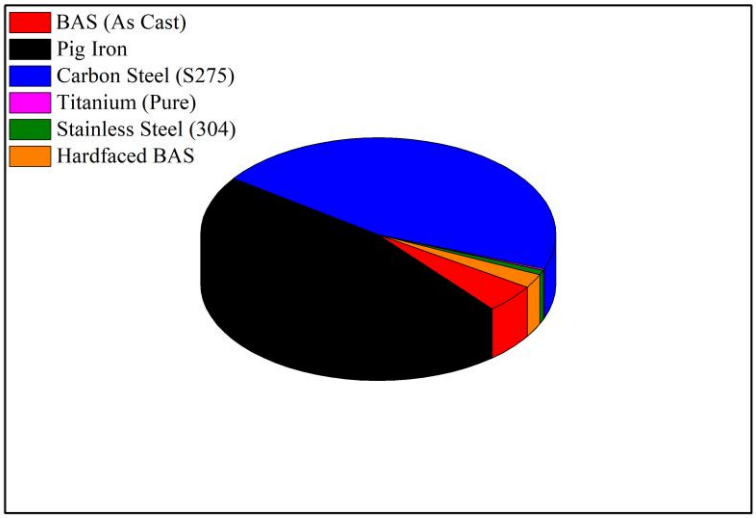

Figure 4.14. Representation of the total weight loss percentage of the all samples in the 0.5M H_2SO_4 solution for 120 days

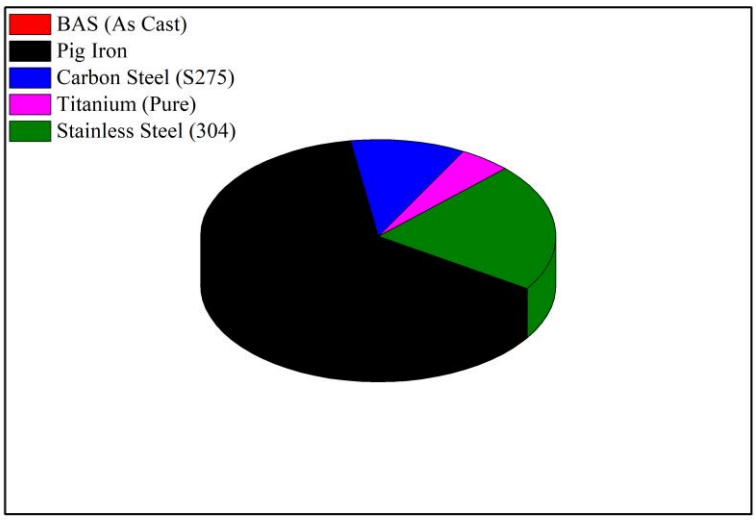

Figure 4.15. Representation of the total weight loss percentage of the all samples in the 1M NaOH solution for 120 days

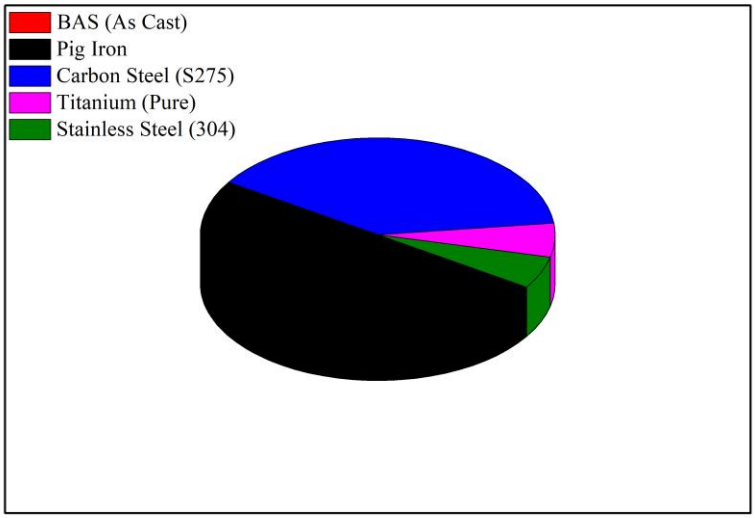

Figure 4.16. Representation of the total weight loss percentage of the all samples in the 0.6M NaCl solution for 120 days

4.2.Industrial Coating/Surface Treatment Application

In the industry, carbon steels are the most preferred material in the design and in the manufacturing of metallic parts which is mainly due to easy machining ability, good weldability, relatively low cost and validity. However, because of their chemical characteristic, under the highhanded environments they can easily form oxides, since they have low chemical resistance. Hence, because of the low chemical durability, the surface protection is a feebleness implementation for carbon steels [60]. Moreover, the most conventional surface treatment implementations involve environmentally hazardous components, nickel in the phosphatization is a good example for this. Moreover, under the aggressive environments, iron alloys form oxide layer so, it is essential to preserve the surface of the metal [62].

4.2.1. Characterization of Hard-faced Layer

While analyzing the surface treated part of the substrates, the main objective is to understand the microstructural change of the sample and, what changes in the

microstructure and whether the amorphous structure is preserved or not during the hardfacing application. The main goal is to achieve same microstructural and mechanical properties after having the hardfacing application.

4.2.2. Microstructural Investigation

As indicated in Table 4.5, to make a correct decision about the microstructures, two different substrates and two different cooling conditions were selected. These are namely; carbon steel (S275) and stainless steel (304) substrates with air cooling and water quenching conditions.

Table 4.5. Prepared hardfaced samples according to their substrate and cooling environments

	1	**2**	**3**	**4**
Substrate	S275 Carbon Steel	304 Stainless Steel	S275 Carbon Steel	304 Stainless Steel
Cooling Environment	Air Cooling (AC)	Air Cooling (AC)	Water Quenching (WQ)	Water Quenching (WQ)

4.2.2.1. Hardfacing Application for Stainless Steel Substrate for Air Cooling and Water Quenching Conditions

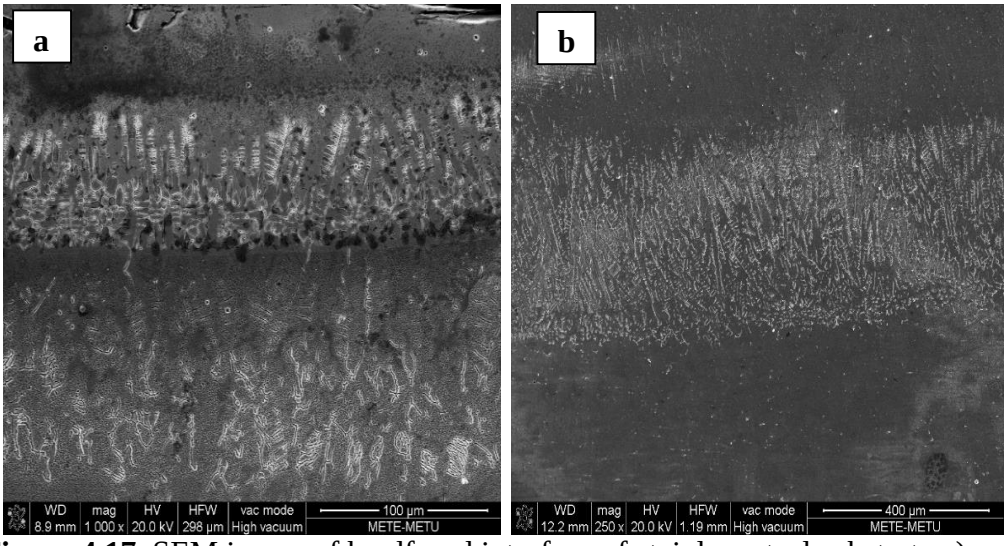

Figure 4.17. SEM image of hardfaced interface of stainless steel substrate a) water quenched and b) air cooling

For stainless steel (304) substrate, there is a high increase in the hardness value of the coated surface. However, for both of the cooling conditions, there is not full penetration at the interface, but there are lots of feature formation in the matrix as indicated in the SEM images (Figure 4.17.) These feature formations basically show that the amorphous structure cannot be maintained in the stainless steel (304) substrate.

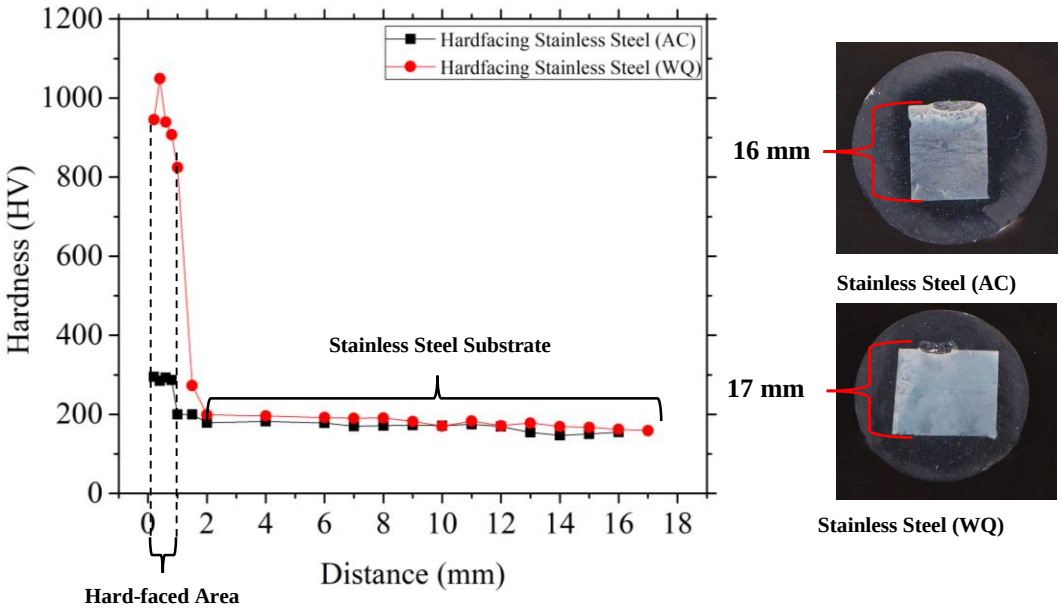

Figure 4.18. Hardness results for stainless steel (304) substrate

According to Figure 4.18

Figure 4.18, hardness value evaluations shows that the increase is in the water quenching condition is higher than in air cooling condition, as expected. In WQ version, nearly 1 mm area has a high hardness value due to the hardfacing application.

4.2.2.2.Hardfacing Application for Carbon Steel Substrate for Air Cooling and Water Quenching Conditions

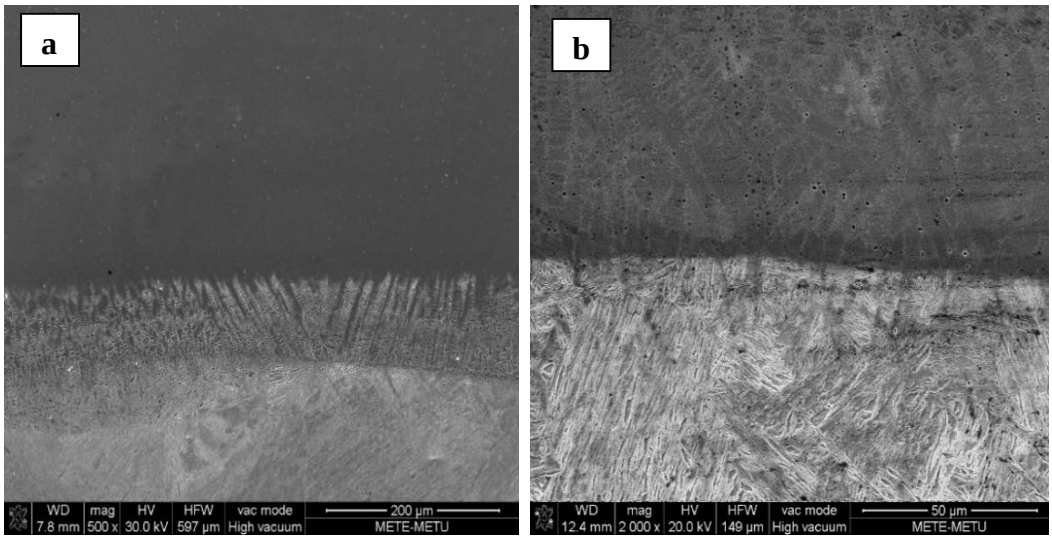

Figure 4.19. SEM image of hardfaced interface of a) carbon steel substrate water quenched and b) carbon steel substrate air cooling

As indicated in Figure 4.19, three is morphological differences between SEM images of the carbon substrate for WQ and AC conditions. Bottom parts of the images show the carbon steel substrate and the upper parts show the hardfaced part. For air cooling condition, there are some feature formation like grain boundaries in the matrix. However, in WQ condition, after the penetration band there is not any feature formation. SEM results showed that dendrites were nucleated and tried to grow on the partially amorphous matrix but the rapid cooling rates did not allow to them to grow. According to these discussions and results, the carbon steel substrate (S275) with water quenching (WQ) condition can be selected as it is more consistent than other conditions.

For carbon steel (S275), there is a high increase in the hardness value of the coated surface, however for only water quenching condition, there is no feature formation in the matrix.

Figure 4.19 a) shows that the amorphous structure can be maintained in the carbon steel (S275) substrate.

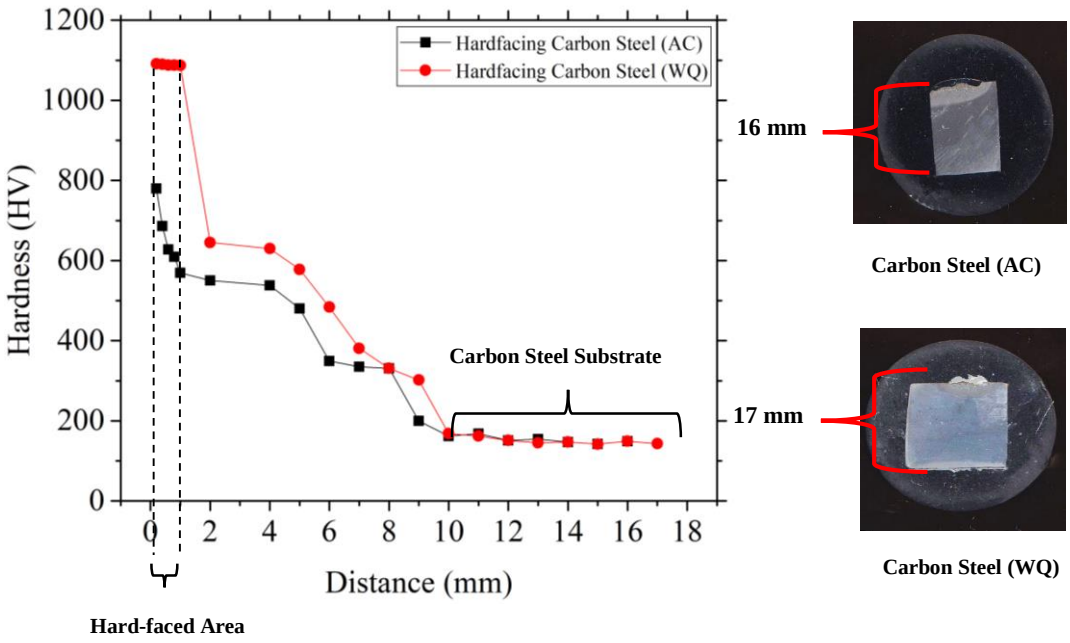

Figure 4.20. Hardness result for carbon steel (S275) substrate

According to hardness results in the Figure 4.20, the hardness value increase is higher in the water quenching condition than in air cooling condition as expected. Also, for water quenching condition, values are similar with the cast condition of the BASs. Figure 4.21 shows that nearly 1 mm area has a high hardness value due to the hardfacing application. For this condition, coated surface has the same hardness value with the cast sample, for this reason, in the rest of the thesis, all the required studies will be carried out in the scope of carbon steel substrate (S275) and water quenching condition.

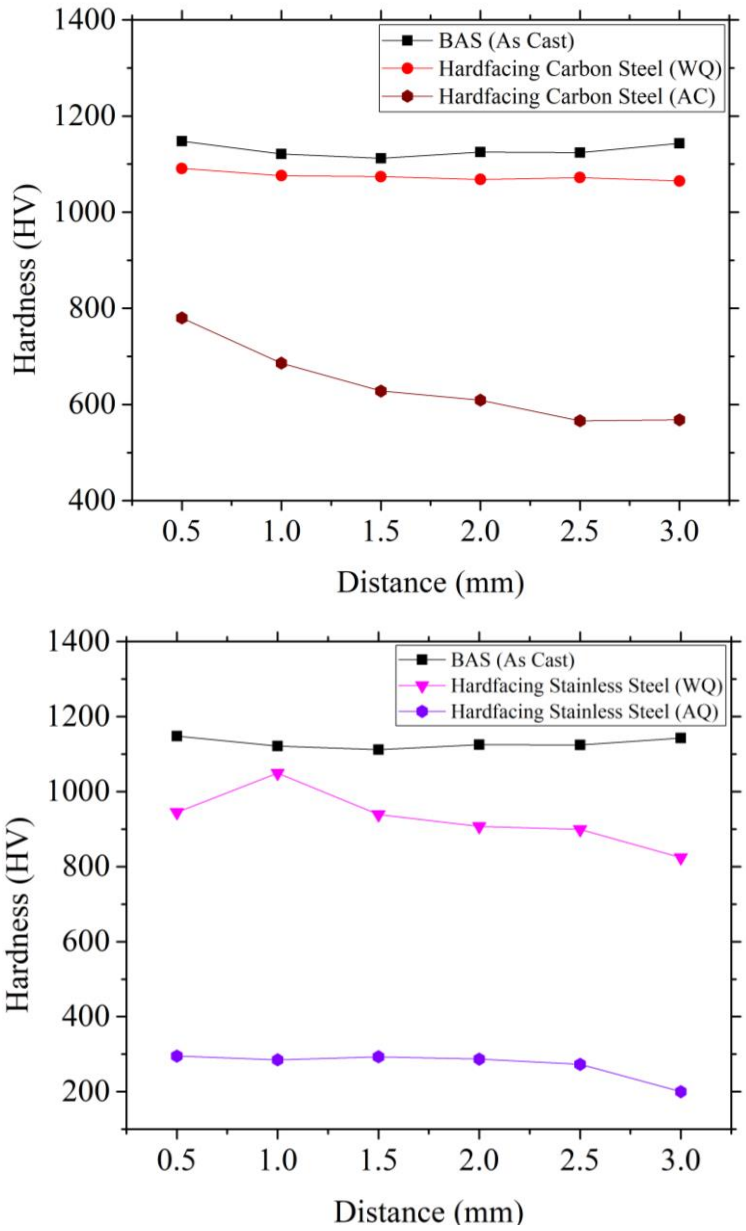

Figure 4.21. Hardness result for carbon steel substrate and stainless steel substrate according to as-cast sample

The overall hardness results were summarized in the Figure 4.21, and it is clear that, WQ hardfaced carbon steel (S275) substrate has the closest hardness value to cast BAS.

After all the conducted examinations, carbon steel substrate with water quenching cooling was selected as candidate process for our hardfacing application. Then, detailed SEM and XRD examinations were carried out based this candidate process.

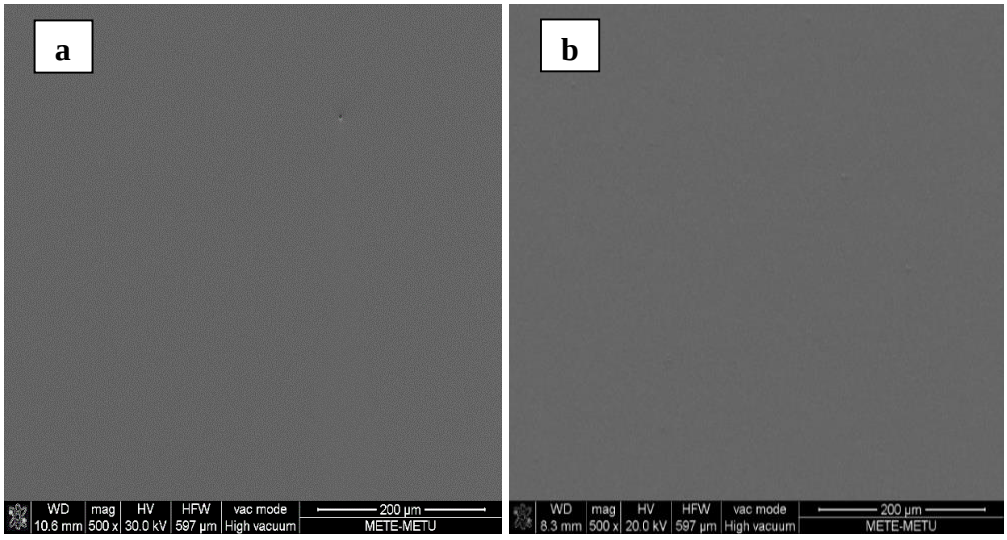

Figure 4.22. a) SEM image of as-cast bas and b) carbon steel substrate with WQ hardfaced layer

As can be seen in Figure 4.22, none of the as-cast and hardfaced sample's matrix does show any contrast in SEM images, which is the natural result of the fully amorphous structures.

Moreover, while comparing as cast and hardfaced samples, the fact that XRD pattern shows some similarities must be considered. Both samples have characteristic amorphous halo shaped XRD patterns (Figure 4.23). For XRD measurement as cast BAS was measured in bulk form. However, hardfaced sample was measured in powder form. So, the result displays the intensity difference in-between.

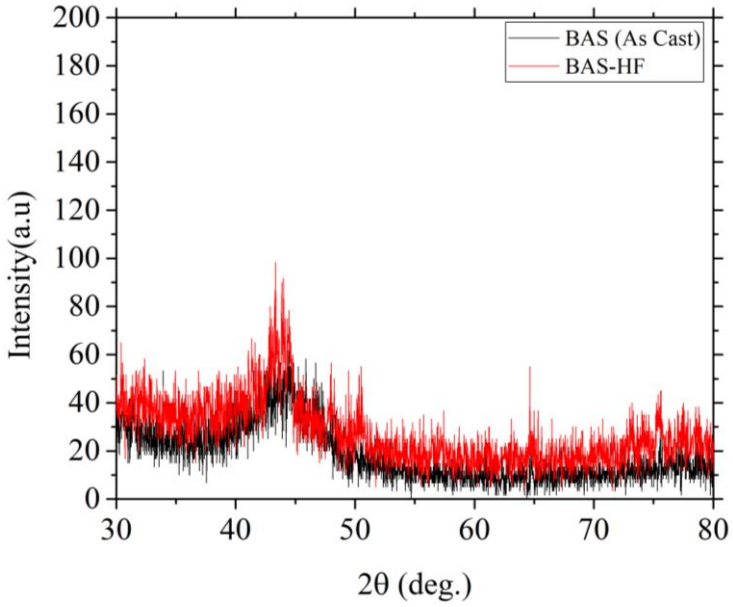

Figure 4.23. Comparable XRD pattern of as cast bas and hardfaced layer

Hence, after industrial coating/surface treatment application by using hardfacing application (WQ cooling condition), amorphous structure could still be obtained according to SEM, XRD and hardness results.

The next step should be the adaption to the industrial applications. For the application to be used in a wider area in the industry, the coating thickness and the coated area should be enlarged. The next hardfacing application was designed to achieve this industrial aim.

4.2.3. Optimization of Coating Thickness

During the optimization studies of the coating thickness, multiple pass technique was applied to obtain larger coated area. The effects on the properties was examined in detail.

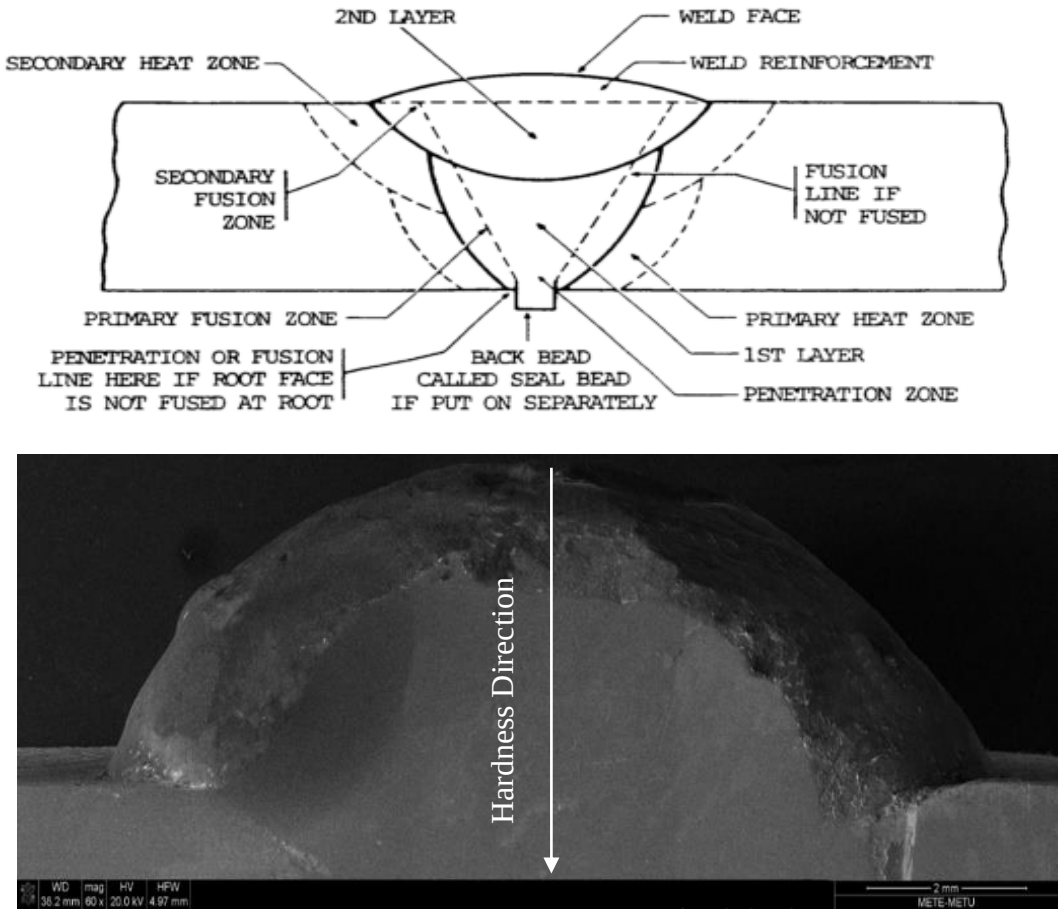

Figure 4.24. Multiple pass hardfacing application

While doing the multiple pass application, following the application on the first coating layer, the second and third layers were applied on the first layer. Hence, due to the additional re-heating and re-cooling steps, the property examination studies were re-performed. Because it might have different properties than single layer hardfacing application.

4.2.3.1. Properties of the Multipass Hardfacing Application

As can be seen in Figure 4.25, the hardness variation of the multiple layered hardfaced sample from bottom to upwards direction is different form single layered hardfaced sample. This variation shows that the hardness of the coating is decreasing from bottom to upwards direction, in the other words, from as quenched to re-heated and re-cooled direction.

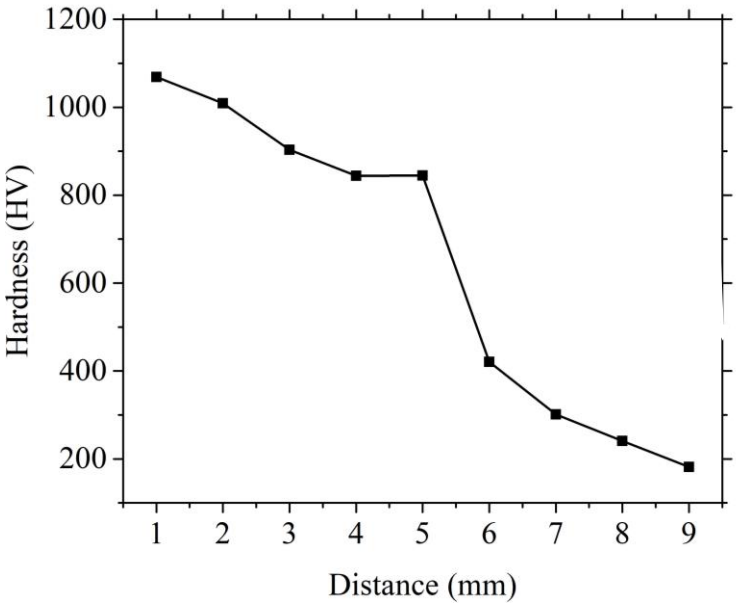

Figure 4.25. Hardness values from bottom to up direction of the multiple hardfaced sample

As can be seen from Figure 4.26, the back-scattered SEM image of the multiple layer hardfaced sample interface, there are some feature formation in the coated (top) section. After this examination, we decided to apply the mapping process to obtain the chemical information about the matrix.

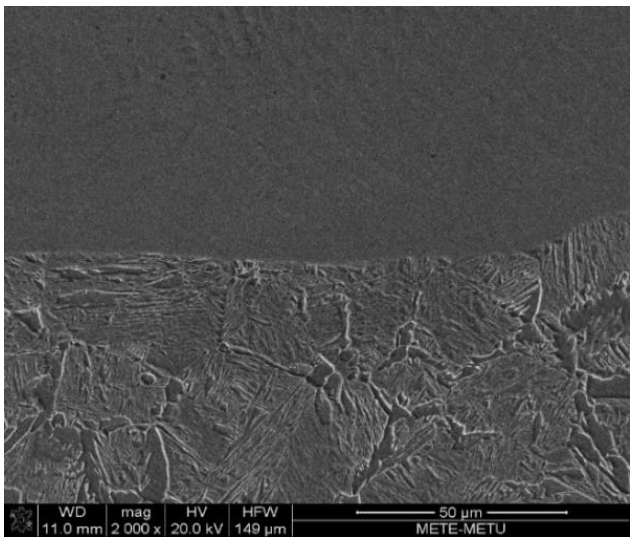

Figure 4.26. SEM Back-scattered images of the multiple layer hardfaced sample interface

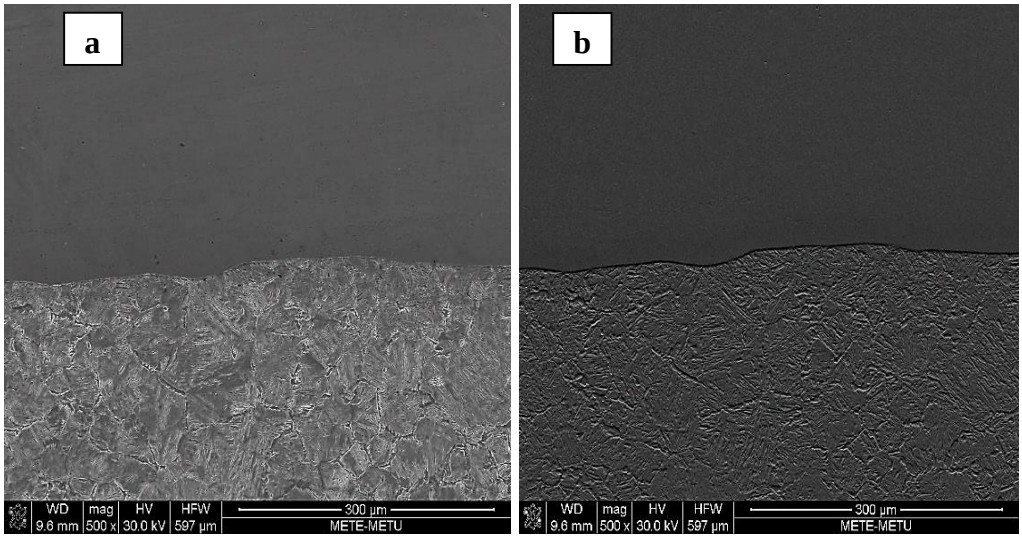

Figure 4.27. a) SEM image and b) Back-scattered image of mapping area

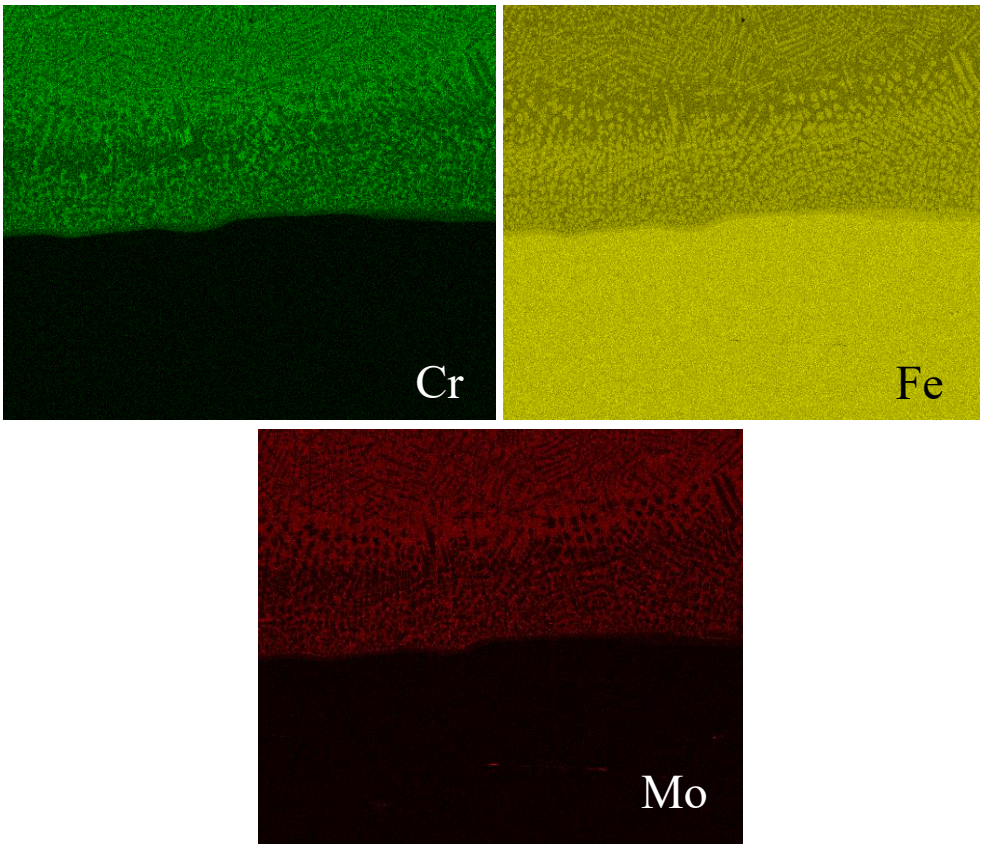

Figure 4.28. Elemental mapping process at the interface

In Figure 4.28, the estimated features in the back-scattered view is clearly seen in the elemental mapping process. This process shows us; the lower hardness regions have some features formations so; we should analyze the high hardness part of the

coating for making comparison. The high hardness region is the upper part of the sample and the analysis were carried out in this part.

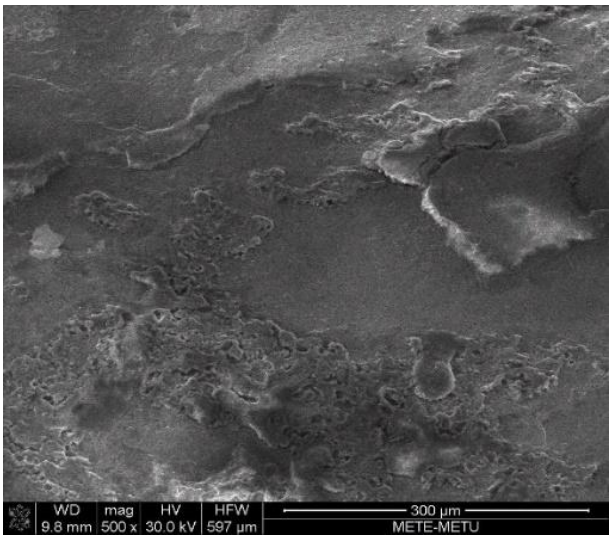

Figure 4.29. SEM image of the bottom part of the Hardfacing

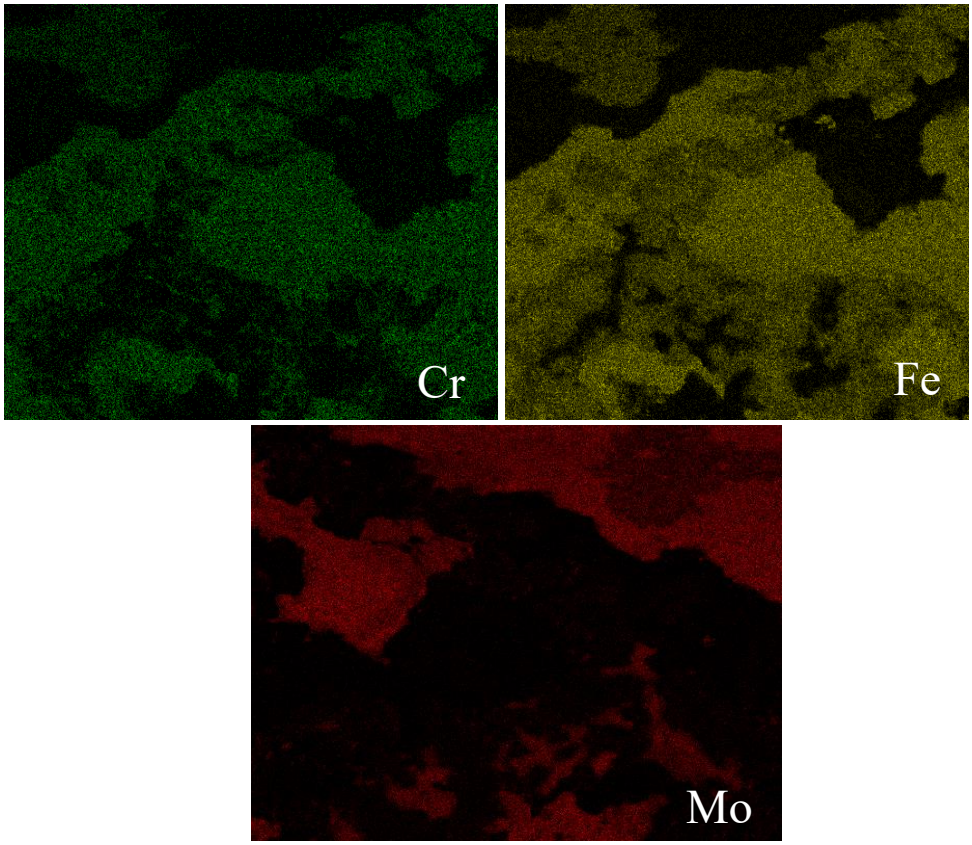

Figure 4.30. Elemental mapping process at the bottom part of Hardfacing

The SEM images clearly show that the only the welding application is remnant at the top of sample (Figure 4.29), and at the higher hardness region, there isn't any new formations as indicated in Figure 4.30. Thus, this mapping study show that in multilayer hardfacing applications, due to the re-melting, in the bottom layer there might be new feature formations. However, at the bottom layer which has high hardness value, there isn't any new feature formations and it prevents their previous morphology.

Hence, although larger coating thickness was obtained by the multiple layer hardfacing process, it did not provide good hardness property and, in the re-heating and cooling regions, amorphous feature cannot be conserved in the structure.

4.2.4. Mechanical Properties

In the industry, carbon steels are the most preferred material in the design and the manufacturing of metallic parts. This is mainly the result of easy machining ability, good weldability, relatively low cost and validity. Amorphous steels could be used in industrial coating/surface treatment application due to their high hardness values. Moreover, in addition to their high hardness characteristic, because of their featureless microstructure they will show greater resistance to wear from abrasion, corrosion or any combination of these factors. After the thickness optimization study results, further wear and corrosion studies were carried out with the specific sample which has thinner coating thickness.

4.2.4.1. Micro Hardness Measurement

Due to rapid cooling rates, an amorphous or ultra-fine-grained coating surface with high hardness was obtained in this study. The hardness values for all studied conditions in this thesis is summarized in the Figure 4.31.

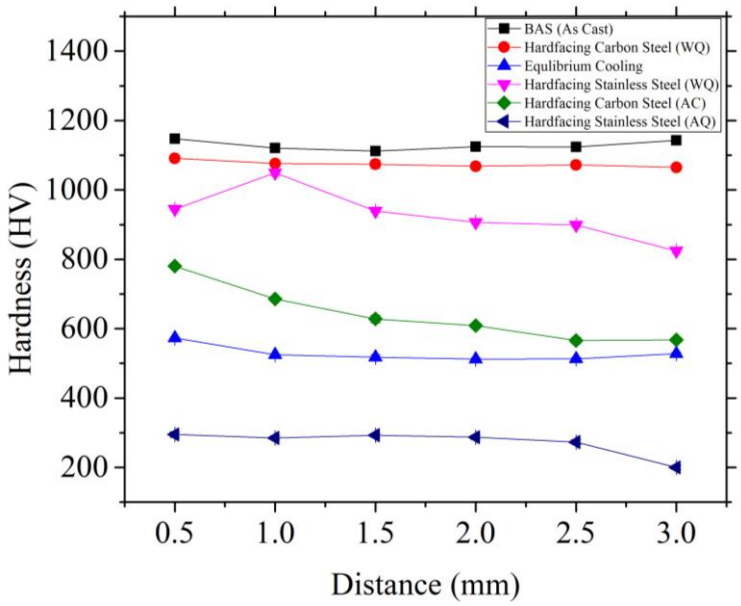

Figure 4.31. Hardness variation for all conditions

As indicated in the Figure 4.31, according to all conditions, hardfacing application on carbon steel substrate with water quenching was almost same with as cast $M_{60}Cr_{13}Mo_{10}B_8Y_2Mn_7$ sample.

4.2.4.2. Tribological Study

Tribology properties become the main topic of conversation when a problem is concerned with carrying some load across interfaces in relative motion [68]. While applying tribological testing there are some critical preparation and testing requirements to be followed, which are;

- Surface finish is critical — while determining the friction coefficient (COF) the surface roughness has an important effect associated with machine marks, inhomogeneous difficulties, etc.,
- Properly clean and dry the specimens,
- Horizontal test surface,
- Selection of proper sliding velocity and normal force [79].

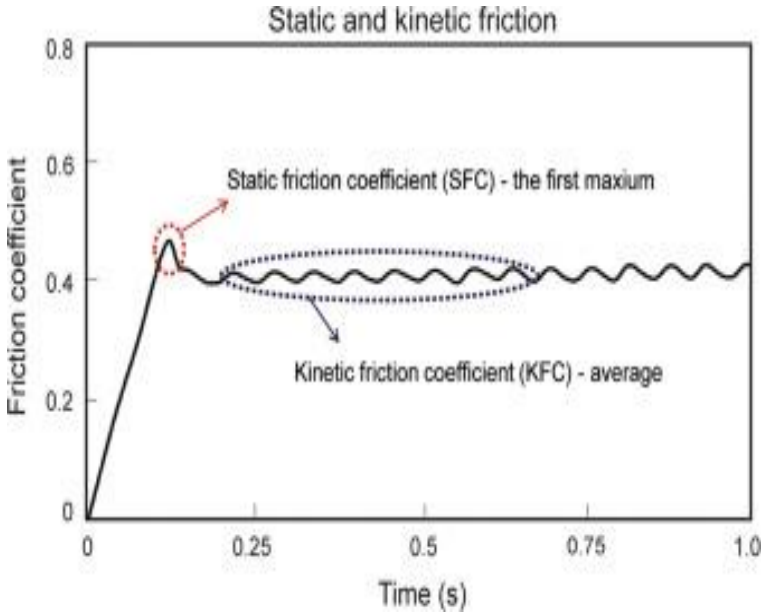

Figure 4.32. A representative friction profile with static friction and kinetic friction [84]

As indicated in Figure 4.32, generally there are two kinds of friction coefficients which are static and dynamic (kinetic). The static friction coefficient can be achieved by dividing the maximum friction force to relative motion to the normal load. The dynamic (or kinetic) friction coefficient can be obtained by dividing the friction force to the applied normal load during sliding.

Static friction is defined as the force that is used get something move and formulated as:

$f_s = F_N \times \mu_s$ (4.1)

μ_S= coefficient of static fraction and F_N is the applied normal load

The force between two moving objects that also has contact is called kinetic friction and it is dependent on the type of the surfaces. While the kinetic force experienced for dry and rough surfaces is high, a pretty low friction force between wet and smooth contacting surfaces is observed.

$f_k = F_N \times \mu_k$ (4.2)

μ_k= coefficient of kinetic fraction and F_N is the applied normal load

In literature, there are some studies related with the tribological properties of BMGs according to different loading types, sliding velocity and duration times. Some of those are presented in Figure 4.33 and Figure 4.34.

.

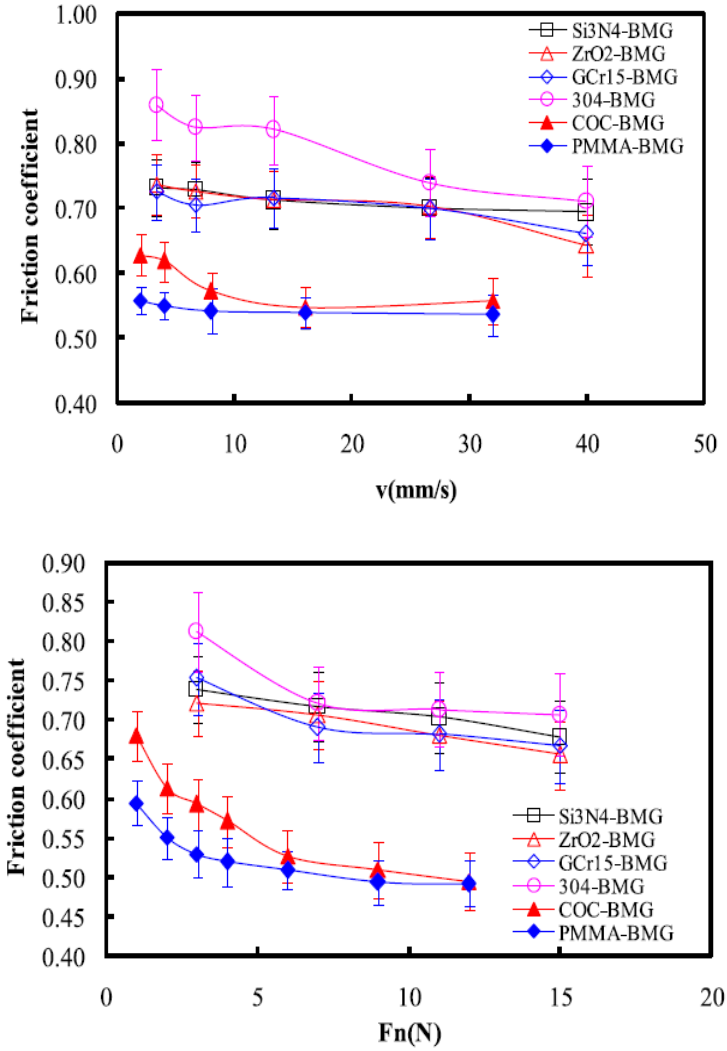

Figure 4.33. Mean friction coefficient of different BMGs as a function of different normal load, sliding velocity and different against pins [85]

The first influence factor on friction coefficient is applied force. According to previous experimental studies, when lower loads were used, the decrease on the frictional coefficient was monitored as sharply, whereas at higher loads, it has a slower rate. The second influence factor is the sliding velocity. By increasing the sliding velocity, frictional coefficient shows a decreasing characteristic [85].

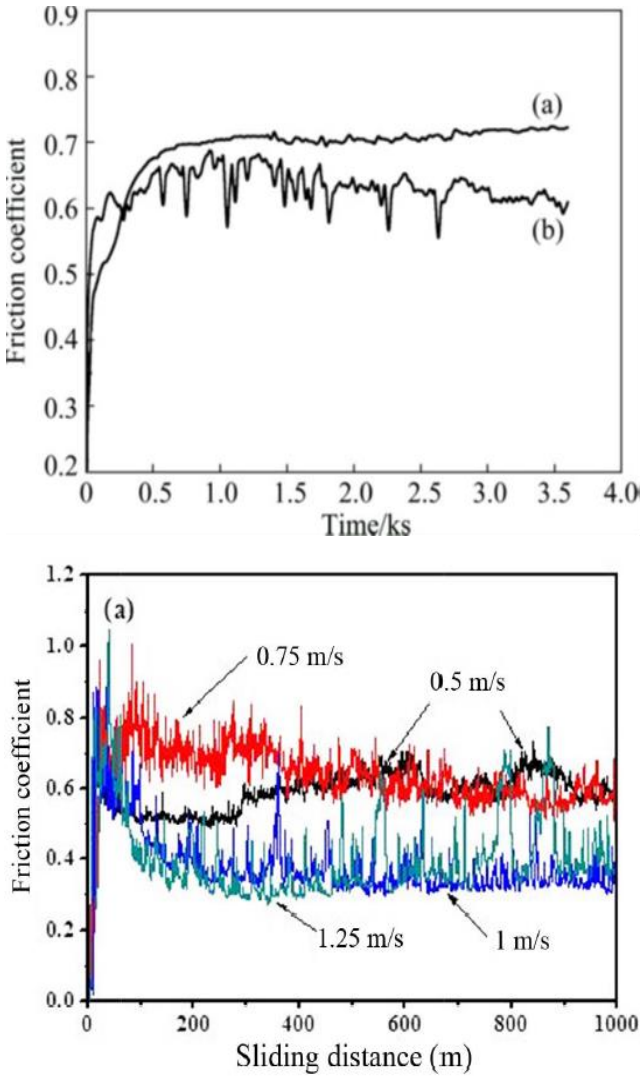

Figure 4.34. Mean friction coefficient of different BMGs with respect to different normal load and sliding velocity[86] (a) Fe-based coating; (b) Q235 stainless steel [87]

When the general trend for friction coefficient of BMGs is considered, their friction coefficient values changes between 0.3-1.0 (Figure 4.34). As indicated in Figure 4.35, they show somehow larger friction coefficient than conventional materials (410 and 316 Stainless Steel Alloy).

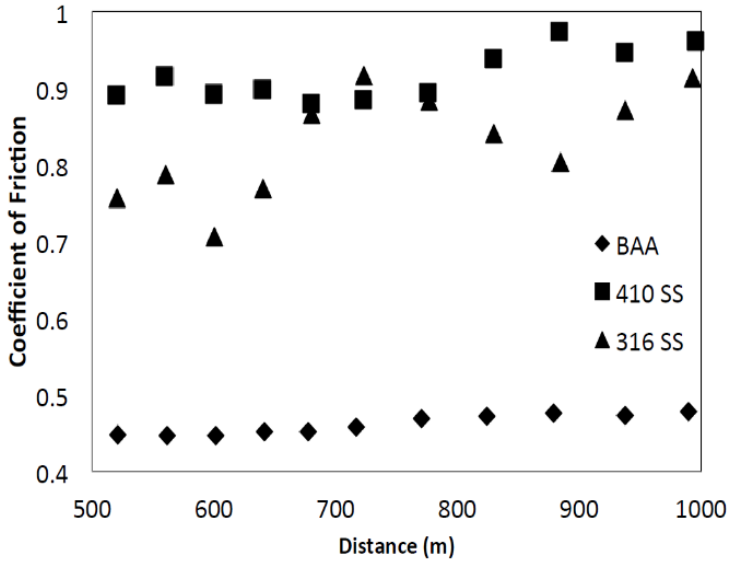

Figure 4.35. Coefficient of friction per sliding distance for Bulk Amorphous Alloy, 410 and 316 Stainless Steel Alloy [88]

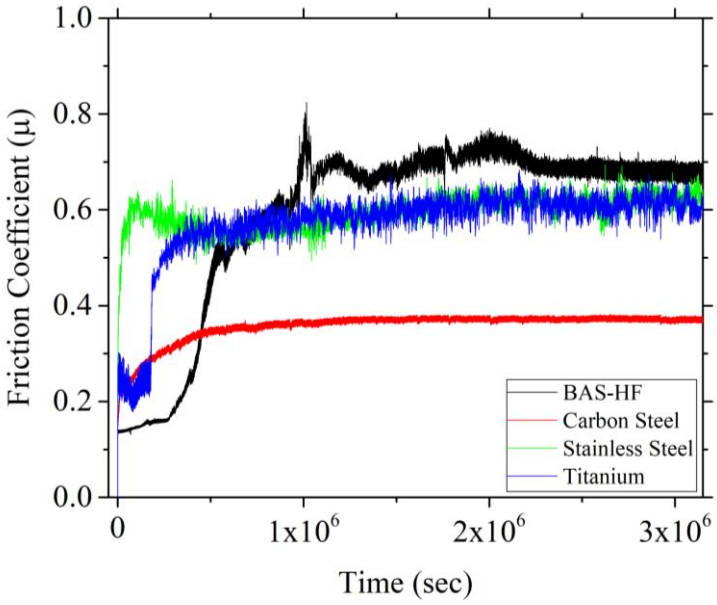

Figure 4.36. Friction Coefficient profile for BAS, Carbon Steel (S275), Stainless Steel (304) and Titanium

The wear rate calculation could not be performed because the test was terminated before the estimated time due to the reasons of excessing the machine's limits. The obtained results from pin-on-disc tribological analysis are shown in the Figure 4.36 and tabulated in Table 4.6 for other tested materials.

Table 4.6. Static and dynamic COFs of the Tested Materials

Sample	Static COFs	Dynamic COFs	Weight Loss
BAS-HF	0.81	0.65	1.7 mg
Carbon Steel (S275)	-	0.37	1 mg
Stainless Steel (304)	0.63	0.59	7 mg
Titanium (Pure)	-	0.60	3 mg

Table 4.7. Static and dynamic COFs of Different Materials with moving Zirconia ball

Sample	Static COFs	Dynamic COFs
BAS-HF	0.81	0.65
Carbon Steel (S275)	-	0.37
Stainless Steel (304)	0.63	0.59
Titanium (Pure)	-	0.60
4340 Steel	-	0.78 [89]
Aluminum	-	0.63 [90]
Chromium	-	0.61 [90]
Iron	-	0.35 [90]

There are some critical reasons for higher friction coefficient of BAS's. One of them is related with the hardness of the contact surfaces. The friction, as widely accepted, depends on the hardness and when the slider is harder than the plate, minimum friction occurs at the maximum hardness point. However, if the slider is softer or has nearly equal hardness, there is some gathering of slider (zirconia) on the plate. Hence, if the slider is softer or has equal hardness the friction is very unstable and there is no exact relationship between hardness and friction coefficient [91]. Moreover, Fe-based metallic glass coating with high hardness indents into the surface of ball and the hard particles dug into the ball surface and scratch out the material (zirconia) as illustrated in Figure 4.37. In the EDS analysis, it was seen that the lighter particles on the wear scar were zirconia particles. In this way, way

of contact changes from ball-to-disk to disk-to-disk, which leads increasing in the roughness and the friction coefficient of the surface [87].

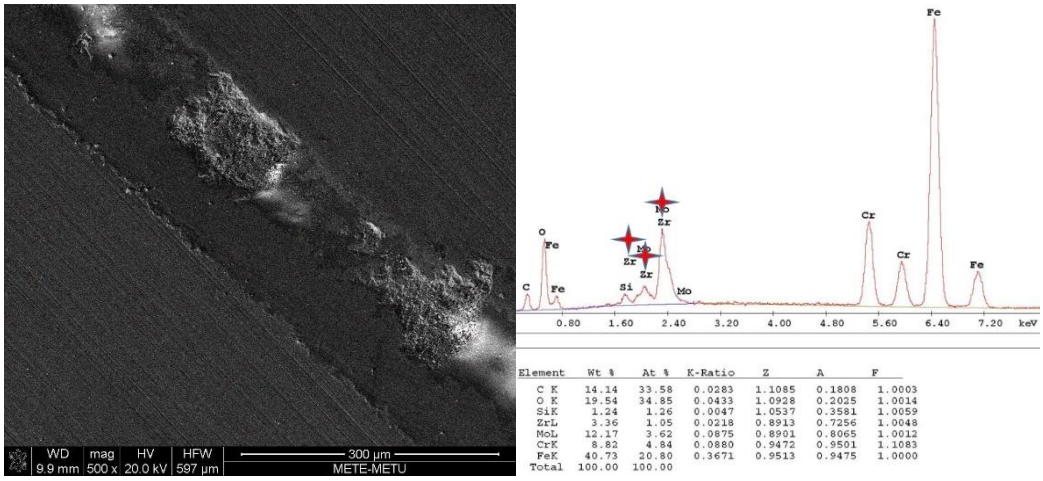

Figure 4.37. SEM and EDS Analysis of sample surface after wearing application

The second reason is related with microstructural mismatch. Mismatches, which are overlapping areas, create taps between the pre-remelted layer and the new ones. Therefore, amorphous/crystalline ratio of the sample decreases throughout the tribological test, and the higher friction results come from the crystalline/crystalline interaction [92].

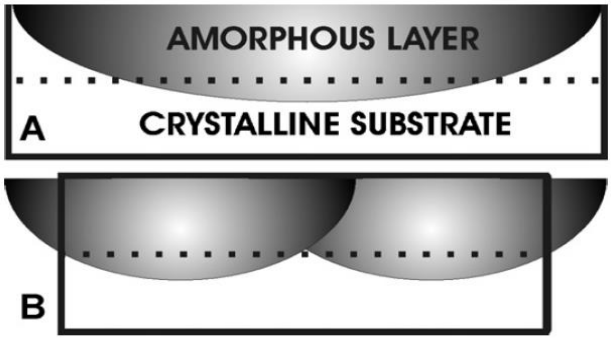

Figure 4.38. Schematic representation of (A) a single pass wear contact and (B) overlapped multiple pass wear contact [92]

4.2.4.3.Corrosion Studies

While comprehending the corrosion resistance of surface coated sample with BAS, again immersion corrosion tests were applied after hardfacing application. Again, 0.5M H_2SO_4 acidic solution with 1.12 pH solution, 1M NaOH basic solution with 14 pH solution and 0.6M NaCl salt solution with 7 pH solutions were applied for 80 days.

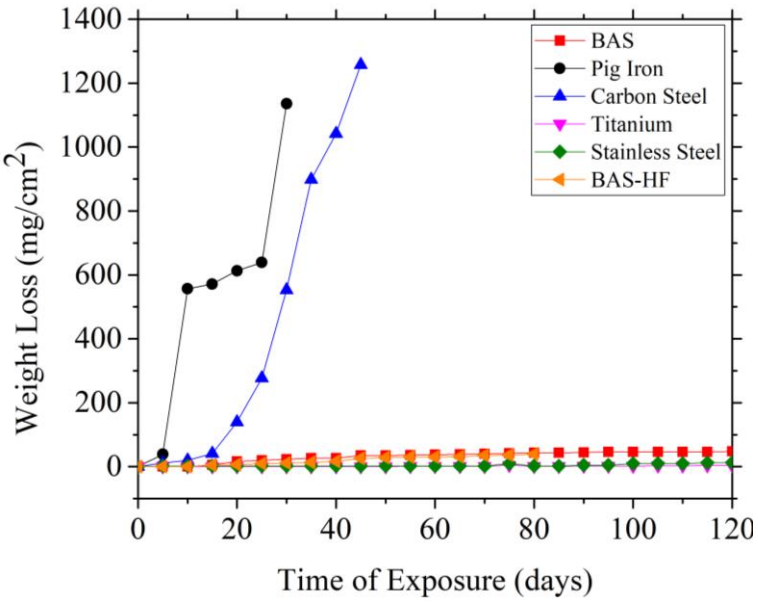

Figure 4.39. Weight loss vs time graph of the all samples in 0.5M H_2SO_4 solution

The corrosion behavior of the all samples, which includes also the hardfacing sample, was shown in the Figure 4.39, Figure 4.40 and Figure 4.41. In between all the samples, it is clearly seen that BAS with hardfacing application shows similar behavior with as cast BAS in the 0.5M H_2SO_4, 1M NaOH and 0.6M NaCl solutions. This result is a strong sign that after coating application, the surface of the substrate acts as cast BAS.

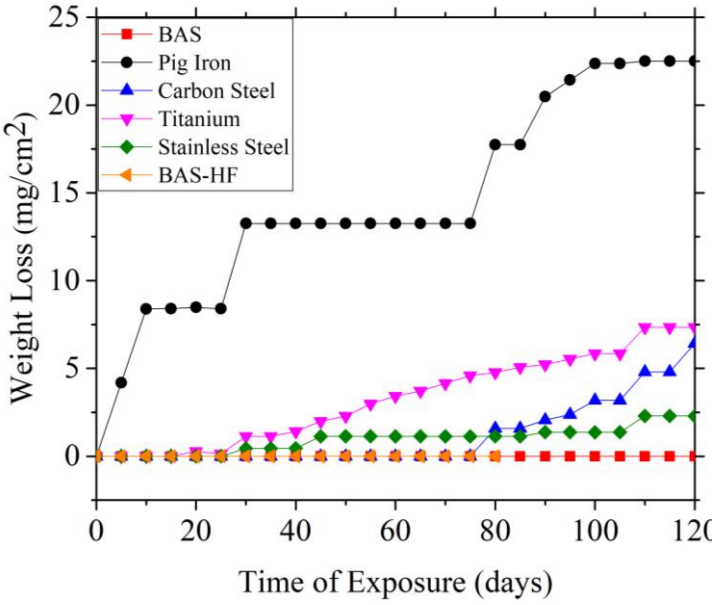

Figure 4.40. Weight loss vs time graph of the all samples in 1M NaOH solution

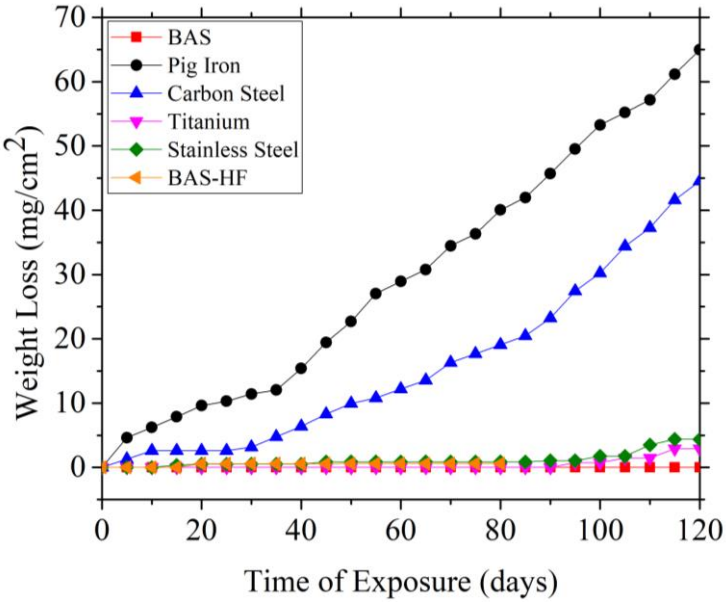

Figure 4.41. Weight loss vs time graph of the all samples in 0.6M NaCl solution

When the detailed comparison is carried out between BAS and hardfaced BAS, in 0.5M H_2SO_4 solution, coated surface shows better corrosion property.

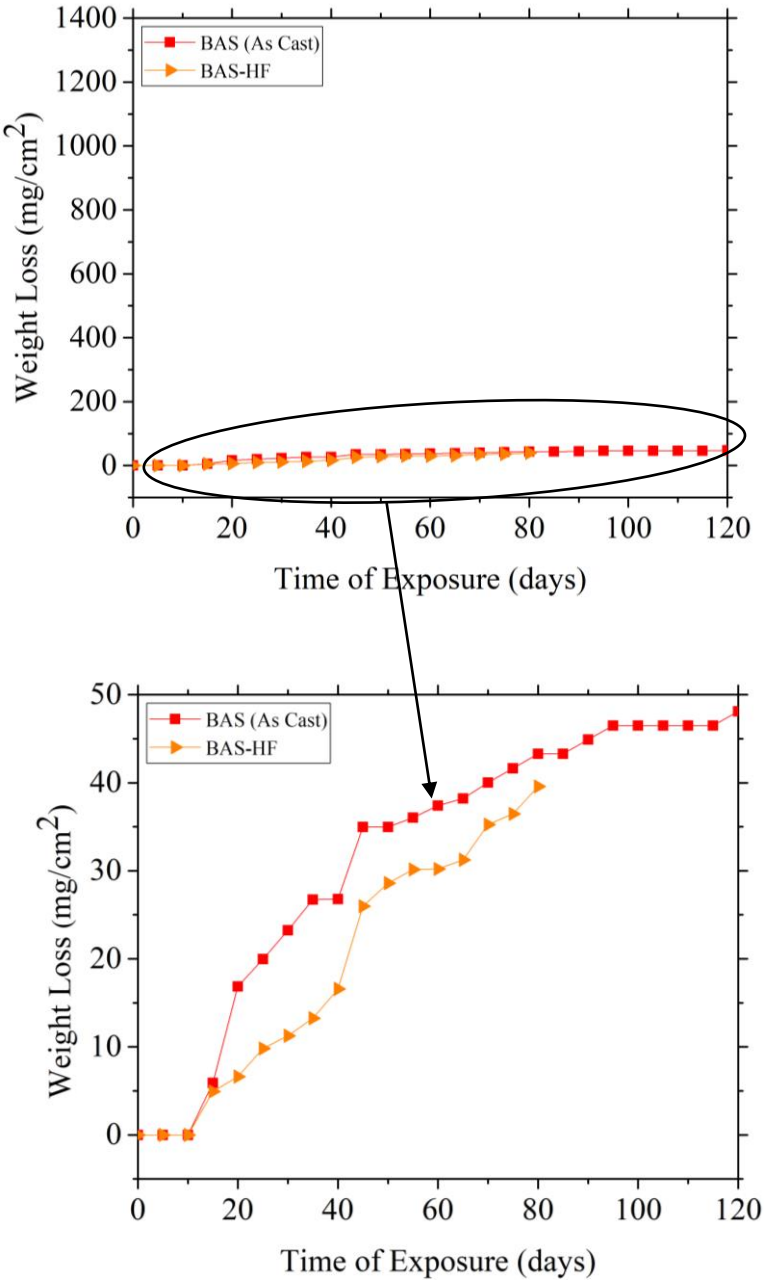

Figure 4.42. Weight loss measurements comparison of the BAS and Hardfaced BAS in 0.5M H_2SO_4 solution

In case of 1M NaOH solution, both have the same corrosion property as shown in Figure 4.43.

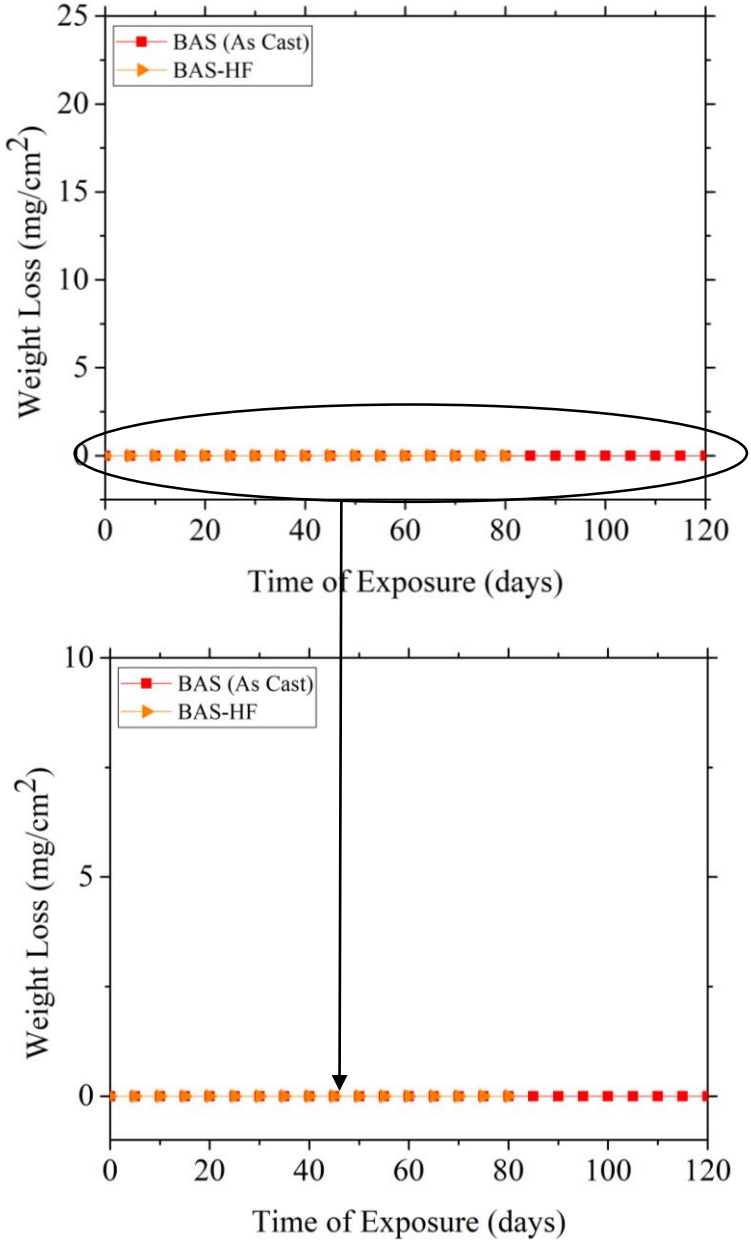

Figure 4.43. Weight loss measurements comparison of the BAS and Hardfaced BAS in 1M NaOH solution

However, in case of 0.6M NaCl solution, coated surface has a bit worse corrosion property according to as cast BAS.

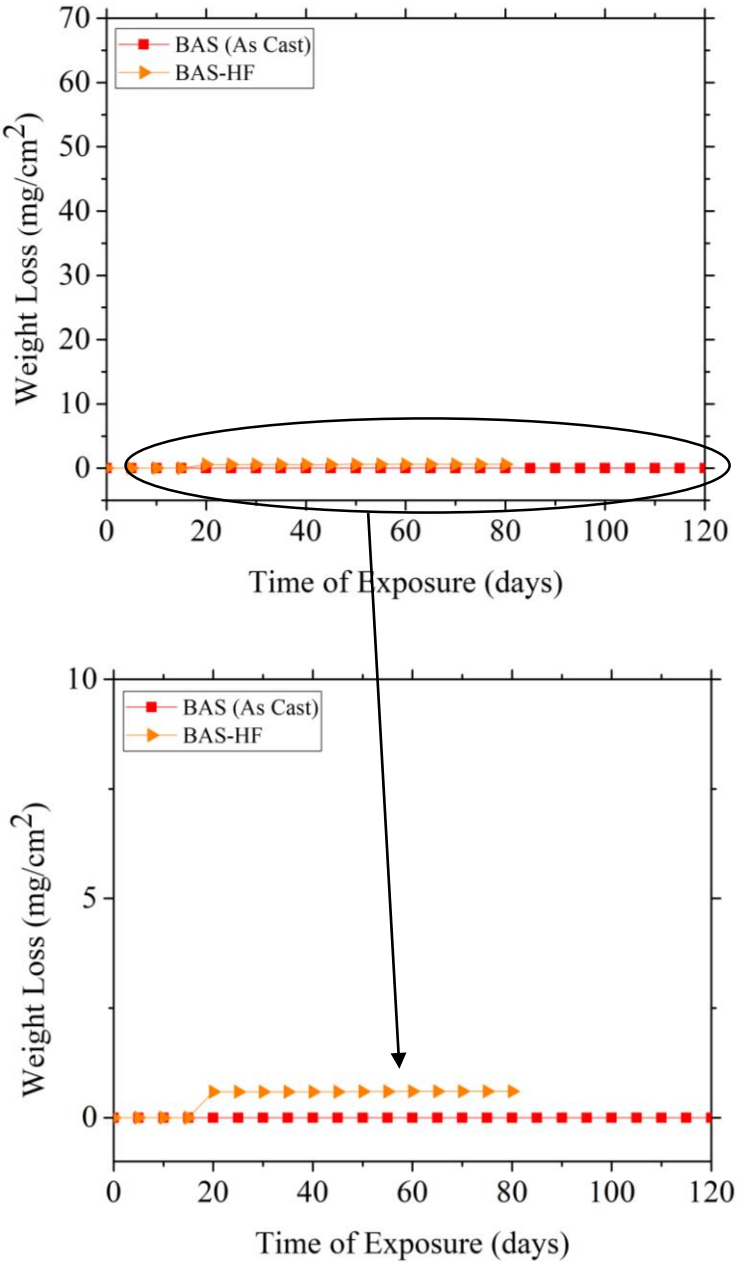

Figure 4.44. Weight loss measurements comparison of the BAS and Hardfaced BAS in 0.6M NaCl solution

As can be seen from, Figure 4.42, Figure 4.43and Figure 4.44 in both partial and full scale, hardfacing application sample also has a good corrosion behavior as BAS. In H_2SO_4 solution, it is better than BAS and it has similar behavior in NaOH solution. However, in NaCl solution, it is little bit worse than BAS. Hence, this

study showed that BAS's do not lose their good corrosion behavior even after hardfacing application.

Table 4.8. Corrosion study results for 80 days

Material	Corrosive Environment	Total Weight Loss (mg/cm^2)	Weight Loss Percentage
BAS (As Cast)	0.5M H_2SO_4	43.295	9.34%
	1M NaOH	0	0%
	0.6M NaCl	0	0%
Hardfaced BAS	0.5M H_2SO_4	39.569	5.12%
	1M NaOH	0	0%
	0.6M NaCl	0.599	0.12%
Pig Iron	0.5M H_2SO_4	1135.458	100%
	1M NaOH	17.749	2.47%
	0.6M NaCl	40.062	2.38%
Carbon Steel (S275)	0.5M H_2SO_4	1257.784	100%
	1M NaOH	1.579	0.13%
	0.6M NaCl	19.070	1.30%
Stainless Steel (304)	0.5M H_2SO_4	2.453	0.34%
	1M NaOH	1.136	0.12%
	0.6M NaCl	0.870	0.08%
Titanium (Pure)	0.5M H_2SO_4	1.509	0.22%
	1M NaOH	4.765	0.69%
	0.6M NaCl	0	0%

All of the corrosive environment outcomes are tabulated in Table 4.8 and the detailed representations of the results are shown in Figure 4.45, Figure 4.46 and Figure 4.47.

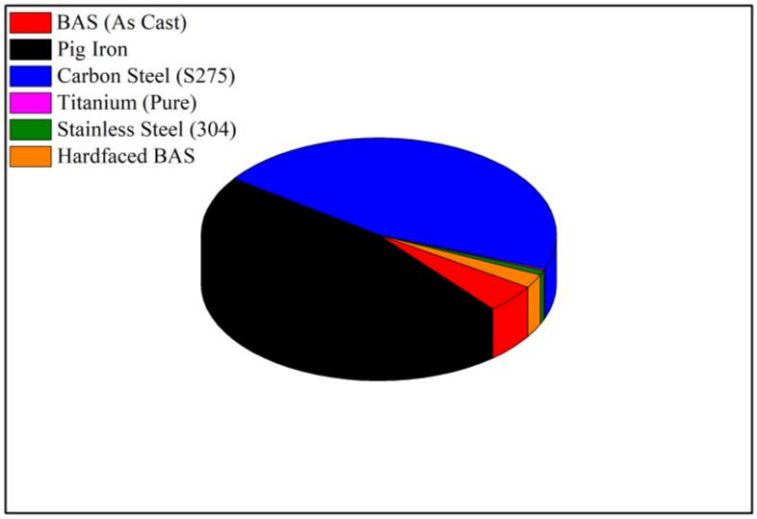

Figure 4.45. Representation of the total weight loss percentage of the all samples which includes hardfacing sample also, in the 0.5M H_2SO_4 solution for 80 days

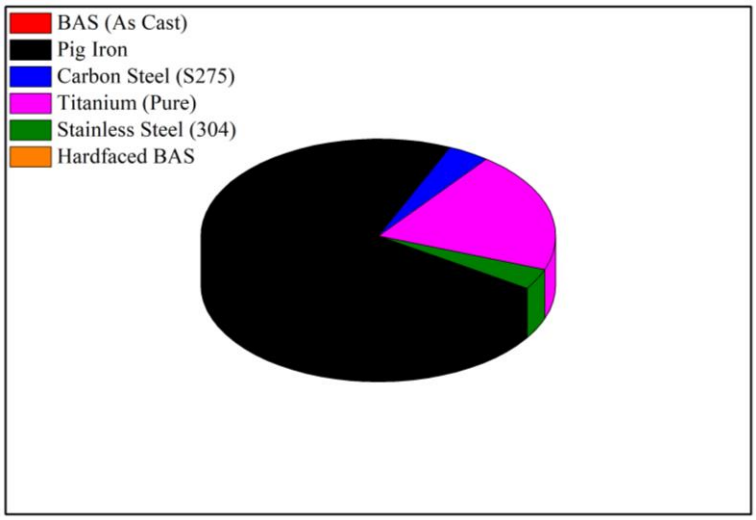

Figure 4.46. Representation of the total weight loss percentage of the all samples which includes hardfacing sample also, in the 1M NaOH solution for 80 days

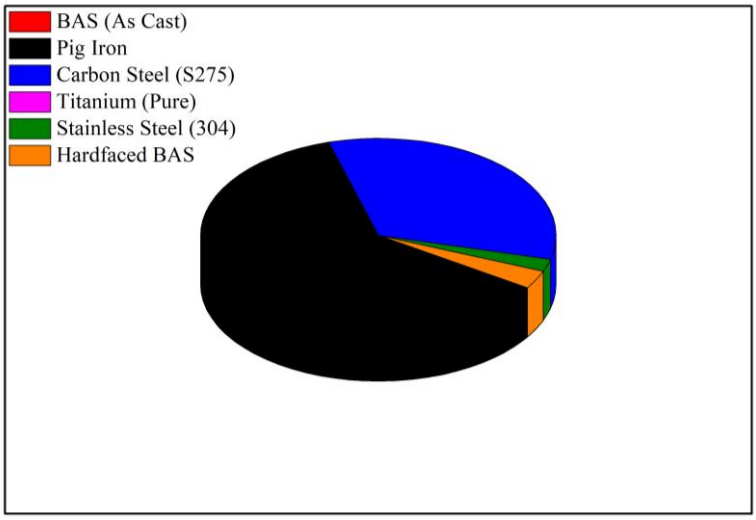

Figure 4.47. Representation of the total weight loss percentage of the all samples which includes hardfacing sample also, in the 0.6M NaCl solution for 80 days

Table 4.9. Weight loss comparison between different material

Materials	**Weight loss in the solutions (mg/cm^2) 5 days**		
	0.5 M H_2SO_4	**1 M NaOH**	**0.6 M NaCl**
BAS (As Cast)	0	0	0
Hardfaced BAS	0	0	0
Pig Iron	38.59	4.18	4.64
Carbon Steel (S275)	11.29	0	1.29
Stainless Steel (304)	2.44	0	0
Titanium (Pure)	0	0	0
AISI 304	3.21 [93]	-	-
AISI 316	1.31 [93]	0.05 [94]	-
18-8 Stainless Steel	-	-	0.022 [95]
Carbon Steel, 0.31% C	2.7 [96]	-	-
Chromium Steel	4.9 [96]	-	-
5456 Aluminum	-	1.125 [97]	-
Nickel 200 Alloy	-	0.11 [94]	-
Mild Steel	-	-	9.87 [98]
T92 Alloy Steel	-	-	0.82 [99]

CHAPTER 5

SUMMARY

In the initial part of the study, the BASs were re-synthesized from cast iron scraps by arc melting under controlled atmosphere. Suction casting technique has been employed for the direct production of 3 mm in diameter, and the reproducibility of the BAS from scrap cast iron were tested.

- For the re-synthesis of the bulk amorphous steels, the scrap cast iron was alloyed with pure Cr, Mo, B, Y and Mn elements.
- The alloying elements like Ti, V, Al and Mn have iron carbide destabilizer nature and according to the related literature work, Al and Mn addition is very critical to be able to reach fully amorphous state.
- Stabilization of the amorphous phase increases with a specific amount of Mn content in the system. According to previously conducted experimental results, after more than 5at. % Mn addition, specimens successfully achieved fully amorphous state. For this reason, 7at. % Mn addition was applied for our test sample.
- When Zr, Fe, Ti and rare earth elements are alloyed with metalloids like C, B, and Si, a large negative heat of mixing is achieved, which improves the GFA of the alloys.
- The Yttrium has an important role while justifying the composition of the BMGs closer to the eutectic point.
- According to common knowledge, high T_g amount leads to higher temperature resistance and better GFA. By interpolation of the refractory materials (Zr, Nb, Mo), higher Tg can be obtained as a result of viscosity increase.
- According to research and experimental data in NOVALAB, Fe-Mo system reveals more negative heat of mixing, and relatively lower critical cooling rate values that provides desired and high glass forming ability.

- During the examination of the amorphous state, SEM, XRD, DSC and VSM studies were conducted. The examined system demonstrated various properties including; T_g of 861K with ΔT_X (=37K), characteristic halo shaped XRD pattern, featureless microstructure and as expected, it acted as soft magnets with 145.39 Oe coercive field (Hc) and 73.23 emu/gr saturation magnetization (Ms).
- Corrosion resistance is an important property of amorphous steels and corrosion resistance is improved by Cr and Mo supplementation. However, the excessive amount of Mo supplementation prevents the dissolution of Cr during passivation.
- $M_{60}Cr_{13}Mo_{10}B_8Y_2Mn_7$ sample displayed the demanded corrosion resistant under different aggressive conditions, and it proved to have very high hardness when compared with other materials.

In the second part, after the sample was successfully produced in the amorphous form, the BAS sample was utilized as a filler material in TIG welding process as a surface treatment application. After this application, coating quality, its coherency and conformity were examined in two different cooling environments.

- Hardfacing application was applied on carbon (S275) and stainless (304) steel substrates and the experiments showed that coherence and conformity is better between carbon steel substrate and BAS.
- It was observed that owing to high bulk glass forming ability (BGFA), BAS coating material preserved its amorphous structure with extreme levels of hardness, which in fact is 3-4 times higher than the substrate metal.
- The friction, as widely accepted, depends on hardness and when the slider is harder than the plate, minimum friction occurs at the maximum hardness point. However, if the slider is softer or has nearly equal hardness, the friction is very unstable and there is no exact relationship between hardness and friction coefficient.
- During the welding application, the mismatches, which are overlapping areas, create taps between the pre-remelted layer and the new ones. Therefore,

amorphous/crystalline ratio of the sample decreases throughout the tribological test, and the higher friction results comes from the crystalline/crystalline interaction.

- Hardfaced samples showed good corrosion behavior with the low weight loss in the different extreme conditions. Hence, this study proved that BASs do not lose their good corrosion behavior even after hardfacing application.
- In all of the experimental results, the hardfaced BASs showed characteristic hollow shape XRD pattern, featureless microstructure, very high hardness values and the good corrosion resistance which are similar with the as cast BAS.

CHAPTER 6

CONCLUSIONS

The aim of the thesis is to develop and make use of a new alternative coating material based on BAS in place of traditional coating materials which will be utilized in industrial coating and surface treatment implementations by hardfacing.

For this application, the BASs were re-synthesized from cast iron scraps, which was derived from NOVALAB's theoretical approach.

- Rather than valuable ingredients, the economical scrap cast iron was used during the synthesization of the bulk amorphous steel.
- According to related thermal parameters and high glass transition temperature (861K), the amorphous nature was successfully acquired with high glass forming ability.
- The amorphous nature of the sample was also proved with characteristic hollow shape XRD pattern, featureless microstructure, very high hardness values, the good corrosion resistance properties and as expected, it acted as soft magnets.

In the second part of the of this study, the superior/unique characteristic of the bulk amorphous steel made them a good candidate for coating applications and the BAS sample was utilized as a filler material in TIG welding process as a surface treatment application.

- Carbon steel substrate and the BAS showed better coherence and conformity
- The hardfaced BAS showed 3-4 times higher hardness values than the substrate metal.

- According to all studies, the characteristic hollow shape XRD pattern, featureless microstructure, very high hardness values and the good corrosion resistance are the proof of the preservation of amorphous structure after coating application.

Recommendations for Future Studies:

i. Based on the conventional testing data, more sensitive surface coating applications (thermal spaying, laser processing etc.) might be used.
ii. More sensitive technique will also improve the thermal expansion and cracking problems of the hardfaced samples which faced during water quenching.
iii. Coating thickness optimization studies might be carried out for industrial applications.
iv. Coating length optimization studies might be carried out for industrial applications.
v. To ensure the wear property of the hardfaced BAS, the wear testing might be carried out with harder ball material.

REFERENCES

1. C. Suryanarayana, A.I., *Bulk Metallic Glasses.* 2011.

2. Drehman, A.J., A.L. Greer, and D. Turnbull, *Bulk formation of a metallic glass: Pd40Ni40P 20.* Applied Physics Letters, 1982. **41**(8): p. 716-717.

3. Kui, H.W., A.L. Greer, and D. Turnbull, *Formation of bulk metallic glass by fluxing.* Applied Physics Letters, 1984. **45**(6): p. 615-616.

4. Ponnambalam, V., et al., *Synthesis of iron-based bulk metallic glasses as nonferromagnetic amorphous steel alloys.* Applied Physics Letters, 2003. **83**(6): p. 1131-1133.

5. Lu, Z.P., et al., *Structural amorphous steels.* Physical Review Letters, 2004. **92**(24): p. 245503-1-245503-4.

6. Gürbüz, S.N., Akdeniz, M.V. and Mekhrabov A.O., *Synthesis and Characterization of Fe-B Bulk Amorphous Alloy Systems*. 2005, İstanbul,Turkey: 12-th International Metallurgy & Materials Congress, UCTEA Chamber of Metallurgical Engineers,. 2094-2101.

7. Yağmurlu, B., Akdeniz M.V., and Mekhrabov A.O., *Bulk Amorphous/Nanocrystalline Materials: Structural Amorphous Steels*. 2014, METU: Ankara, Turkey.

8. Joshi, S.S., et al., *Amorphous Coatings and Surfaces on Structural Materials.* Critical Reviews in Solid State and Materials Sciences, 2015. **41**(1): p. 1-46.

9. Stoica, M., *Fe-Based Bulk Metallic Glasses : Understanding the Influence of Impurities on Glass Formation.* 2017.

10. Stoica, M., *Fe-Based Bulk Metallic Glasses: Alloy Optimization, Focused on Understanding the Influences of Impurities on the Glass Formation.* 2015.

11. Greer, A.L., *Metallic Glasses.* Physical Metallurgy 2014. **5th Edition**: p. 305-385.

12. Chen, H.S. and D. Turnbull, *Evidence of a glass-liquid transition in a gold-germanium-silicon alloy.* The Journal of Chemical Physics, 1968. **48**(6): p. 2560-2571.

13. Chen, H.S. and D. Turnbull, *Formation, stability and structure of palladium-silicon based alloy glasses.* Acta Metallurgica, 1969. **17**(8): p. 1021-1031.

14. Chen, H.S., *Thermodynamic considerations on the formation and stability of metallic glasses.* Acta Metallurgica, 1974. **22**(12): p. 1505-1511.

15. Zhang, T., A. Inoue, and T. Masumoto, *Amorphous Zr-Al-TM (TM=Co, Ni, Cu) alloys with significant supercooled liquid region of over 100 K.* Materials Transactions, JIM, 1991. **32**(11): p. 1005-1010.

16. Inoue, A. and K.j. Hashimoto, *Amorphous and nanocrystalline materials : preparation, properties, and applications*. Advances in materials research. 2001, Berlin ; New York: Springer. 206 p.

17. Angell, C.A., *Formation of glasses from liquids and biopolymers.* Science, 1995. **267**(5206): p. 1924-1935.

18. Wang, W.H., C. Dong, and C.H. Shek, *Bulk Metallic Glasses.* Materials Science and Engineering: R: Reports, 2004. **44**(2-3): p. 45-89.

19. Busch, R., J. Schroers, and W.H. Wang, *Thermodynamics and Kinetics of Bulk Metallic Glass.* MRS Bulletin, 2011. **32**(08): p. 620-623.

20. Shen, T.D. and R.B. Schwarz, *Bulk ferromagnetic glasses prepared by flux melting and water quenching.* Applied Physics Letters, 1999. **75**(1): p. 49-51.

21. Mivšek, K., *Metallic glass.* 2006.

22. Inoue, A., *Recent progress of Zr-based bulk amorphous alloys.* Science Reports of the Rerearch Institutes Tohoku University Series A-Physics, 1996. **42**(1): p. 1-11.

23. Senkov, O.N. and D.B. Miracle, *Effect of the atomic size distribution on glass forming ability of amorphous metallic alloys.* Materials Research Bulletin, 2001. **36**(12): p. 2183-2198.

24. Senkov, O.N. and D.B. Miracle, *A topological model for metallic glass formation.* Journal of Non-Crystalline Solids, 2003. **317**(1-2): p. 34-39.

25. Pehlivanoğlu, M.K., Akdeniz, M.V., and Bor, A.Ş., *Structural characterization of iron-based bulk metallic glass alloys produced by centrifugal casting.* Chemical Engineering Communications, 2003. **190**(5-8): p. 925-935.

26. Courtney, T.H., *Mechanical behavior of materials*. 2nd ed. ed. McGraw-Hill series in materials science. 2000: Boston : McGraw Hill.

27. Grant, W.A., *A review of: "Rapidly Quenched Metals, Section II, Edited by N. J. Grant and B. C. Giessen (Proceedings of the Second International Conference on Rapidly Quenched Metals, Cambridge, Massachusetts, November 17–19, 1975). Elsevier Sequoia S.A. (Lausanne), 1976.".* Radiation Effects, 1978. **36**(3/4): p. 255.

28. Cantor, B., *Rapidly quenched metals III : proceedings of the Third International Conference on Rapidly Quenched Metals, organised jointly by the Materials Science Group of the University of Sussex and the Metals Society, London, and held at the University of Sussex, Brighton, on 3-7 July, 1978*. Book - Metals Society: no. 198. 1978: London : Metals Society, 1978.

29. Inoue, A. and A. Takeuchi, *Recent development and application products of bulk glassy alloys.* Acta Materialia, 2011. **59**(6): p. 2243-2267.

30. Yue, X., et al., *The Development of Structure Model in Metallic Glasses.* Materials Research, 2017

31. Nair, B. and B. Geetha Priyadarshini, *Process, structure, property and applications of metallic glasses.* AIMS Materials Science, 2016. **3**(3): p. 1022-1053.

32. Guo, S.F., et al., *Fe-based bulk metallic glasses: Brittle or ductile?* Applied Physics Letters, 2014. **105**(16): p. 161901.

33. Inoue, K.A.A., *Fe-(Cr, Mo)-(C, B)-Tm Bulk Metallic Glasses With High Strength And High Glass-Forming Ability.* Adv.Mater.Sci., 2008.

34. Gu, X.J., S.J. Poon, and G.J. Shiflet, *Mechanical properties of iron-based bulk metallic glasses.* Journal of Materials Research, 2011. **22**(02): p. 344-351.

35. Ivo Stloukal, L.K.a.J.Č., *Iron-Based Bulk Metallic Glasses – Optimization Of Casting.* Hradec nad Moravicí, 2009.

36. Paufler, P., *Structure of Materials. An Introduction to Crystallography, Diffraction and Symmetry. By Marc De Graef and Michael E. McHenry. Pp. xxxi+844. Cambridge: Cambridge University Press. 3rd printing, 2010. Price (hardback) USD 118.00. ISBN: 978-0521651516.* Acta Crystallographica Section A, 2012. **68**(4): p. 523.

37. Suryanarayana, C. and A. Inoue, *Iron-based bulk metallic glasses.* International Materials Reviews, 2013. **58**(3): p. 131-166.

38. Buschow, K.H.J., *Handbook of Magnetic Materials*, in *Handbook of Magnetic Materials*, K.H.J. Buschow, Editor. 2013, Elsevier. p. v-viii.

39. Amiya, K. and A. Inoue, *Fe-(Cr,Mo)-(C,B)-Tm Bulk Metallic Glasses with High Strength and High Glass-Forming Ability.* MATERIALS TRANSACTIONS, 2006. **47**(6): p. 1615-1618.

40. Henein, H., V. Uhlenwinkel, and U. Fritsching, *Metal Sprays and Spray Deposition*. 2017: Springer International Publishing.

41. Xing, L.Q., et al., *Atomic ordering and magnetic properties in Nd57Fe20B8Co5Al10 solids.* Journal of Applied Physics, 2000. **88**(6): p. 3565-3569.

42. Inoue, A., et al., *Hard magnetic bulk amorphous nd-fe-ai alloys of 12 mm in diameter made by suction casting.* Materials Transactions, JIM, 1996. **37**(4): p. 636-640.

43. Wei, B.C., et al., *Nd65Al10Fe25-xCox (x=0,5,10) bulk metallic glasses with wide supercooled liquid regions.* Journal of Applied Physics, 2001. **89**(6): p. 3529-3531.

44. Inoue, A., Y. Shinohara, and J.S. Gook, *Thermal and Magnetic Properties of Bulk Fe-Based Glassy Alloys Prepared by Copper Mold Casting.* Materials Transactions, JIM, 1995. **36**(12): p. 1427-1433.

45. Inoue, A., *Bulk amorphous alloys with soft and hard magnetic properties.* Materials Science and Engineering A, 1997. **226-228**: p. 357-363.

46. Inoue, A., et al., *New bulk amorphous Fe-(Co,Ni)-M-B (M=Zr,Hf,Nb,Ta,Mo,W) alloys with good soft magnetic properties.* Journal of Applied Physics, 1998. **83**(11): p. 6326-6328.

47. Shen, T.D. and R.B. Schwarz, *Bulk ferromagnetic glasses in the Fe–Ni–P–B System.* Acta Materialia, 2001. **49**: p. 837-847.

48. Poon, S.J., et al., *Synthesis and properties of high-manganese iron-based bulk amorphous metals as non-ferromagnetic amorphous steel alloys.* Materials Research Society Symposium - Proceedings, 2003. **754**: p. 167-177.

49. Kassner, M.E., *Fundamentals of creep in metals and alloys*. 3rd edition ed. 2015: Waltham, MA : Elsevier/Butterworth-Heinemann, [2015].

50. Pang, J., et al., *Thermal properties of metallic glasses: Heating rate dependence and their correlation.* Materials Letters, 2014. **126**: p. 81-84.

51. Zhang, W. and A. Inoue, *Thermal and magnetic properties of Fe-Co-Ln-B (Ln=Nd, Sm, Tb or Dy) amorphous alloys with high magnetostriction.* Materials Transactions, JIM, 1999. **40**(1): p. 78-81.

52. Itoi, T. and A. Inoue, *High-frequency permeability of (Fe,Co,Ni)62Nb8B30 amorphous alloys with a wide supercooled liquid region.* Applied Physics Letters, 1999. **74**(17): p. 2510-2512.

53. Pang, S.J., et al., *Synthesis of Fe-Cr-Mo-C-B-P bulk metallic glasses with high corrosion resistance.* Acta Materialia, 2002. **50**(3): p. 489-497.

54. Chen, Q.J., et al., *Glass-forming ability of an iron-based alloy enhanced by co addition and evaluated by a new criterion.* Chinese Physics Letters, 2005. **22**(7): p. 1736-1738.

55. Scully, J.R., A. Gebert, and J.H. Payer, *Corrosion and related mechanical properties of bulk metallic glasses.* Journal of Materials Research, 2011. **22**(02): p. 302-313.

56. Pang, S.J., et al., *Bulk glassy Fe-Cr-Mo-C-B alloys with high corrosion resistance.* Corrosion Science, 2002. **44**(8): p. 1847-1856.

57. Waseda, Y., Aust, K. T. , *Corrosion behaviour of metallic glasses.* Journal Of Materials Science 1981.

58. Chen, N., et al., *Role of Alloying Additions in Glass Formation and Properties of Bulk Metallic Glasses.* Materials, 2010. **3**(12): p. 5320-5339.

59. A. Bouchareb, B.B., R. Piccin and M. Baricco, *Formation and thermal properties of Fe-based BMG's with Y or Gd addition.* Nanoelectronics and Materials, 2010.

60. Xu, D., G. Duan, and W.L. Johnson, *Unusual glass-forming ability of bulk amorphous alloys based on ordinary metal copper.* Physical Review Letters, 2004. **92**(24): p. 245504-245504.

61. Gürbüz, S.N., Mekhrabov A.O. and Akdeniz M.V., *Modelling of Glass Forming Ability of Fe-B based Alloy Systems*. 2005, İstanbul, Turkey: 12-th International Metallurgy & Materials Congress, UCTEA Chamber of Metallurgical Engineers.

62. Viomar, A., et al., *Improving the Carbon Steel Surface Treatment Process.* Materials Science Forum, 2014. **805**: p. 161-166.

63. Khangura, S.S., Singh, P., Singh, H., Brar, G.S., *Proceedings of the International Conference on Research and Innovations in Mechanical Engineering*. 2014, New York: Springer. pages cm.

64. Olofsson, J., *Friction and Wear Mechanisms of Ceramic Surfaces.* Digital Comprehensive Summaries of Uppsala Dissertations from the Faculty of Science and Technology 2011. **841**.

65. Shibe, V. and V. Chawla, *An Overview of Research Work in Hardfacing.* Mechanica Confab 2013. **2**(3).

66. *Advanced Coating*. [cited 2018 20.04]; Available from: www.advanced-coating.com.

67. Mohammed Yunus, M.S.A.a.M.I., *Application of QC Tools for Continuous Improvement in an Expensive Seat Hardfacing Process Using TIG Welding.* International Journal for Quality Research 2016. **10**(3): p. 641-660.

68. Atamert, S., *Stability, Wear Resistance, and Microstructure of Iron, Cobalt and Nickel-Based Hardfacing Alloys.* 1988.

69. *Welding Consumables | Hardfacing.* Afrox Product Reference Manual, 2016. **Product Reference Manual**.

70. Yüksel, N. and S. Şahin, *Wear behavior–hardness–microstructure relation of Fe–Cr–C and Fe–Cr–C–B based hardfacing alloys.* Materials & Design, 2014. **58**: p. 491-498.

71. Kirchgaßner, M., E. Badisch, and F. Franek, *Behaviour of iron-based hardfacing alloys under abrasion and impact.* Wear, 2008. **265**(5-6): p. 772-779.

72. International, A., *Surface Hardening by Coating or Surface Modification*. Surface Hardening of Steels. 2002.

73. Pradeep, G.R.C., Ramesh, A. and Prasad, B. D. , *A Review Paper On Hardfacing Processes And Materials.* International Journal of Engineering Science and Technology, 2010. **2(11)**.

74. Group, W., *An Introduction to TIG Welding.*

75. Yağmurlu, B., Akdeniz M.V., and Mekhrabov A.O., *Production of Bulk Amorphous Steels from Cast Iron Scraps*. Book of Abstracts of Material Research Society 2013 Fall Meeting. 2013, Boston,USA.

76. Yağmurlu, B., Akdeniz M.V., and Mekhrabov A.O., *Synthesis of Bulk Amorphous Steels Having Extreme High Hardness*. 17th International Mettallurgy & Materials Congress-IMMC 2014. 2014, İstanbul,Turkey: UCTEA Chamber of MEtallurgical Engineers. 637-644.

77. Bernecki, T., *Surface Science.* Handbook of Thermal Spray Technology, 2004.

78. *Gas Tungsten Arc Welding − GTAW.* 2000.

79. Li, D., *Static Coefficient of Friction Measurement.* NANOVEA, 2014.

80. Ponnambalam, V., S.J. Poon, and G.J. Shiflet, *Fe-Mn-Cr-Mo-(Y,Ln)-C-B (Ln = Lanthanides) bulk metallic glasses as formable amorphous steel alloys.* Journal of Materials Research, 2004. **19**(10): p. 3046-3052.

81. Akdeniz, M.V., Mekhrabov, A.O., and Pehlivanoğlu, M.K., *Solidification behaviour of bulk glass-forming alloy systems.* Journal of Alloys and Compounds, 2005. **386**(1-2): p. 185-191.

82. *Online Materials Information Resource.* Online, 2018.

83. Tsai, P.H., et al., *Prominent Fe-based bulk amorphous steel alloy with large supercooled liquid region and superior corrosion resistance.* Journal of Alloys and Compounds, 2014. **586**: p. 94-98.

84. Cho, D.-H., B. Bhushan, and J. Dyess, *Mechanisms of static and kinetic friction of polypropylene, polyethylene terephthalate, and high-density polyethylene pairs during sliding.* Tribology International, 2016. **94**: p. 165-175.

85. Tian, P., et al., *Tribological behavior of Zr-based bulk metallic glass sliding against polymer, ceramic, and metal materials.* Intermetallics, 2015. **61**: p. 1-8.

86. Jang, B. and S. Yi, *Tribological Behavior of Fe-based Bulk Amorphous Alloy in a Distilled Water Environment.* Journal of the Korean Society of Tribologists and Lubrication Engineers, 2014. **30**(5): p. 295-302.

87. Wu, H., et al., *Fabrication, tribological and corrosion behaviors of detonation gun sprayed Fe-based metallic glass coating.* Transactions of Nonferrous Metals Society of China, 2016. **26**(6): p. 1629-1637.

88. Dittrick, S., *Iron Bulk Amorphous Alloy Coating for Reduced Wear Damage of Turbine.* 2013(Washington State University).

89. C. Meran, V.K., A. Alptekin, *Friction stir welding of AISI 304 austenitic stainless steel.* Mat.-wiss. u. Werkstofftech, 2007. **38**(10).

90. Handbook, A., *Friction, Lubrication, and Wear Technology*. Vol. 18. 1992. 70-75.

91. Tegart, A.J.W.M.a.W.J.M., *Relation between Friction and Hardness.* Proceedings of the Royal Society of London. Series A, Mathematical and Physical Sciences, 1952. **Vol. 212**(No. 1111).

92. Matthews, D.T.A., V. Ocelík, and J.T.M. de Hosson, *Tribological and mechanical properties of high power laser surface-treated metallic glasses.* Materials Science and Engineering: A, 2007. **471**(1-2): p. 155-164.

93. A. Pardo , M.C.M., M. Carboneras, F. Viejo, R. Arrabal, J. Munoz, *Influence of Cu and Sn content in the corrosion of AISI 304 and 316 stainless steels in H_2SO_4.* Corrosion Science, 2006. **48**: p. 1075-1092.

94. International, A., *Corrosion: Understanding the Basics*. 2000, Materials Park, Ohio.

95. Morrill, H.H.U.a.M.C., *Corrosion of 18-8 Stainless Steel in Sodium Chloride Solutions.* Industrial and Engineering Chemistry. **33**(7).

96. International, A., *Casting design and performance*. 2009: Materials Park, OH.

97. Salah Eid, M.A., E. M. Kamar, A. Y. El-Etre, *Corrosion inhibition of aluminum and aluminum silicon alloys in sodium hydroxide solutions by methyl cellulose.* J. Mater. Environ. Sci, 2015. **6 (3)**.

98. Soni, R.M.a.A., *Mild steel deterioration with time in various aqueous salt solutions.* Indian Journal of Chemical Technology, 2002. **9**: p. 74-78.

99. Yi Long, C.F., Bicao Peng, Yi Xie, Jun Wang, Minghua Zhang, Yuanhui Wu, Tangqing Wu, Fucheng Yin, *Corrosion Behaviour of T92 Steel in NaCl Solution.* International Journal of Electrochemical Science, 2017. **12**: p. 5104-5120.

APPENDICES A

T_g Determination

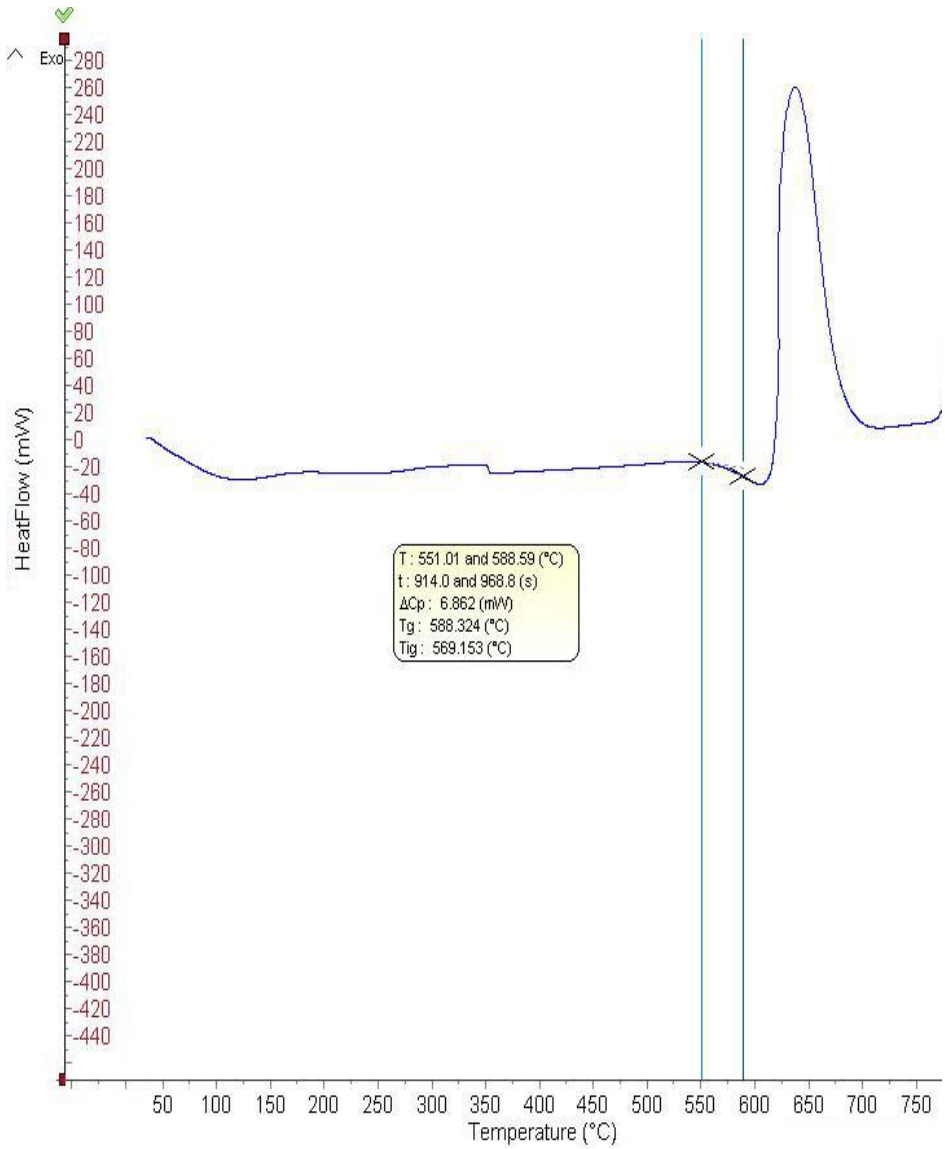

Figure A.1. Determination of the T_g from DSC SETERAM software